TARTU ÜLIKOOLI
TOIMETISED

УЧЕНЫЕ ЗАПИСКИ ТАРТУСКОГО УНИВЕРСИТЕТА

ACTA ET COMMENTATIONES UNIVERSITATIS TARTUENSIS

947

AIR IONS AND ELECTRICAL AEROSOL ANALYSIS

TARTU 1992

TARTU ÜLIKOOLI TOIMETISED
ACTA ET COMMENTATIONES UNIVERSITATIS TARTUENSIS
Alustatud 1893.a. VIHIK 947

AIR IONS AND ELECTRICAL AEROSOL ANALYSIS

TARTU 1992

Tartu Ülikooli toimetised.
Vihik 947.
AIR IONS AND ELECTRICAL AEROSOL ANALYSIS.
Tartu Ülikool.
EW2400 Tartu, Ülikooli 18.
Vastutav toimetaja J. Salm.
10,54.10,75.T.297.350.
TÜ trükikoda. EW2400 Tartu, Tiigi 78.

CONTENTS

FOREWORD

Systematic research in air electricity at Tartu University has been going on over forty years. An English-language survey of the history of the Air Electricity Laboratory (AEL) and a bibliography of publications up to 1985 (761 titles) can be found in the book [Ионизация, аэрозоли, электрометрия. Библиографический указатель научных публикаций Тартуского государственного университета за 1946-1985 гг. - Тарту, 1986]. A greater part of the scientific results of AEL has been published in Russian and in publications relatively little known to the scientific community at large. Since 1990 the results of AEL are published mainly in English. Most of the recent results are to a significant extent based on earlier publications and without this information several questions might arise in reading the recent papers.

To remedy the situation AEL has decided to publish a collection of English-language translations and summaries of its earlier papers which have originally been published in Russian. However, the present collection dealing with air ion and aerosol science does not reflect the whole range of research carried out in AEL.

The collection contains two types of papers: unchanged translations, and surveys written specially for this volume. A respective note can be found at the end of all translated articles. It is recommended to refer to the original publication in the cases of unchanged translations, and to this volume in other cases.

The collection also contains a bibliography of AEL's recent titles, which is a sequel of the above book. As in the above book the Estonian and Russian titles are provided with English translations. Differently from the above book only papers on air ions and aerosols are listed.

The editor wishes to thank Mati Limberg for his help in translating the articles and Karmen Veldre for her typing.

Tartu, February, 1992

Jaan Salm and Hannes Tammet

MODELING OF THE EVOLUTION OF SMALL TROPOSPHERIC IONS

A. Luts and J. Salm

Introduction

Researchers have been interested in the chemical composition of small ions since the first quarter of the 20th century [1]. Experimental study of the chemical composition of ions in the troposphere is a complicated task. Measurements of ion electric mobilities give only approximate information about the masses and sizes of ions [2]. Mass-spectrometric studies in the troposphere were carried out only since 1983 [3] and data obtained contained but limited information: only the masses of the cores (more stable parts) of the ions were found out. This explains the interest in theoretical modeling of ion evolution. The modeling has been carried out mostly on the basis of the methods of chemical kinetics: proceeding from the known ion-molecular reactions and the chemical composition of the troposphere, respective differential equations are composed, and the temporal changes of ion concentrations are calculated till the steady state is reached.

The foundation of the modern conception of the evolution of tropospheric small ions was laid down in [4], where the possible transformation processes of ions have been dealt with mainly qualitatively. The importance of ion-molecular reactions has also been pointed out. However, when the paper [4] was published, only a relatively small number of rate constants of ion-molecular reactions were known.

Subsequent research of major importance has been concerning quantitative modeling of ion evolution up to an age of 1 ms [5,6]. $O_2^-(H_2O)_n$ were found to be dominant negative ions and $H_3O^+(H_2O)_k$ dominant positive ions. These results were supported by experimental results. The steady state of negative tropospheric ions has been computed in [7]. In comparison with the paper [5] considerably more ion-molecular reactions and neutral compounds have been taken into account. It has been found out that in the steady state the cluster ions $NO_3^-(H_2O)_k(HNO_3)_m$ are dominant, there are less clusters with the cores HSO_4^-. It should be noted that ions of the same type have also been measured with a mass spectrometer [3].

Ion evolution with a considerably expanded number of reactions and neutral compounds has been modeled in the papers [8,9]. Below we will mainly summarize the results of these papers.

1. Description of the method

1.1. Characterization of the system of equations and previous methods of solution

The formation, evolution, and decay of small tropospheric ions can be mathematically described by the following system of differential equations:

$$\frac{d\mathbf{Y}}{dt} = \mathbf{AY} - \mathbf{BY} + \mathbf{Q} , \qquad (1)$$

where **Y** is the vector of ion concentrations,
A is the matrix describing the rates of ion-molecular reactions,
B is the matrix describing the decay of ions,
Q is the vector of the rate of ion generation.

The elements a_{jk} of matrix **A** are products of the rate constants of the respective ion-molecular reactions (where an ion with the number k becomes an ion with the number j) and the concentrations of the neutral compounds participating in the reactions [5,6]. In the modeling of small tropospheric ions the concentrations of neutral compounds are usually considered to be constant, in this case matrix **A** = const.

By the decay of ions we understand both recombination with the small ions of the opposite sign and attachment to aerosol particles. In both cases the small ion is lost. Thus the elements of matrix **B** can be expressed by

$$b_{jk} = \delta_{jk}(\alpha n + \beta Z), \qquad (2)$$

where δ_{jk} is the symbol of Kronecker,
α is the coefficient of recombination,
n is the total concentration of small ions,
β is the effective coefficient of attachment to aerosol particles,
Z is the concentration of aerosol particles [7,10].

Evidently

$$n = \sum y_j(t), \qquad (3)$$

where $y_j(t)$ are the concentrations of particular ion species.

For the modeling of ion evolution the system (1) is to be solved. In principle this could yield both the evolution and the steady state, but the solution is complicated by the following reasons:

- the system (1) is large (the number of equations in the order of magnitude of 100),
- the system (1) is nonlinear even on the assumption of constancy of matrix **A**,
- the system (1) is stiff as the elements of matrix **A** differ from one another up to 10^{11} times.

Due to the solution difficulties, the system (1) has been solved partially. In [5,6] only the linear system

$$\frac{d\mathbf{Y}}{dt} = \mathbf{AY} \tag{4}$$

has been solved using the Runge-Kutta method. The Runge-Kutta method is widely used for the solution of differential equations, but it is not suitable for the solution of stiff equation systems in the case of a long domain of integration. The Gear method has been used for the solution of stiff differential equations in the work [11], but the experience of the authors of that work and of the authors of the present paper shows that difficulties arise also with Gear method.

In the paper [7] only the steady problem

$$\frac{d\mathbf{Y}}{dt} = 0 \tag{5}$$

has been solved using a method based on the theory of signal flow graph. This method makes it possible to find out the steady concentrations of ions and additionally to evaluate the relative importance of different reactions, whereas it does not give information about the evolution of ions.

The authors of the present paper have developed a method suitable for modeling the ion evolution and the steady state [10]. The next section gives a short summary of the method.

1.2. The computation method for the evolution of ions and the steady state according to the paper [10]

Assuming that matrix **A** of the problem (1) is constant, the solution of the problem (4) can be written as

$$\mathbf{Y} = \mathbf{Y}_0 e^{\mathbf{A}t}, \tag{6}$$

where $\mathbf{Y}_0$ is the vector of initial concentrations. It is reasonable to choose $\mathbf{Y}_0$ to be parallel with vector $\mathbf{Q}$. The solution method of the problem (4), using the peculiarities of the shape of solution (6) has been elaborated in [12].

The solution (6) corresponds to real processes as far as the recombination has not become important, i.e. up to an age of ions of about 10 s, but this fact does not hinder the use of the solution (6) in the computation of the steady state.

Having solved the problem of modeling the ageing of ions (4), we will deal with the problem of the steady state (5). The concentration of small ions corresponding to the steady state n_{st} is constant and can be found from the equation

$$q = \alpha n_{st}^2 + \beta Z n_{st} , \qquad (7)$$

where $q = \sum q_j$ is the summary rate of ion generation.

In accordance to the equation (3)

$$n_{st} = \sum y_{j,st} . \qquad (8)$$

Thus in the steady state matrix $\mathbf{B}$ (see equation 2) is also constant.

According to equations (1) and (5)

$$\mathbf{A}\mathbf{Y}_{st} - \mathbf{B}_{st}\mathbf{Y}_{st} + \mathbf{Q} = 0 \qquad (9)$$

and

$$\mathbf{Y}_{st} = (\mathbf{B}_{st} - \mathbf{A})^{-1}\mathbf{Q} . \qquad (10)$$

In principle the steady concentrations of ions could be found by the formula (10), but first, the finding of the inverse matrix in the case of a stiff system may be complicated and second, the finding of a large inverse matrix is time consuming.

The paper [10] presents and proves another possibility of finding the steady concentration. As we already have the solution in the shape (6), we are looking for steady concentrations in the shape

$$\mathbf{Y}_{st} = \mathbf{Q}_0 \int \frac{\mathbf{Y}}{|\mathbf{Y}_0|} e^{-\mathbf{B}_{st} t} dt , \qquad (11)$$

where $\mathbf{Q}_0$ is the matrix whose elements are determined by the formula

$$q_{0,jk} = \delta_{jk} q ,$$

$\mathbf{Y}$ is the solution (6),

$|\mathbf{Y}_0| = \sum y_{0,j}$ is the norm of vector $\mathbf{Y}_0$.

In paper [10] the identity of equations (10) and (11) has been proved (we will not repeat the proof here).

Matrix $\mathbf{B}_{St}$ is to be computed according to equations (2) and (7), i.e.

$$b_{St,jk} = \delta_{jk}\{\beta Z + [(\beta Z)^2 + 4\alpha q]^{1/2}\}/2 \equiv \delta_{jk} b_{St} \qquad (12)$$

The computation is organized as follows. First the solution (6) is found and it is obtained in the shape of the table (t_j ; $y_{k,j}$). Then equation (13) is used for the approximate computation of the integral (11):

$$y_{St,k} = \frac{q}{|Y_0|} \sum_{j=1}^{n_0-1} \frac{t_{j+1}-t_j}{2} (y_{k,j} e^{-b_{St} t_j} + y_{k,j+1} e^{-b_{St} t_{j+1}}) \qquad (13)$$

where $k = 1, \ldots, N_0$ (N_0 is the number of concentrations),

n_0 is the number of the points where the solution (6) has been found.

If the solution (6) is found, then the time spent for the solution of the problem (5) on the basis of equation (11) or (13) is negligible.

1.3. Separation of more important variables.

To decrease the number of differential equations in the system (4) $d\mathbf{Y}/dt = \mathbf{AY}$ before starting to find the solution (6) we separated more important reactions, ions, and neutral compounds before each solution. The procedure of the separation of important data is described in detail in [13]. The set of the obtained important data depends on the concentrations of neutral compounds used in the particular problem. This way it is usually possible to decrease the number of equations two times.

2. Data for the modeling of ion evolution

Data necessary for formulating the problem (1) are the description of ion-molecular reactions, the concentrations of neutral compounds participating in ion-molecular reactions, the vectors of initial ion concentrations $\mathbf{Y}_0$ (equation 6) and the quantities α , β , Z , q (equation 7), characterizing ion formation and recombination.

Preferences among existing data on ion-molecular reactions cannot be made randomly. The preliminary determination of the concentrations of neutral compounds also causes problems, as the concentrations of many compounds are not known. Paper [13] contains a more detailed description of the method of forming the set of ion-molecular reactions, and the concentrations of neutral compounds considered natural in the present paper. Here we will only point out that the model describing the kinetics of positive ions contains 1044 reactions, 198 ions and 131 neutral compounds, and the model for negative ions contains 474 reactions, 143 ions and 106 neutral compounds.

As the shape of the solution (6) does not depend on vector Y_0, the norm of vector Y_0 can be taken equal to 1. The real concentrations of ions are included in the computation of steady concentrations according to equation (11). The values of elements $y_{0,j}$ of vector Y_0 are presented in [13].

The intensity of ion generation in natural troposphere (near the ground) is about $q \approx 10\ cm^{-3}s^{-1}$. In our studies $q = 14\ cm^{-3}s^{-1}$. The value of the coefficient of mutual recombination of small ions is taken to be nearly independent of particular ions, in the troposphere its value would be $\alpha = 1.6 \cdot 10^{-6}\ cm^3s^{-1}$ [7]. As there are numerous measurement data on the equilibrium concentration of ions in the troposphere (n about a couple of hundred of ions cm^{-3}), the value of the quantity βZ can be estimated by formula (7). In our studies $\beta Z = 0.04\ s^{-1}$.

3. The evolution of positive ions

The basic diagram of the reactions with positive ions has been presented in Fig. 1. The main routes of the evolution of ions are depicted by the continuous lines, the less important routes by the dashed lines. The term "route" may denote direct or mediated (through ions which have not been mentioned) transformation process.

The formulae surrounded by frames signify final ions, the rest are transitional ions. The formulae of ions which are formed in smaller quantities than the main ions are in brackets (e.g. less CH_3^+ ions are formed than N_4^+ ions).

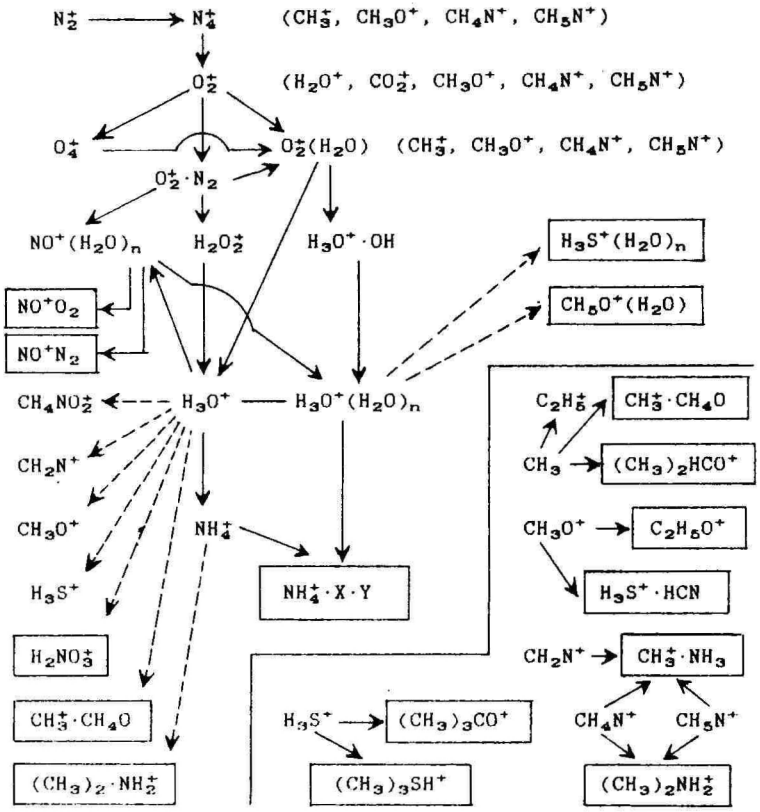

Fig. 1. Diagram of the evolution of positive ions.

3.1. Modeling results for natural concentrations of neutral compounds

The evolution of positive ions during ageing is presented in Fig. 2. The percentages of the dominant ions in the steady state are given in Table 1.

As can be seen in Figs. 1 and 2 , the initial ions (mainly N_2^+ and O_2^+) are transformed into the ions $H_3O^+(H_2O)_k$ in 10^{-8} s. The latter achieve their equilibrium concentrations at an age of about 10 μs, and this state remains nearly unchanged up to an age of about 1 s. The final ions start to be formed from the ions $H_3O^+(H_2O)_k$.

The dominance of the ions $H_3O^+(H_2O)_k$ at an age of about 1 ms agrees with experimental results [6].

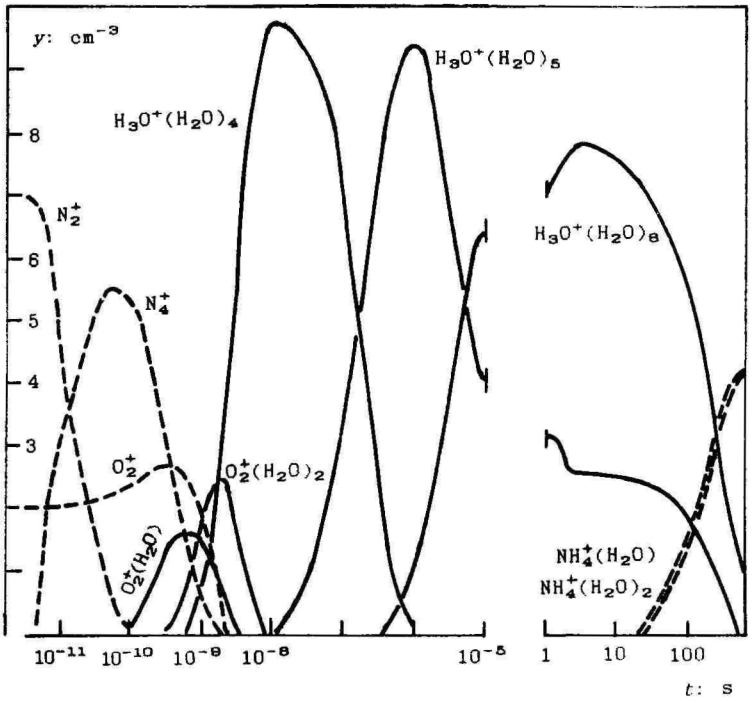

Fig. 2. Time variation of the evolution of positive ions.

According to the modeling results the final ions have cores NH_4^+. As can be seen from the first column of Table 1, the ions $H_3O^+(H_2O)_k$, and not final ions are dominant in the steady state at natural concentrations of neutral compounds. It is to be pointed out that this does not agree with the measurement results. According to the paper [14] the steady state of the troposphere should not have a significant amount of the ions $H_3O^+(H_2O)_k$. There are two explanations of this discrepancy with the modeling results. First, according to section 3.2. Second, measurement data indicate that alongside with the ions $NH_4^+ \cdot X \cdot Y$ many other not exactly identified ions are significant in the troposphere. For instance, clusters with pyridine basis are suggested as such unidentified ions in [14]. Due to the absence of data about relevant reactions the formation of such ions cannot be modeled. And in this case, it does not seem necessary to pay too serious attention

to a great number of the ions $H_3O^+(H_2O)_k$ in comparison with empirical data. We will handle this excess as a measure of incompleteness of the present data, the more so because in view of the fact a "correction" of the rate constants of some reactions has made it possible to significantly decrease the number of the ions $H_3O^+(H_2O)_k$.

Table 1

Relative weights of ions in the steady state, in per cents

Ions \ $[NH_3]$ (cm^{-3})	$4 \cdot 10^{11}$	$1 \cdot 10^{11}$	$1 \cdot 10^{12}$	$1 \cdot 10^{13}$
$H_3O^+(H_2O)_k$	77	93	56	1
$NH_4^+ X \cdot Y$	23	6	43	98

The influence of the variation of some important rate constants on the behaviour of the model deserves a separate treatment. Our experience shows that by relatively small changes of the rate constants of the reactions it is possible to adjust the model in several necessary directions. In the model under discussion we did not use 'corrections', mainly for the reason that we do not know all the reactions which make it possible to simulate the formation of all the clusters presented in empirical data.

3.2. The dependence of the evolution on the concentrations of neutral compounds

We have modeled the influence of the changes in the concentrations of the following compounds on the evolution of positive ions: NH_3, CH_3OH, CH_4, CH_3NH_2, CH_3NO_2, CO, H_2S, SO_2, $(CH_3)_2S$, SF_6, CH_3CH, C_2HF_3, CH_2CF_2, C_2H_3F, C_2H_3Cl, CH_2F_2, C_2H_5Cl, C_2H_2, C_2H_4, C_2H_6, C_3H_6, C_3H_8, N_2H_4, HCN, C_2N_2, C_2H_3N, NO_2, $(CH_3)_2NH$, H_2O_2, CH_3COOH, $(CH_3)_2CO$, $CH_3OC_3H_7$, CH_3CHO, O_3. It appears that only the concentration of NH_3 has a strong influence on evolution, whereas a moderate influence is exerted by CH_3OH, CH_4, CH_3NH_2, CH_3NO_2, CO, H_2S, and N_2O. The change of the concentration of the rest of the compounds by at least three times did not have a significant influence on the evolution of positive ions.

The influence of the change of the concentration of NH_3 is presented in Table 1. If the presumably natural concentration of this compound ($4 \cdot 10^{11}$ cm^{-3}) is diminished 4 times, then the ions $H_3O^+(H_2O)_k$ become dominant in the steady state. If we increase the concentration 2.5 times, the content of the ions $H_3O^+(H_2O)_k$ in the steady state is roughly equal to the content of final ions $NH_4^+ \cdot X \cdot Y$. If the concentration is further increased, then the ions $NH_4^+ \cdot X \cdot Y$ become dominant instead of the ions $H_3O^+(H_2O)_k$. Thus, if we suppose that the concentration of NH_3 considered natural is too low, and that the concentration of NH_3 should be increased, then the simulation results agree better with experimental results (where the ions $NH_4^+ \cdot X \cdot Y$ are dominant). In this case the modeling results agree with the measurement data according to which the composition of positive ions is independent of the concentration of NH_3 [15]. Indeed, if the concentration of NH_3 exceeds a certain critical limit, then the composition of ions is not influenced any more by the further increase of its concentration.

Due to the influence of the other compounds that have an effect on the evolution of positive ions new final ions are formed instead of the former final ions $NH_4^+ \cdot X \cdot Y$ (see Fig. 1). The reactions of the formation of the new final ions are the slowest in comparison with the reactions of the formation of the ions $NH_4^+ \cdot X \cdot Y$. Thus in the case of a thousandfold increase of all the above compounds, the relative weight of the new final ions will be below 5%.

4. The evolution of negative ions

The general diagram of the reactions taking place with negative ions is significantly more complex than the diagram of the evolution of positive ions. An example of this diagram can be found in [7]. In the case of natural concentration of neutral compounds it is still possible to separate from the general diagram a part depicting the main routes of transformation. This part is depicted in Fig. 3.

The solid lines denote the more important, and the dashed lines the less important transformations. The ions not surrounded with frames are of lesser importance in comparison with the ions surrounded with frames.

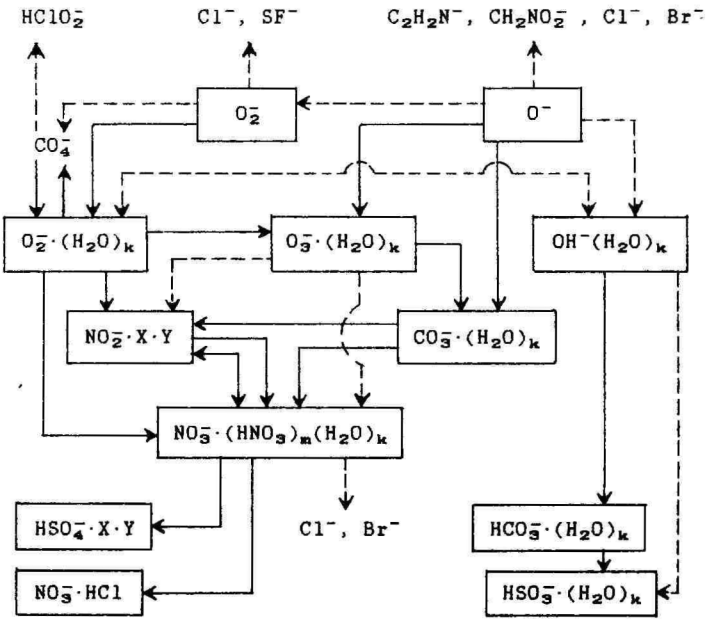

Fig. 3. Diagram of the evolution of negative ions.

4.1. Modeling results for natural concentrations of the neutral compounds

The evolution of negative ions in their ageing is shown in Fig. 4.

The ions $O_2^-(H_2O)_k$, $k > 0$ are formed of the initial ions (mostly O_2^-). The former achieve their balanced concentrations at ages below 1 μs. The ions $CO_4^-(H_2O)_k$, which in their turn are in balance with the ions $O_2^-(H_2O)_k$ are, in the case of a normal concentration of CO_2, a couple of hundreds of times less numerous than the ions $O_2^-(H_2O)_k$. This state is practically unchanged till an age of about 0.1 s, when the formation of the ions of the next stage starts. The result that at an age of about 1 ms the ions $O_2^-(H_2O)_k$ are dominant agrees with experimental data. At an age of about 0.1 s the reactions with the participation of

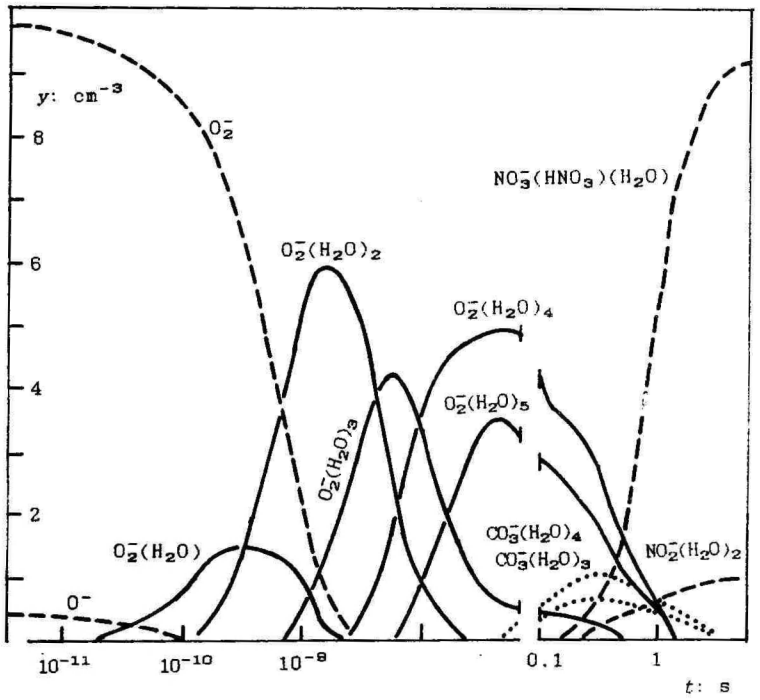

Fig. 4. Time variation of the evolution of negative ions.

three neutral gases become important. First, NO_2 participates mostly in the transformations $O_2^-(H_2O)_k$ --> $NO_2^-\cdot X\cdot Y$. Second, NO participates in the transformations $O_2^-(H_2O)_k$ --> --> $NO_3^-\cdot X\cdot Y$. Third, ozone participates in the transformations $O_2^-(H_2O)_k$ --> $O_3^-(H_2O)_k$. Generally, the final ions $NO_3^-\cdot X\cdot Y$ are formed directly through the chain $O_2^-(H_2O)_k$ --> --> $NO_2^-\cdot X\cdot Y$ --> $NO_3^-\cdot X\cdot Y$. However, if the concentration of ozone is sufficiently high, or the concentrations of NO and NO_2 are sufficiently low, the formation of the final ions through the ions $CO_3^-(H_2O)_k$ becomes important, whereas the ions $CO_3^-(H_2O)_k$ are then formed in a considerable amount.

The ions $NO_3^-(HNO_3)_m(H_2O)_k$ generally do not have the time to be transformed into the ions $HSO_4^-\cdot X\cdot Y$ and $NO_3^-\cdot HCl$, i.e. in natural conditions this transformation becomes important not earlier than at an age of a couple of hundreds of seconds. The relative weight of the ions $HCO_3^-(H_2O)_k$ will at a normal concentration of water be below 1%.

According to the modeling results, in the steady state of negative ions there are about 65% of the ions $NO_3^-(HNO_3)_m(H_2O)_n$, 10% of the ions $NO_2^-\cdot X\cdot Y$, 2.5% of the ions $O_2^-(H_2O)_k$. The result that the ions $NO_3^-(HNO_3)_m(H_2O)_n$ are dominant agrees with experimental data [14]. However, too many $NO_2^-\cdot X\cdot Y$ ions are formed according to the model. In principle, it could be possible to eliminate the discrepancy by changing the rate constants, but as there would be other discrepancies left (as will be explained in section 4.2), we did not worry about the small superfluous part of the ions $NO_2^-\cdot X\cdot Y$.

4.2. The dependence of the evolution on the concentrations of neutral compounds.

In the case of negative air ions the dependence of the evolution on the concentrations of H_2O, O_3, NO, NO_2, HNO_3, SO_2, H_2SO_4, N_2O, CH_4 and chlorine compounds has been modeled. The results are presented in the Tables 2 and 3 and in the numbered passages of the following text. State A in Tables 2 and 3 denotes the case where the concentrations of neutral compounds were natural.

1. An increase of the concentration of **water** shifts the balance of the ions $O_2^-(H_2O)_k$ towards larger ions. But as the final ions are formed mostly from the ions $O_2^-(H_2O)$ and $O_2^-(H_2O)_2$, the formation of the final ions is slowed down. Rows B1 in Tables 2 and 3 present the results for the concentration $4.4\cdot10^{17}$ cm^{-3}.

On the other hand, a decrease of the concentration of water speeds up the formation of the final ions (rows B2, $[H_2O] = 1.3\cdot10^{17}$ cm^{-3}).

We can see that the model is rather sensitive to the concentration of water. This result agrees with experimental data [16]. Indeed, on the basis of this paper we can also say that an increase of the concentration of water slows down the formation of the final ions.

2. The concentration of **ozone** influences the formation of the final ions through the chain $O_2^-(H_2O)_k$ --> $O_3^-(H_2O)_k$ --> --> $CO_3^-(H_2O)_k$ --> $NO_3^-(H_2O)_k$. It appears that this chain is quite important in the formation of the final ions. If we increase the concentration of ozone 4 times in comparison with the normal concentration (rows C1, $[O_3] = 3\cdot10^{12}$ cm^{-3}), the formation of the final ions is significantly sped up. On the other hand, a tenfold decrease of the concentration

Table 2

The abundances of negative ions (on age of ions 1 s), on various concentrations of neutral gases, in per cents

Ions / State*	$NO_3^-\cdot(HNO_3)_m\cdot(H_2O)_n\cdot$	$NO_2^-(H_2O)_k$	$O_2^-(H_2O)_k$	$CO_3^-(H_2O)_k$	HSO_4^-	$NO_3^-HCl\,Cl^-(H_2O)_k$	SO_3^- SO_4^- $NO_2^-SO_2$
A	60	8	13	17	-	-	1
B1	44	4	50	-	-	-	-
B2	86	12	-	0,5	-	-	1
C1	90	2	-	6	-	-	-
C2	14	14	66	-	-	-	-
D1	55	-	20	16	-	-	-
D2	56	44	-	-	-	-	-
D3	68	6	10	10	-	-	-
E1	82	6	12	-	-	-	-
E2	25	10	24	37	-	-	-
F	21	9	18	16	35	-	-
G1	58	8	14	18	-	-	1
G2	58	8	14	18	-	-	1
H1	22	14	16	-	-	-	46
H2	65	6	14	14	-	-	-
L1	37	11	40	11	-	-	1
L2	58	8	14	18	-	-	1
M	21	-	14	17	-	46	1

* The states, presented in Tables 2 and 3, are:

B1 : $[H_2O] = 4.4\cdot10^{17}$ cm^{-3}; B2 : $[H_2O] = 1.3\cdot10^{17}$ cm^{-3};

C1 : $[O_3] = 3\cdot10^{12}$ cm^{-3}; C2 : $[O_3] = 8\cdot10^{10}$ cm^{-3};

D1 : $[NO] = 1.6\cdot10^{10}$ cm^{-3} $[NO_2] = 2.2\cdot10^{9}$ cm^{-3};

D2 : $[NO] = 1.6\cdot10^{8}$ cm^{-3} $[NO_2] = 2.2\cdot10^{11}$ cm^{-3};

D3 : $[NO] = 1.6\cdot10^{10}$ cm^{-3}; E1 : $[HNO_3] = 1\cdot10^{12}$ cm^{-3};

E2 : $[HNO_3] = 1\cdot10^{8}$ cm^{-3}; F : $[H_2SO_4] = 4\cdot10^{12}$ cm^{-3};

G1 : $[CH_4] = 3.9\cdot10^{15}$ cm^{-3} G2 : $[CH_4] = 3.9\cdot10^{11}$ cm^{-3};

H1 : $[SO_2] = 3\cdot10^{13}$ cm^{-3}; H2 : $[SO_2] = 3\cdot10^{9}$ cm^{-3};

L1 : $[N_2O] = 1\cdot10^{15}$ cm^{-3}; L2 : $[N_2O] = 1\cdot10^{11}$ cm^{-3};

M : $[HCl] = 1.2\cdot10^{14}$ cm^{-3} $[Cl_2] = 2\cdot10^{14}$ cm^{-3}

$[HBr] = 4\cdot10^{11}$ cm^{-3} $[Cl] = 4.4\cdot10^{13}$ cm^{-3}.

Table 3

The abundance of negative ions in steady state, on various concentrations of neutral gases, in per cents

Ions / State	$NO_3^-\cdot(HNO_3)_m\cdot(H_2O)_n$	$NO_2^-(H_2O)_k$	$O_2^-(H_2O)_k$	$CO_3^-(H_2O)_k$	HSO_4^-	$NO_3^-HCl\,Cl^-(H_2O)_k$	$SO_3^-\,SO_4^-\,NO_2^-SO_2$
A	88	9	2	1	-	-	-
B1	89	5	6	-	-	-	-
B2	91	8	-	-	-	0.5	0.5
C1	95	4	-	1	-	-	-
C2	48	41	10	-	-	1	0.5
D1	94	2	2	1	-	-	-
D2	55	43	1	-	-	1	0.5
D3	88	10	1.5	1	-	-	-
E1	96	3	1	-	-	-	-
E2	74	14	3	5	1	2	0.5
F	19	9	3	1	67	2	-
G1	88	9	2	1	-	-	-
G2	88	9	2	1	-	-	-
H1	44	24	2	-	-	0.5	0.5
H2	87	8	2.5	1	-	-	-
L1	84	11	5	1	-	-	-
L2	88	9	2	1	-	-	-
M	14	-	2	1	-	83	-

of ozone (rows C2, $[O_3] = 8\cdot10^{10}$ cm^{-3}) is accompanied by slowing down of the formation of the final ions. At the same time, in this case more $NO_2^-\cdot X\cdot Y$ ions are formed, as the transformation process $O_2^-(H_2O)_n$ --> $NO_2^-\cdot X\cdot Y$ --> $NO_3^-\cdot X\cdot Y$ becomes more important. The influence of ozone on the behaviour of the model is more significant than the influence found in the experiment [15,16].

3. The influence of the concentrations of **NO** and **NO_2** on the evolution of ions is also rather significant. NO mostly influences the rates of the transformations $O_2^-(H_2O)_k$ --> --> $NO_3^-\cdot X\cdot Y$ and $CO_3^-(H_2O)_k$ --> $NO_2^-\cdot X\cdot Y$; NO_2 influences the rates of the transformations $O_2^-(H_2O)_k$ --> $NO_2^-\cdot X\cdot Y$ and $CO_3^-(H_2O)_k$ ---> $NO_3^-\cdot X\cdot Y$, and also the balance of the ions $NO_2^-\cdot X\cdot Y$ and $NO_3^-\cdot X\cdot Y$.

If we increase [NO] 10 times and decrease [NO_2] 10 times ([NO] = $1.6 \cdot 10^{10}$ cm^{-3}, [NO_2] = $2.2 \cdot 10^{9}$ cm^{-3}), then in the region of 1 s age ion formation is slowed down, whereas at the same time summarily it is sped up (see rows D1 in Tables 2 and 3). On the other hand, if we decrease [NO] 10 times and increase [NO_2] 10 times, then the loss of the ions $O_2^-(H_2O)_k$ is sped up, but at the same time a significant amount of the ions $NO_2^- \cdot X \cdot Y$ is formed, as the former balance of the ions $NO_2^- \cdot X \cdot Y$ and $NO_3^- \cdot X \cdot Y$ is shifted.

If we increase only the concentration of NO 10 times, then the evolution of the ions is near to that of the normal state (see Tables 2 and 3, rows D3).

Indeed, the concentration of NO_2 influences the evolution of negative ions also according to the experimental results [15]. At the same time the influence of the concentration of NO should not be noticeable.

4. The concentration of HNO_3 influences the balance of the ions $NO_3^-(HNO_3)_m(H_2O)_n$, and also the formation of these ions of the ions $CO_3^-(H_2O)_k$. If [HNO_3] is higher then the ions $NO_3^- \cdot X \cdot Y$ are larger, which also decreases their transformation into the ions HSO_4^- and $NO_3^- \cdot HCl$. If [HNO_3] is lower, then the ions $NO_3^- \cdot X \cdot Y$ contain more smaller ions, which are capable of being transformed into the ions HSO_4^- and $NO_3^- \cdot HCl$.

The concentration of HNO_3 influences mainly the composition of the ions of 1 s age, the influence on the ion composition of the steady state is weaker. Even if we decrease [HNO_3] a hundred times in comparison with the normal state, the steady state remains relatively unchanged, whereas the part of 1 s final ions is significantly decreased (Tables 2 and 3, rows E2, [HNO_3] = $1 \cdot 10^{8}$ cm^{-3}). If we increase the concentration of [HNO_3] 100 times in comparison with the normal concentration, then the part of the final ions is weakly increased (Tables 2 and 3, rows E1). The fact that the concentration of HNO_3 in general influences the composition of 1 s ions agrees with experimental data [15].

5. Due to the influence of H_2SO_4 the normal final ions $NO_3^-(HNO_3)_m(H_2O)_n$ are transformed into the ions HSO_4^-. However, the influence of changing the concentration is rather weak. If we want the part of the ions HSO_4^- to become important, it is necessary to increase the concentration 10^4 times (see Tables 2 and 3, rows F, where the concentration of H_2SO_4 is equal to $4 \cdot 10^{12}$ cm^{-3}).

There are no experimental data confirming the influence of the change of the concentration of H_2SO_4. On the other hand, it is known that in the steady state of the troposphere, alongside with the ions $NO_3^-\cdot X\cdot Y$, there is a small amount of ions with the core HSO_4^- [3].

6. A hundred-fold change of the concentration of CH_4 did not have a significant influence on the evolution of ions. This agrees with experimental data [15].

7. If the concentration of N_2O is increased a hundred times, then at an age of 1 s there are more $O_2^-(H_2O)_k$ ions and less $CO_3^-(H_2O)_k$ and $NO_3^-(HNO_3)_m(H_2O)_n$ ions. The steady state remains practically unchanged. A hundred-fold decrease of the concentration of N_2O does not have significant influence on the evolution of ions.

The result agrees with experimental data, where N_2O also belongs to the group of compounds having a weak influence on the evolution of ions [15].

8. Due to the influence of SO_2 the ions $HCO_3^-(H_2O)_k$ (there are generally few such ions) are transformed into the ions $HSO_3^-(H_2O)_k$, also SO_3^- ions are formed, which can be transformed into the ions $NO_3^-\cdot X\cdot Y$, thus creating one more channel of formation of final ions. The influence of changing the concentration of SO_2 is weak. A decrease of the concentration has practically no influence, whereas a hundredfold increase of the concentration generates a certain amount of SO_3^- ions (Tables 2 and 3, rows H1, $[SO_2] = 3\cdot10^{13}$ cm^{-3}).

The computational influence of the concentration of SO_2 is weaker than it could be on the basis of the results presented in [15].

9. An at least thousand-fold increase of the concentrations of **chlorine compounds (HCl, Cl_2, freons)** has the remarkable influence on the evolution of ions. This result generally agrees with experimental data [15], which predict an extremely strong influence in the case of these compounds, but the influence obtained by computation is too weak.

Conclusions

In the present paper and in papers [8,9] an attempt has been made to compare the behaviour of a model based on chemical kinetics with the measurement data obtained by mass

and mobility spectrometry. The ions of 1 s age and the influence of adding neutral gases to them have been studied only with mobility spectrometry.

Thus, the ions of an age of about 1 ms are similar on the basis of both measurements and modeling. The same (with certain reservations presented in sections 3.1. and 4.1.) is true of the ions of the steady state. However, it is not possible to conclude that the model is sufficiently correct. Namely, certain discrepancies appear between the measurement results and modeling in the case of 1 s ions. First, the influence of many admixtures found to be very important in [15] (HCl, CCl_3COOH, $(CH_3)_2 \cdot NH$, $CHCl_3$, etc.) could not be modeled. Second, the model predicts a strong influence of ozone on the evolution of ions; on the basis of measurements such a strong influence should not exist.

At the same time there are many results coinciding with the measurements of 1 s ions. Indeed, in modeling, as in paper [16], a higher concentration of water slows down the formation of final ions. Indeed, the model is sensitive to the concentration of NO_2 and HNO_3, and weakly sensitive to CH_4 and N_2O in the case of negative ions and to most gases in the case of positive ions.

Finally, we have to point out that though our models have used a relatively large quantity of data and the results agree with relevant measurement results in many respects, a lack of data about several important reactions is still evident.

References

1. Nolan, J.J. The nature of the ions produced in air by radioactive bodies // Proc. Roy. Irish Acad.- 1920.- Vol. 35.- P. 38-45.

2. Plasma Chromatography / Ed. by T.W. Carr.- N.Y. and Lond.: Plenum Press, 1984.

3. Heitman, H., Arnold, F. Composition measurements of tropospheric ions // Nature.- 1983.- Vol. 306.- P. 747-751.

4. Mohnen, V.A. Formation, nature and mobility of ions of atmospheric importance // Electrical Processes in Atmospheres.- Darmstadt: D. Steinkopff Verlag, 1977.- P. 1-17.

5. Huertas, M.L., Fontan, J., Gonzalez, J. Evolution times of tropospheric negative ions // Atmos. Envir.- 1978.-

Vol. 12.- P. 2351-2362.

6. Huertas, M.L., Fontan, J. Evolution times of tropospheric positive ions // Atmos. Envir. - 1975. - Vol.9.- P. 1018-1026.

7. Kawamoto, H., Ogawa, T. First model of negative ion composition in the troposphere // Planet. Space Sci.- 1986.- Vol. 34, No. 12.- P. 1229-1239.

8. Сальм Я.Й., Лутс А.М. Кинетика образования отрицательных легких аэроионов в тропосфере // Уч. зап. Тарт. ун-та.- 1988.- Вып. 809.- С. 64-70.

9. Лутс А.М., Сальм Я.Й. Кинетика образования положительных легких аэроионов в тропосфере // Уч. зап. Тарт. ун-та.- 1988.- Вып. 824.- С. 60-68.

10. Сальм Я.Й., Лутс А.М. Метод вычисления стационарных концентраций одного класса задач химической кинетики // Уч. зап. Тарт. ун-та.- 1988.- Вып. 824.- С. 52-59.

11. Лившиц А.Н., Портнов Ф.Г., Шмидт А.Б. Моделирование химической кинетики образования отрицательных ионов в воздухе с нулевой влажностью // Изв. АН Латв. ССР.- Сер. хим.- 1983.- N 4.- С. 449-451.

12. Ракитский Ю.В., Устинов С.М., Сениченков Ю.В., Воскобойников С.П. Алгоритмы и программы интегрирования дифференциальных уравнений.- Ленинград: Изд. ЛГУ.- 1984.- 88 с.

13. Luts, A. Chemical kinetics of tropospheric ions at higher ionization rates // Acta et comm. Univ. Tartuensis.- - 1992.- (in print).

14. Eisele, F.L., McDaniel, E.W. Mass spectrometric study of tropospheric ions in the southwestern and northeastern United States // J. Geophys. Res..- 1986.- Vol.91.- P. 5183- -5188.

15. Ихер Х.Р., Сальм Я.Й. Зависимость спектра подвижности легких аэроионов от химических примесей в воздухе // Уч. зап. Тарт. ун-та.- 1982.- Вып. 631.- С. 27-34.

16. Сальм Я.Й., Ихер Х.Р. Исследование спектра подвижности легких аэроионов // Тр. ин-та эксперим. метеорологии.- 1983.- - Вып. 30(104).- С. 116-121.

THE EFFECT OF PYRIDINE AND ITS HOMOLOGUES ON MOBILITY SPECTRA OF POSITIVE SMALL AIR IONS

T. Parts and J. Salm

Introduction

Natural air contains permanent gases (N_2, O_2, Ar, Ne, He, Kr, H_2, N_2O, Xe), and variable components (H_2O, CO_2, CH_4, CO, O_3, NH_3, NO, NO_2, SO_2, H_2S, hydrocarbons, organic compounds containing oxygen, nitrogen, and sulphur, element-organic compounds, etc.) [1, 2]. The concentration c of unpermanent gases in the troposphere varies between traces ($c < 1$ ng) to several microgrammes (in the case of H_2O to several grammes) in m^3 [2, 3]. Biosphere is the largest source of organic emissions into the troposphere. These emissions include also pyridine bases, i.e. mixtures of heterocyclic organic compounds (pyridine, picolines, lutidines, collidines). Pyridine bases are formed also in combustion processes of fossil fuels, oil shales, turf, and in the incineration of wood and bone [4]. Mass-spectrometric measurements confirm their presence in natural air [5].

In addition to neutral molecular components the air also contains a certain amount of radicals O, OH, HO_2, CH_3O_2, etc. (10^4-10^9 molecules in cm^3), and air ions (small air ions of an order of 10^2-10^3 pairs in cm^3). Cosmic irradiation and radiation of radioactive compounds cause the formation of primary ions (N_2^+, O_2^+, H_2O^+, CO_2^+, O_2^-, O^-, OH^-, etc.) from neutral molecules. In ion-molecular reactions with molecules the primary ions are transformed into small air ions. The composition of the latter in the troposphere has not been finally established.

It is known that the mobility spectrum of small air ions is sensitive to a number of admixtures in the air [6, 7]. The difference between urban and rural spectra of positive small air ions [8] may be connected with the differences in the chemical composition of the air. Pyridine and its homologues may influence the composition of positive small air ions [5]. The present paper will consider the influence of pyridine, 2-picoline, 2,3-, 2,4-, 2,5-, 2,6-lutidine and γ-collidine on the mobility spectrum of small air ions.

Objects and methods of the investigation

The objects of the investigation are ordinary urban air in a relatively clean laboratory of 50 m^3, and admixtures: pyridine, methylpyridine, dimethylpyridines, trimethylpyridine. Table 1 presents certain physical-chemical properties of the latter and of NH_3 and H_2O [9]. Water and ammonium have an important role in the formation of positive air ions [5].

Table 1

Physical-chemical properties of some pyridines, NH_3, and H_2O

Compound	Formula	Molecular mass amu	Boiling point °C	Proton affinity eV
Pyridine	C_5H_5N	79	115.3	9.6
2-picoline	$CH_3C_5H_4N$	93	128	9.75
2,4-lutidine	$(CH_3)_2C_5H_3N$	107	157	9.83
2,6-lutidine	$(CH_3)_2C_5H_3N$	107	143	9.83
γ-collidine	$(CH_3)_3C_5H_2N$	121	172	10
Ammonium	NH_3	17	-33.5	9.4
Water	H_2O	18	100	7.3

In the laboratory room people worked only in the case of extreme necessity (adjustment of apparatuses). During the measurement the room was empty. The floor of the room was made of glazed plates. The walls and the ceiling were painted with pentaphtal paint which is a relatively slow gas absorber. There were very few pieces of furniture in the room and most of them were metallic. Smoking was prohibited in the laboratory and in neighbouring rooms.

The measurement was carried out with an air ion spectrometer *UT-7509* [8,10] which was slightly rebuilt and supplemented with an *Iskra 226* computer. The program KAIS used for spectrometer control and data collection was compiled by H. Tammet. The program executed the measurement and recording of the mobility spectrum of small air ions of both polarities in 64 points located logarithmically uniformly by mobility.

The background spectra were measured in maximally clean room. After that some certain chemicals in very low concentrations were added to the air.

The concentrations presented in this paper were roughly estimated. Actual measurements of concentrations were not made. The concentrations were calculated by the estimated volume of the admixture evaporating from a surface of 1 cm^2 at T = 295 K, $p = 10^5$ Pa. The time of evaporation and the distance of the admixture dish from the spectrometer were taken into account in the calculations.

Experimental results

The background spectra of one-second small air ions in laboratory air have a typical form (Fig. 1).

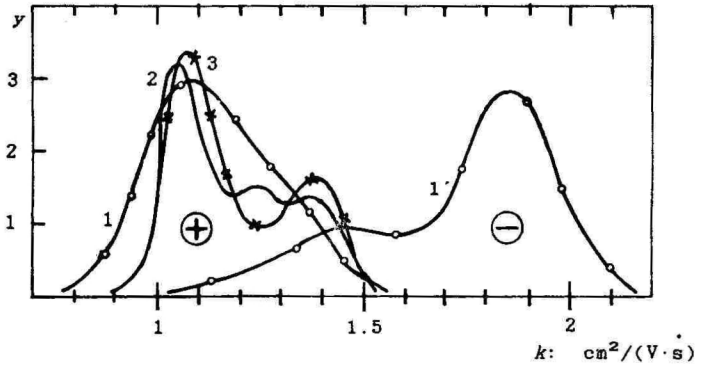

Fig. 1. Mobility spectra of small air ions. 1 and 1′ – – background spectra, monthly average (March 1986); 2 and 3 – traces of pyridines in the room (2 – the next day, 3 – a week after the experiments). The ordinate y of the spectra is in arbitrary units.

After the experiments with pyridine and its homologues and airing of the room, the mobility spectrum of positive air ions always contains three peaks, whereas 1.05 $cm^2/(V \cdot s)$ is dominant. Pyridine, picoline, lutidines, and collidine influence the mobility spectrum of small positive air ions (Figs. 2-4). They do not influence the spectrum of negative air ions. On the wide background peak 0.7-1.6 $cm^2/(V \cdot s)$ there are evident peaks 1.05 $cm^2/(V \cdot s)$ (background after all pyridines), 1.2 $cm^2/(V \cdot s)$ (2-picoline, 2,6-lutidine, collidine), and 1.4 $cm^2/(V \cdot s)$ (2,3-lutidine, 2,4-lutidine). In the case of pyridine the peak is widened towards higher mobilities.

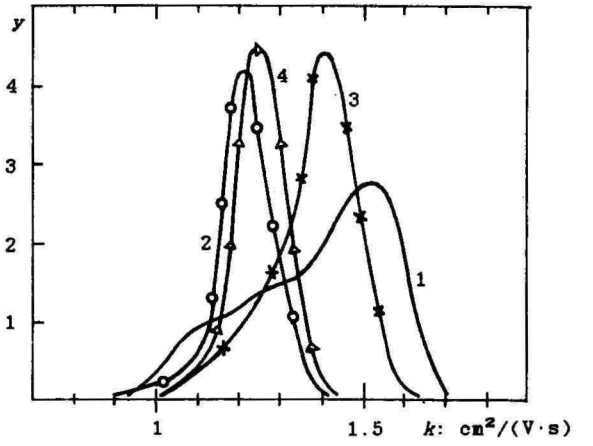

Fig. 2. The influence of pyridines on the spectrum of positive air ions. 1 - pyridine, 2 - 2-picoline, 3 - 2,3-lutidine, 4 - collidine.

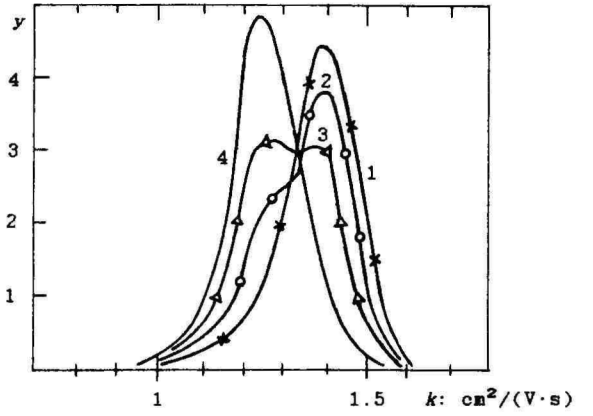

Fig. 3. The influence of dimethylpyridines on the spectrum of positive air ions. 1 - 2,3-lutidine, 2 - 2,4-lutidine, 3 - 2,5-lutidine, 4 - 2,6-lutidine ($c \approx 10^{-2}$ μg/m³).

Fig. 3 presents the mobility spectra of various dimethylpyridines: 2,3-, 2,4-, 2,5-, and 2,6-lutidines. The mobility

spectra of 2,3-, and 2,6-lutidine have discrete peaks of 1.4 $cm^2/(V \cdot s)$ and 1.2 $cm^2/(V \cdot s)$ respectively. The mobility spectra of 2,4- and 2,5-lutidine are in an intermediate position, and have two peaks whose relations depend on the concentration of the admixture.

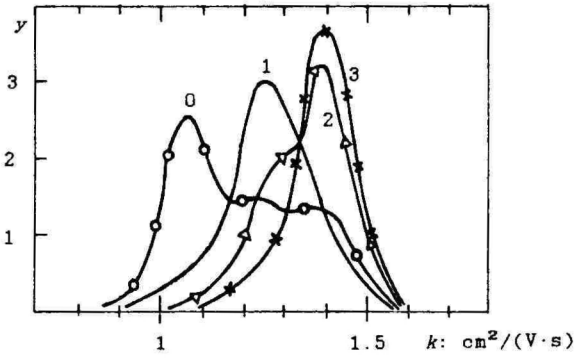

Fig. 4. The dependence of the spectrum of positive small air ions on the concentration of 2,4-lutidine ($c_3 > c_2 > c_1 > c_0$, $c_3 = 10^{-1}$ μg/m³, $c_0 \approx 10^{-3}$ μg/m³).

Discussion

In recent studies of air ions in the troposphere using mass spectrometry and gas chromatography it is supposed that $NH_4^+(H_2O)_n$ are the final dominant positive air ions in natural air, however the composition of positive air ions is influenced by organic admixtures always present in the troposphere [5].

In addition to dominant air ions the atmosphere also contains $O_2^+(H_2O)_n$, $NO^+(H_2O)_n$, $H_3O^+(H_2O)_n$, $NH_4^+(NH_3)_m(H_2O)_n$, etc., depending on temperature, pressure, humidity, age of ions, and the particular admixtures of the air.

The main parameters that determine the mobility of an ion in a gas are its mass and effective dimensions. The mass of an ion is determined by its chemical composition, the dimensions are determined by composition and other physical-chemical properties of the ion.

An increase in the concentration of an admixture or the appearance of new admixtures in the air leads to a change in

the composition of air ions on account of their collisions with the molecules of the admixture. As a result air ions with new chemical compositions are formed. Masses and dimensions, and consequently also mobilities of the ions are changed.

Our measurements show that in some cases admixtures with remarkably different molecular masses ($CH_3C_5H_4N$, $(CH_3)_2C_5H_3N$ and $(CH_3)_3C_5H_2N$) give mobility peaks in one and the same region 1.2 $cm^2/(V \cdot s)$ (Figs. 2 and 3).

Pyridine, picoline, lutidines, and collidine have higher proton affinities than ammonium (Table 1) and they easily enter the reactions of proton transfer (Table 2) which take place at a reaction rate of about 10^{-9} $cm^3 \cdot s^{-1}$ [5].

Table 2

Proton transfer reactions with pyridines

Initial compounds			Final products	
C_5H_5N	+ $NH_4^+(H_2O)_n$	-->	$C_5H_5NH^+(H_2O)_n$	+ NH_3
$CH_3C_5H_4N$	+ $NH_4^+(H_2O)_n$	-->	$CH_3C_5H_4NH^+(H_2O)_n$	+ NH_3
$(CH_3)_2C_5H_3N$	+ $NH_4^+(H_2O)_n$	-->	$(CH_3)_2C_5H_3NH^+(H_2O)_n$	+ NH_3
$(CH_3)_3C_5H_2N$	+ $NH_4^+(H_2O)_n$	-->	$(CH_3)_3C_5H_2NH^+(H_2O)_n$	+ NH_3

Changes in the spectra may be connected with the above reactions, but other reactions are also possible (e.g. decay of complexes, changes of hydration rates, etc.). Measurements of mobility spectra of small air ions show that pyridine and its homologues manifest individual physical-chemical properties both in the reactions of proton transfer and in the reactions of cluster formation - decomposition.

Conclusions

1. Pyridines as nucleophilic chemical reagents have a strong influence on the mobility of positive small air ions of one-second age, whereas they do not influence the mobility of negative ions.

2. The form of the mobility spectrum of positive small air ions depends on the concentrations of the admixtures injected into the air, but on very low concentrations the effect is similar: a peak at the mobility 1.05 $cm^2/(V \cdot s)$ is induced.

3. Lutidines (dimethylpyridines) have a characteristic influence on the spectrum of positive small air ions. The mobility spectrometry of one-second small air ions makes it possible to identify 2,3-, 2,4-, 2,5-, and 2,6-lutidines at their low concentrations in air.

References

1. Leithe, W. Die Analyse der Luft und ihrer Verunreinigungen in der freien Atmosphäre und am Arbeitsplatz.- Stuttgart: Wissenschaftliche Verlagsgesellschaft mbH, 1974.- 340 S.

2. Исидиров В.А. Органическая химия атмосферы. - Л.: Химия, 1985. - 265 с.

3. Защита атмосферы от загрязнений. - Вильнюс, 1983. - Вып. 7. - 98 с.

4. Краткая химическая энциклопедия. - М.: Сов. Энцикл., 1964. - Т. 3. - С. 1057.

5. Eisele, F.L. Identification of tropospheric ions // J. Geophys. Res. - 1986. - Vol. 91, D 7. - P. 7897-7906.

6. Таммет Х.Ф. Зависимость спектра подвижности легких аэроионов от микропримесей воздуха // Уч. зап. Тарт. ун-та. - 1975. - Вып. 348. - С. 13-15.

7. Ихер Х.Р., Сальм Я.Й. Зависимость спектра подвижности легких аэроионов от химических примесей в воздухе // Уч. зап. Тарт. ун-та. - 1982. - Вып. 631. - С. 27-31.

8. Таммет Х.Ф., Ихер Х.Р., Миллер Ф.Г. Спектр подвижностей односекундных легких аэроионов в природном воздухе // Уч. зап. Тарт. ун-та. - 1985. - Вып. 707. - С. 26-36.

9. Справочник химика. - Л.-М.: Химия, 1964. - Т. 3. - С. 195-196.

10. Таммет Х.Ф., Хилпус А.О. и др. Спектрометр аэроионов для обнаружения некоторых примесей воздуха // Уч. зап. Тарт. ун-та. - 1977. - Вып. 409. - С. 84-88.

Translated from:

Партс Т.М., Сальм Я.Й. Воздействие пиридина и некоторых его гомологов на спектр подвижности положительных легких аэроионов // Уч. зап. Тарт. ун-та.- 1988.- Вып. 803.- С. 71-78.

MEASUREMENT OF AIR ION MOBILITY SPECTRA IN A WIDE RANGE

J. Salm and M. Reinart

The main purpose of this research was to obtain information about the mobility spectrum of air ions in indoor (laboratory) conditions. The article also deals with the testing of a relatively modern air ion spectrometer.

A ten-channel air ion spectrometer *UT-7914* was used for the measurements, a short description of the device is provided in [1]. The general design of *UT-7914* is quite similar to that of its prototype [2]. The main differences between the new spectrometer and the prototype are the reduced number of channels, the use of individual smallsize electrometers [3] for each channel instead of commutated electrometers, the control unit built of modern microchips, and the use of a unit of analogous indication of the signals from separate channels. The spectrometer has two aspiration measuring capacitors with divided effective capacitance. Thus there are 10 limiting mobilities with a logarithmically uniform distribution: 0.00048; 0.001; 0.0022; 0.0048; 0.01; 0.022; 0.048; 0.1; 0.22; 0.48 $cm^2/(V \cdot s)$.

For the computation of the mobility spectra H. Tammet has written programs for *NAIRI* computers on the basis of the piecewise linear spectrum model [4]. The present paper employs the program yielding the so-called λ-spectrum which is composed of 9 values of the conductivity function $\lambda(k)$ for the above mobility values k = 0.00048; 0.001; 0.0022; 0.0048 etc. up to 0.22 $cm^2/(V \cdot s)$, and of the concentration of small air ions which have conventionally been given the mobility of 1 $cm^2/(V \cdot s)$. The values of the conductivity function at k = = 0.48 $cm^2/(V \cdot s)$ are a priori taken to be zero. The program, alongside with the values of spectra, also yields the respective estimates of random errors.

The spectra were measured during 6 months from November 1981 to May 1982, as a rule, the measurements were conducted on weekdays from 17:00 to 18:00 (Moscow time). The measurements were carried out in laboratory without special sources of air ions and aerosols. One person servicing the spectrometer was in the room during the recording of spectra. The ventilation window was closed. In the whole measurement

period 630 negative and 665 positive air ion spectra were obtained. Before the calculation of average values the data were checked and in two cases some parts of it were not used: 1) if the computer issued a special symbol indicating the inexactness of the computation due to strongly anomalous data; 2) if the negative values of the spectra (in principle impossible) in their absolute values at least two times exceeded the estimate of the mean square error in the same fraction. In the first case the whole spectrum was rejected, in the second case the anomalous value and two neighbouring values on the right and on the left were rejected. The latter rule is based on special mathematical experiments which show that the deviance of the signal in one spectrometer channel causes error in several neighbouring fractions of the spectrum. The rejected values of the spectra were distributed roughly uniformly between the two above criteria.

The above rejection procedure left 4172 values, i.e. the average of 417 spectra for negative air ions, and 4805 values, i.e. the average of 480 spectra for positive ions. The averaged λ-spectrum for the whole measurement period is presented in Table 1 and Fig. 1.

Table 1

Air ion spectra in laboratory conditions

Mobility k $cm^2/(V \cdot s)$	Values of the spectral function $\lambda(k)$: e/cm^3	
	Negative air ions	Positive air ions
0.00048	1005	1534
0.001	1522	1927
0.0022	397	438
0.0048	287	376
0.01	120	239
0.022	15	120
0.048	28	-1
0.1	-1	4
0.22	1	1
1	181	196

The resulting spectrum demonstrates that the maximum value of the spectral function is about 10^{-3} $cm^2/(V \cdot s)$ and that

ions are practically absent in the mobility range from 0.05 $cm^2/(V \cdot s)$ before small ions.

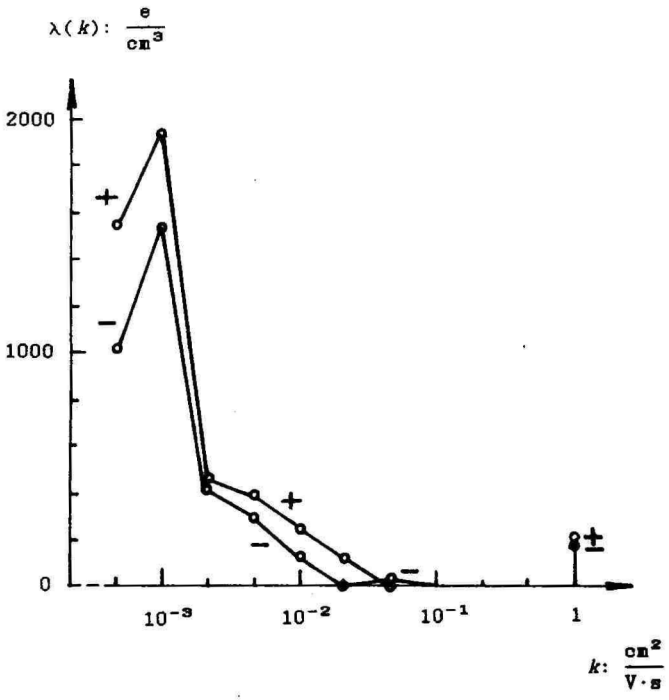

Fig. 1. Air ion mobility spectrum in laboratory conditions.

The spectral distribution of small air ions has not been specially studied in the present paper, however, according to existing data, small air ions are located approximately in the range from 0.5 to 2.5 $cm^2/(V \cdot s)$ [5, 6]. Thus, the mobility spectrum has a large gap approximately in the range from 0.05 to 0.5 $cm^2/(V \cdot s)$.

The a priori zeroing of the spectral function at $k = 0.48$ $cm^2/(V \cdot s)$ turned out to be justified: in the opposite case there would have been a significant value of the function at $k = 0.22$ $cm^2/(V \cdot s)$. The fact that almost all papers on air ion spectra published up to now do not show such a gap, can probably be explained by low resolution of the equipment and by significant measurement errors. The gap can be explained

by the diffusion charging model of intermediate and large air ions, considering the ultra-low probability of the appearance of charged particles in the range of radii approximately from 1 to 3 nm (which correspond to the mobility range from 0.05 to 0.5 $cm^2/(V \cdot s)$) [7].

References

1. Сальм Я.Й. Десятиканальный спектрометр аэроионов // Методы и приборы биоинформации и контроля параметров окружающей среды. Межвузовый сборник.- Вып. 150.- 1981.- Л.: ЛЭТИ. - С. 34-38.

2. Таммет Х.Ф., Якобсон А.Ф., Сальм Я.Й. Многоканальный автоматический спектрометр аэроионов // Уч. зап. Тарт. ун-та. - 1973.- Вып. 320.- С. 48-75.

3. Миллер Ф.Г. К разработке электрометров прямого усиления для многоканальных спектрометров аэроионов // Уч. зап. Тарт. ун-та.- 1981.- Вып. 588.- С. 124-131.

4. Таммет Х.Ф. Кусочно-линейная модель спектра в аэроионных и аэрозольных измерениях // Уч. зап. Тарт. ун-та.- 1980.- Вып. 534.- С. 45-54.

5. Mohnen, V.A. Formation, nature and mobility of ions of atmospheric importance // Electrical Processes in Atmospheres. Proc. 5 Int. Conf. Atmos. Electr. - Darmstadt: Dr. Dietrich Steinkopff Verlag, 1977. - P. 1-17.

6. Ихер Х.Р., Сальм Я.Й. Зависимость спектра подвижности легких аэроионов от химических примесей в воздухе // Уч. зап. Тарт. ун-та.- 1982.- Вып. 631.- С. 27-34.

7. Israël, H. Atmosphärische Elektrizität. T. I. - Leipzig: Akad. Verlagsges. Geest & Portig, K.-G., 1957.

Translated from:

Сальм Я. Й., Рейнарт М. А. Измерение спектра подвижности аэроионов в широком диапазоне // Уч. зап. Тарт. ун-та.- 1983. - Вып. 648.- С. 41-45.

SPECTRUM OF ATMOSPHERIC IONS IN THE MOBILITY RANGE 0.32-3.2 $cm^2/(V \cdot s)$

H. Tammet, H. Iher and J. Salm

Introduction

The authors have carried out continuous measurements of ion spectra in the mobility range from 0.32 to 3.2 $cm^2/(V \cdot s)$, whereas the whole range was logarithmically divided into 10 intervals. The spectrum was represented by a corresponding set of fraction concentrations. Instruments and methods used are described in [1]. The present paper presents preliminary conclusions from the results of measurements carried out from 04.06.85 to 10.06.85 in the city of Tartu, Estonia, and from 10.06.85 to 15.09.85 at Tahkuse village, Estonia. In 1984 systematic measurements of mobility spectra of small ions of one-second age were carried out at the same village [2]. The measurement point at Tahkuse was situated in a typical sparsely populated rural region 27 km to the north-east of the city of Pärnu.

In the measurement point at Tahkuse the spectrometers with the sensors were located in the attic of a one-storeyed country house. The air was sucked in through an opening in the vertical frontone of the attic at a height of about 5 m from the ground. The house was surrounded by tall trees and there were fields nearby. The computer, controller, and the sensor of pressure were situated in a room with a microclimate of normal living premises.

The measurements were carried out round the clock, interruptions were due to technical failures and power cuts. All the measurements were controlled by the computer program described in [1].

Processing of results

The results were first recorded on a compact cassette and subsequently rewritten on a hard disk of *Iskra-226* computer with the help of the system described in [3]. Further processing was carried out by *Iskra-226* computer using Basic-02 programming system.

The first stage of processing included technical recoding of information and elimination of all the data where at least one overloading of at least one electrometer had occurred. At

the second stage fraction concentrations of ion spectra were computed and the times when measurement precision had failed to meet certain criteria, were eliminated. The method of the computation of spectra is presented in [1]. The elimination of results is described in Table 1. The eliminated times were not uniformly distributed over the whole day; a heightened probability of insulation failures was observed in high-humidity morning hours. Similarily, the probability of failures and noise in power input was increased in the morning hours.

Table 1

The extent of measurements

Place	Time (Moscow, Summer) Beginning	End	No. of hrs. possible	actual	passed stage 1	passed stage 2
Tartu	04.06.85. 18:00	10.06.85. 7:00	133	102	91	90
Tahkuse	10.06.85. 19:00	15.08.85. 19:00	2328	2025	1763	1700

The results obtained at stage 2 were the basis of all the statistical conclusions. No further elimination of results on the basis of quality was carried out.

It can be hypothesized that the apparatus matrix proposed in [1] is designed on the basis of an overly modest estimate of apparatus smoothing of the spectrum and leads to systematic "undercorrection" of spectra, especially in the conditions of strong turbulence. The apparatus matrix can be improved after further experiments in the laboratory. As it is, we have considered it best to stick to the lower limit of the estimate of apparatus smoothing, as "overcorrection" would lead to even more considerable distortions of results, than the retention of residual apparatus smoothing in the case of "undercorrection".

At the second stage of processing, an additional correction was used for the adsorption of ions on the input grid of the measurement capacitor. According to a semi-empirical estimate [4] the adsorption is about 4% for a mobility of 2 $cm^2/(V \cdot s)$.

The form of the spectrum and the classification of ions according to their mobilities.

To determine the average spectra of small air ions on the basis of 1700 hours of measurements at Tahkuse, only the hours where none of the four main parameters exceeded the interval $x \pm \sigma_x$ (neither for positive, nor for negative ions) were chosen. There were 443 such hours and they were more or less uniformly distributed over the whole period of measurement. The respective spectra were averaged arithmetically. The results are presented in Fig.1.

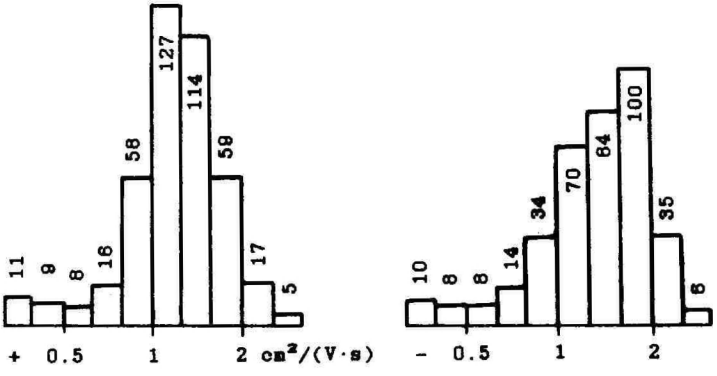

Fig. 1. Average spectra of small atmospheric ions. Henceforth the fractions will be indicated in the descending order of numbers and ascending order of the mobilities. The number of ions/cm^3 is indicated at every column. The limits of mobility intervals are: 0.32; 0.40; 0.50; 0.63; 0.79; 1.00; 1.26; 1.58; 2.00; 2.51; 3.16.

The standard deviation of random error of the measurement of fraction concentrations in an one-hour spectrum was about several ions in cm^3. Random errors in the average spectra in Fig. 1 were much lower. However, considerable systematic errors which do not diminish in averaging are not excluded. One of the possible sources of errors is residual apparatus smoothing of the spectrum. It is very likely that positive results in the mobility interval over 2.5 cm^2/(V·s) are only a result of smoothing, and that actually there are no such ions. Results pointing to the existence of high-mobility ions

in the atmosphere have been published for several times, e.g. [5, 6]; however, in all these cases it cannot be excluded that the apparent presence of such ions has been caused by low resolution of the instruments and resulting smoothing of spectrum.

The presence of low-mobility ions in the results cannot be explained by apparatus distortions. Such ions that are not always present, are of special interest.

In the spectra with a clear-cut "heavy tail" a minimum is observed in the mobility range 0.5-0.6 $cm^2/(V \cdot s)$. The minimum is observed also in the average spectra (Fig. 1). An analysis of a set of spectra creates an impression that the physical nature of ions changes at the limit 0.5-0.6 $cm^2/(V \cdot s)$. It seems that in the case of high mobilities the ions could be considered as molecular clusters, whereas in the case of low mobilities the properties of macroscopic particles are dominant.

The above regularity confirms the correctness of using the boundary 0.5-0.6 $cm^2/(V \cdot s)$ for the classification of ions. Henceforth, in accordance with numerous other studies, we will use 0.5 $cm^2/(V \cdot s)$ as the standard value of the border, whereas only ions with higher mobilities will be called small ions. Ions with lower mobilities will be classified as intermediate ions. In the following discussion of the intermediate ions we will consider only the ions with mobilities 0.32--0.5 $cm^2/(V \cdot s)$, recorded during the measurements.

Intermediate ions are mostly distributed symmetrically by polarities. However, there are cases where intense formation of intermediate ions takes place only for one of the polarities. Respective examples are presented in Fig. 2, the examples are extreme also with a view to relative proportions of intermediate and small ions.

These examples permit to hypotesize that at the division of ions into small and intermediate according to their physical nature it is necessary to consider the respective mobility intervals as partially overlapping. For instance, positive ions with the mobilities 0.63-0.8 $cm^2/(V \cdot s)$ in the spectrum (Fig. 2a) are likely to be intermediate ions physically.

In the spectrum of small positive ions at the achieved resolution always only one maximum is discovered, whereas its location is highly variable. In the spectrum of negative ions often two peaks were observed (see Fig. 2b). In ordinary

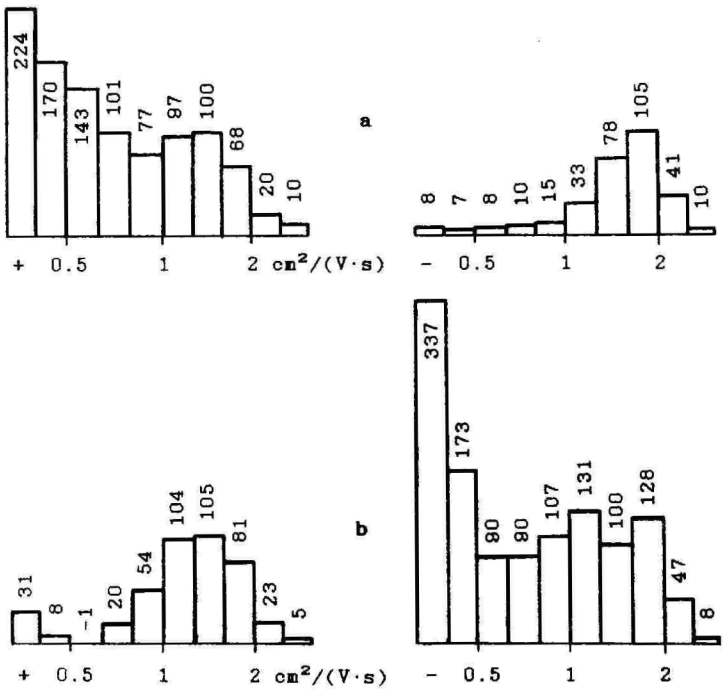

Fig. 2. Examples of extreme spectra.
a - at 3 a.m. 13.06.85; b - at 5 p.m. 05.09.85.
Estimates of standard deviation of random errors are less than 3 ions/cm³ for any fraction.

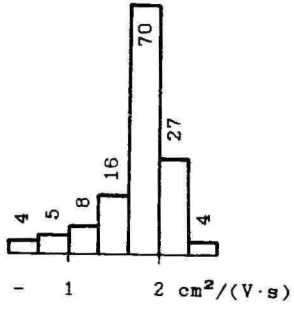

conditions the more mobile peak in the spectrum is strongly dominant and there is no intermediate minimum. Fig. 3 presents an extremely narrow spectrum. This sample also demonstrates an extremely high average mobility and a rather low concentration of small ions.

Fig. 3. Extremely narrow spectrum of small negative ions. Midnight 30.08.85.

Our results concerning the form of spectrum agree well with an example by Yunker [7], with the observations of Misaki et al. [8], and also with the results of [9].

Parameters of the spectrum

For statistical analysis it is necessary to describe the basic properties of the spectrum by means of a small amount of numeric parameters. The following set of parameters is based on the above conclusion about the expedience of dividing the whole spectral range into a subrange of small ions with mobilities over 0.5 $cm^2/(V \cdot s)$ (8 first fractions) and a subrange of intermediate ions with mobilities below this limit (2 last fractions). The main parameters are determined and denoted as follows:

1. Concentration of small ions $n = \sum_{j=1}^{8} \varphi_j$.

2. Average mobility of small ions for standard conditions

   $\bar{k} = \sum_{j=1}^{8} k_j \varphi_j / n$, where k_j is geometric mean of boundary mobilities of the fraction.

3. Relative width of the spectrum of small ions

   $$s = \sqrt{\left(\sum_{j=1}^{8} k_j^2 \varphi_j / n - \bar{k}^2 \right)} / \bar{k}.$$

4. Fraction concentration of intermediate ions

   $$m = \varphi_9 + \varphi_{10}$$

Natural average mobility of small ions is viewed as a supplementary parameter.

$$\bar{k}' = \left(\frac{101325\ \text{Pa}}{p} \frac{T}{273.15\ \text{K}} \right) \bar{k}.$$

Statistical averages and distributions

Average values and standard deviations of the parameters of all 1700 pairs of spectra recorded at Tahkuse are presented in Table 2.

By way of comparison it can be pointed out that in summer 1984 on the island of Vilsandi it was found that $k_+ = 1.35 \pm \pm 0.48\ cm^2/(V \cdot s)$ and $k_- = 1.59 \pm 0.44\ cm^2/(V \cdot s)$ [10]. These values were obtained using an integral aspiration counter and

Table 2

Average parameters of spectra at Tahkuse

Parameter	Polarity	Average	Standard deviation	Unit of measurement
n	+	408	145	cm^{-3}
n	-	359	136	"
m	+	24	16	"
m	-	24	20	"
$\bar{k}$	+	1.31	0.10	$cm^2/(V \cdot s)$
$\bar{k}$	-	1.47	0.13	"
$\bar{k}'$	+	1.39	0.10	"
$\bar{k}'$	-	1.56	0.13	"
s	+	0.305	0.022	1
s	-	0.317	0.033	"

respectively higher random errors of measurement are reflected in the high estimates of standard deviations.

Average conductivities $\lambda_+ = 9.20$ fS/m and $\lambda_- = 9.12$ fS/m are nearly equal; this is evidence of the suppression of the electrode effect under tall trees. The presented values do not include the conductivity caused by ions with mobilities below 0.32 $cm^2/(V \cdot s)$.

The statistical distribution of hourly averages of mobilities is described by Table 3.

Table 3

Distribution of hourly averages of small ion mobilities at Tahkuse

	1.0	1.1	1.2	1.3	1.4	1.5	1.6	1.7	1.8	1.9
$\bar{k}_+$	12	235	584	577	234	53	5	0	0	
$\bar{k}_-$	2	41	135	321	463	475	196	65	2	
$\bar{k}'_+$	0	28	294	652	520	179	25	2	0	
$\bar{k}'_-$	0	5	47	150	324	487	457	188	41	

Mobilities below 1.1 $cm^2/(V \cdot s)$ occurred only when ions which were intermediate according to their physical nature, formally fell into the mobility range of small ions. The Sherman distributions [11] differ from those in Table 3 first of all in their greater width. A possible explanation is the

effect of random measurement errors.

The statistical distribution of the average mobility is rather close to normal distribution. The distribution of small ion concentration has a noticeable positive asymmetry and a large excess. The distribution of intermediate ion concentration is significantly different from normal distribution: the coefficient of asymmetry exceeds 9 and the coefficient of excess is 180 (see also Table 9).

The distribution of the coefficient of unipolarity is shown in Table 4.

Table 4

Distribution of the unipolarity coefficient n_+/n_- at Tahkuse. The first line contains the values and the second line the frequencies.

0.8	0.9	1.0	1.1	1.2	1.3	1.4	1.5	1.6
4	66	440	747	353	72	12	3	

Daily variation

The daily variation of main spectral parameters is weakly expressed. The data are presented in Table 5.

The strong daily variation of the concentration of small ions in inhabited locations is caused by the daily rhythm of anthropogenic pollution of the air. The concentration of small air ions is determined by both the intensity of ion formation and aerosol density. In a relatively sparsely inhabited rural location variations of both factors evidently cancel each other.

The nightly maximum of the concentration of small ions was caused by rare cases of anomalously heightened concentration exceeding $n + 3\sigma_n$. None of these anomalies was accompanied by anomalies of unipolarity. A likely reason of high concentrations is an anomalously low concentration of aerosols which occurred only at night. If to eliminate 2% of the data on the basis of the criterion of high ion concentration, then the average daily variation is strongly suppressed - peaks of n_+ at 23:00 and 3:00 fall to 418 cm^{-3}.

The daily variation of the average mobility is closely connected with the daily variation of temperature which will be dealt with separately.

Table 5

Daily variation of spectral parameters at Tahkuse. First column - beginning of the interval by Moscow Summer Time. υ - number of days covered, t - temperature in °C, η - correlation ratio.

	υ	t	n_+	m_+	$\bar{k}_+$	$\bar{k}'_+$	n_-	m_-	$\bar{k}_-$	$\bar{k}'_-$
0	78	14.3	441	23	1.332	1.406	386	23	1.481	1.562
1	74	13.6	443	23	1.338	1.409	391	22	1.500	1.579
2	75	13,0	437	22	1.343	1.410	384	20	1.510	1.586
3	73	12.5	452	28	1.343	1.409	392	21	1.514	1.588
4	72	12.3	440	23	1.355	1.419	380	22	1.516	1.588
5	71	11.6	437	23	1.356	1.417	376	21	1.526	1.595
6	72	11.5	406	24	1.354	1.414	350	22	1.528	1.597
7	67	11.9	399	23	1.347	1.410	344	20	1.526	1.598
8	57	12.5	307	23	1.336	1.401	341	22	1.504	1.578
9	52	14.5	401	27	1.298	1.371	348	24	1.462	1.546
10	58	15.8	391	26	1.299	1.380	338	21	1.463	1.554
11	61	16.9	385	25	1.293	1.377	334	25	1.467	1.562
12	66	18.0	396	28	1.267	1.354	347	31	1.431	1.544
13	70	18.9	399	29	1.262	1.352	348	30	1.441	1.544
14	72	19.3	392	26	1.269	1.361	343	28	1.460	1.566
15	74	19,7	389	27	1.265	1.360	341	30	1.449	1.557
16	76	19.8	379	27	1.266	1.361	334	30	1.435	1.543
17	77	20.0	381	26	1.263	1.358	338	35	1.424	1.532
18	75	19.7	373	23	1.278	1.373	331	24	1.441	1.548
19	75	18.9	381	21	1.281	1.373	340	21	1.443	1.547
20	78	18.7	387	21	1.285	1.376	344	20	1.438	1.540
21	78	17.7	400	20	1.287	1.384	364	19	1.436	1.532
22	75	16.5	420	21	1.307	1.389	381	19	1.443	1.534
23	74	15.4	444	23	1.309	1.387	405	23	1.444	1.530
η	-	64%	17%	17%	32%	23%	17%	19%	26%	19%

Dependence of mobility on temperature

The dependence of mobility on temperature is described in Table 6.

In the case of ions with stable structure the increase of temperature leads to the growth of natural mobility which is inversely proportional to the density of the air. Actually,

Table 6

Dependence of average mobility
on temperature at Tahkuse

°C	$\bar{k}'_+$	$\bar{k}_+$	$\bar{k}'_-$	$\bar{k}_-$
0-5	1.52	1.48	1.71	1.63
5-10	1.45	1.40	1.62	1.55
10-15	1.40	1.33	1.57	1.49
15-20	1.38	1.28	1.54	1.46
20-25	1.34	1.24	1.51	1.41
25-30	1.32	1.21	1.52	1.39
η	33%	48%	26%	35%

natural mobility decreases with the growth of temperature. This gives evidence of the dependence of the structure of ions on temperature. This dependence may partially be caused by the growth of the concentration of air trace-gases together with the temperature.

The data in Table 6 can be taken to pose a problem of the reduction of mobilities proportionally to the density of the air. To obtain more information, the dependence of the reduced mobility on air pressure was computed. The results shown in Table 7 demonstrate a lack of a linear tendency, at the same time a non-linear tendency is evident.

Table 7

Dependence of average reduced
mobility on air pressure

Pressure	995-1005	1005-1015	1015-1025	1025-1035 hPa
$\bar{k}_+$	1.35	1.30	1.30	1.36 $cm^2/(V \cdot s)$
Frequency	66	785	669	158

The investigation of the mobilities of one-second aged ions did not reveal a dependence of the reduced mobility on temperature [2]. It seems that the dependence on temperature is caused by admixtures of such low concentrations that the relaxation time of their reactions with ions is substantially over one second.

Linear correlations

The estimate of linear statistical correlations in the set of basic parameters is presented in Table 8. Disregarding the problem discussed above, the data in Table 8 do not contradict the accepted understanding of the regularities of the behaviour of air ions.

Table 8

Estimates of the coefficients of linear correlation r for the whole period of measurement. Number of realizations is 1780, and the 99% confidence level is r_{99} = 6%.

r: %	t	n_+	m_+	$\bar{k}_+$	n_-	m_-	$\bar{k}_-$
t	+100	-12	-7	-49	-10	+2	-39
n_+	-12	+100	+20	-23	+97	+15	-28
m_+	-7	+20	+100	-24	+17	+63	-23
$\bar{k}_+$	-49	-23	-24	+100	-24	-28	+86
n_-	-10	+97	+17	-24	+100	+20	-33
m_-	+2	+15	+63	-28	+20	+100	-37
$\bar{k}_-$	-39	-28	-23	+86	-33	-37	+100

Ionization and aerosol formation

The formation of intermediate air ions is one of the most frequently discussed mechanisms of atmospheric aerosol generation. Especially interesting is the condensation on ions of substances other than water which can form stable particles. Some mechanisms of this process are known [12]. The results of the present measurements clearly demonstrate and quantitatively describe the formation of intermediate ions in the atmosphere which makes it possible to draw several conclusions about aerosol formation.

In earlier measurements of the spectra of one-second aged ions at Tahkuse intermediate ions were not discovered [2]. In a special experiment (22:00. 09.06.85) with the air of the city of Tartu a weak radioactive substance was used, this increased the concentration of small ions to 1500 cm^{-3} but did not lead to the growth of the concentration of intermediate ions which remained at a level of 20 cm^{-3}. This indicates that the concentration of intermediate ions does

not grow together with increased ionization rate, but is kept at a certain low level by some limiting factor. This factor can be the concentration of certain trace-gases in the air which is necessary for the formation of intermediate ions. As the effect of intermediate ion formation is almost always saturated at the level of natural ionization rate, it is understandable that artificial ion formation in laboratory conditions does not lead to intense aerosol formation.

The air component controlling the formation of intermediate ions cannot be water, as the amount of water in the air cannot be responsible for the effect of saturation. According to measurement data the concentration of intermediate ions is not any function of humidity. Spectra with and without intermediate ions can be accompanied by both foggy and fair weathers. Examples of strong charge asymmetry presented in Fig. 2 point towards the existence of different trace-gases capable of forming intermediate ions of either one or the other polarity. The chemical nature of such trace-gases is presently unknown. The task of identification of these trace--gases would be easier, if it were possible to find conditions where intermediate ions are generated with stability. According to [18] it can be supposed that such conditions were in the caves of Carlsbad, USA where average mobilities +0.35 $cm^2/(V \cdot s)$ and -0.50 $cm^2/(V \cdot s)$ were recorded for a sum of small and intermediate ions, whereas the concentrations were above 600 000 cm^{-3}.

In Tartu the average $m_+ = m_- = 57$ cm^{-3} was observed from 04.06.85 to 10.06.85 (for Tahkuse the respective figure was 24 cm^{-3}). The limited measurement period in the city (90 hrs) does not make it possible to draw any conclusions about the increased concentration of intermediate ions in the conditions of higher anthropogenic air pollution.

A quantitative description of statistical distribution of concentration of intermediate ions and charge symmetry are presented in Table 9. On the background of low concentrations detailed in Table 9 there are some conspicuous samples. Some of those are the samples depicted in Fig. 2, where m_+ achieves the value 394 cm^{-3} (a), and m_- 510 cm^{-3} (b).

Above it was assumed that intermediate ions are formed as a result of condensation of substances on small ions. However, there is another hypotesis which claims that particles are formed in a neutral state and only subsequently charged,

Two-dimensional distribution of concentrations of intermediate ions of different polarities with mobilities from 0.32 to 0.5 $cm^2/(V \cdot s)$ at Tahkuse

m_+ \ m_-	<10	10-20	20-30	30-40	40-50	50-60	>60	Σ
<10	22	39	7	3	0	0	0	71
10-20	109	375	106	27	4	1	0	622
20-30	28	232	291	70	16	2	6	645
30-40	2	27	66	70	31	10	4	210
40-50	1	2	6	21	21	15	11	77
50-60	0	0	0	1	7	13	17	38
>60	1	1	1	0	2	5	27	37
Σ	163	676	477	192	81	46	65	1700

as a result of diffusion of small ions to particles similarly to large ions. The mobility range 0.32-0.5 $cm^2/(V \cdot s)$ corresponds to the diameter range 2-2.7 nm. According to the most reliable of the available results [14] the mean probability of the presence of charge of one polarity for this range is about 0.007. If m = 500 (see Fig. 2), then in one cm^3, there should be about 70000 neutral particles of the size 2-2.7 nm. Data in [15] show that the average concentration of such particles in air does not exceed several hundreds in cm^3 which leads to the formation of several intermediate ions in cm^3. The hypothesis of intermediate ion formation from neutral particles also runs into difficulties if it has to be used to explain the observed cases of charge asymmetry.

Be that as it may, the above-said cannot be taken to refute conclusively the hypothesis that a certain part of intermediate ions is formed from neutral particles. It is possible that both mechanisms have their own role in the real atmosphere. The sample in Fig. 2b could have the following hypothetical explanation. Particles arise due to rapid growth of negative small ions. These particles are neutralized in recombination with positive ions and this causes the emergence of an anomalously high quantity of small neutral particles. Due to the diffusion of positive ions to the neutral particles positive ions with the mobility 0.32-0.5 $cm^2/(V \cdot s)$ emerge (see Fig. 2b).

On the basis of the above measurement results and speculative argumentations a double classification of atmospheric ions can be proposed. The traditional classification distinguishes *small*, *intermediate* and *large ions* on the basis of mobility. The conditional limit 0.5 $cm^2/(V \cdot s)$ between small and intermediate ions found empirical proof in this investigation. To increase the exactness of the formal limit further measurements are necessary.

The other classification is based on the physical nature of ions:
- *cluster ions* - particles with the properties of clusters,
- *condensation ions* - particles with the properties of macroscopic bodies, emerging from cluster ions by a growth of their size.
- *aerosol ions* - particles emerging as a result of adsorption of cluster or condensation ions to aerosol particles.

The difference between the physical properties of molecular clusters and those of microscopic bodies has been dealt with e.g. in [16].

The mobility ranges of different groups of ions overlap. If to accept the above explanation of the spectra in Fig. 2b. it can be said that negative ions with mobilities 0.32-0.5 $cm^2/(V \cdot s)$ are condensation ions in this particular case but positive ions in this same mobility range are aerosol ions.

To check the proposed hypothesis and to find out about the role of atmospheric ions in the balance of atmospheric aerosol it is necessary to carry out systematic measurements of atmospheric ion spectra in a wider mobility range.

References

1. Таммет Х.Ф. и др. Аппаратура и методика спектрометрии подвижностей легких аэроионов // Уч. зап Тарт. ун-та.- 1987.- Вып. 755.- С. 18-28.

2. Таммет Х.Ф., Ихер Х.Р., Миллер Ф.Г. Спектр подвижностей односекундных легких аэроионов в природном воздухе // Уч. зап. Тарт. ун-та.- 1985.- Вып. 707.- С. 26-36.

3. Бернотас Т.П. и др. Система сбора и обработки данных в спектрометрии аэрозолей и аэроионов // Уч. зап. Тарт. ун-та. -1985.- Вып. 707.- С. 45-53.

4. Tammet, H. The aspiration method for the determination

of atmospheric-ion spectra.- Jerusalem, 1970.- 200 p.

5. Eichmeier, J., Braun, W. Beweglichkeitsspektrometrie atmosphärischer Ionen // Meteorol. Rdsch..- 1972.- Jg. 25.- S. 14-19.

6. Cabane, M., Milani, M.R. Study of the mobility of small ions in air // Res. Lett. Atmos. Elect.- 1983.- Vol. 3.- P. 55-59.

7. Yunker, E.A. The mobility spectrum of atmospheric ions // Terr. Magn. Atmos. Elect.- 1940.- Vol. 45.- P. 127-132.

8. Misaki, M., Ohtagaki, M., Kanazawa, I. Mobility spectrometry of the atmospheric ions in relation to atmospheric pollution // PAGEOPH.- 1972.- Vol. 100, N 8.- P. 133-145.

9. Thomson, B.A., Iribarne, J.V. Positive and negative ion mobility spectra of spray-produced ions // Electrical Processes in Atmospheres.- Darmstadt: Dr. Dietrich Steinkopff Verlag, 1977.- P. 18-23.

10. Хыррак У.Э. Статистические сводки результатов измерения ионов и аэрозолей на о. Вилсанди летом 1984 года // Уч. зап. Тарт. ун-та.- 1987.- Вып. 755.- С. 47-57.

11. Sherman, K.L. Atmospheric electricity at the College-Fairbanks Polar Year Station // Terr. Magn. Atmos. Elect.- 1937.- Vol. 42.- P. 371-390.

12. Banic, S.M., Diamond, G.L., Iribarne, J.V. Ion-induced gas-to-particle reactions // Proceedings in Atmospheric Electricity.- Hampton: A. Deepak Publishing, 1983.- P. 36-38.

13. Wilkening, M. Characteristics of atmospheric ions in contrasting environments // J. Geophys. Res.- 1985.- Vol. 90. - P. 5933-5935.

14. Hoppel, W.A. Ion-aerosol attachment coefficients, ion depletion, and the charge distribution on aerosols // J. Geophys. Res.- 1985.- Vol. 90.- P. 5917-5923.

15. Смеркалов Б.А. Аппроксимация среднего распределения аэрозольных частиц по размерам // Изв. АН СССР ФАО.- 1984.- Т. 20.- С. 7-321.

16. Петров Ю.И. Физика малых частиц.- М.: Наука, 1982.- 360 с.

Translated from:

Таммет Х.Ф., Ихер Х.Р., Сальм Я.Й. Спектр атмосферных ионов в диапазоне подвижности 0,32-3,2 $см^2/(В \cdot с)$ // Уч. зап. Тарт. ун-та.- 1987.- Вып. 755.- С. 29-46.

THE DEPENDENCE OF SMALL AIR ION MOBILITY SPECTRA IN THE GROUND LAYER OF THE ATMOSPHERE ON TEMPERATURE AND PRESSURE

J. Salm, H. Tammet, H. Iher and U. Hõrrak

First, we will consider the theoretical side of the problem of dependence of mobility on temperature and pressure. In the formula of ion mobility in the first approximation of the Chapman-Enskog theory which in our conditions is sufficiently exact, the inverse proportionality of mobility and gas density is clearly expressed [1]. This relation is easy to prove if the gas is sufficiently rarefied, so that the processes of transport are determined only by paired collisions of particles, and the strength of the electric field is sufficiently weak. Therefore it is generally accepted to reduce the mobility to standard conditions with the equation

$$k = k' \frac{p}{101325} \frac{273.15}{T} , \qquad (1)$$

where k' is the natural mobility,
p is the pressure in Pa ,
T is the absolute temperature in K.

In addition to that, mobility depends on temperature also at constant gas density. This dependence is determined by the character of the interaction of ions and neutral particles. Unfortunately, for our conditions the character of this interaction is not sufficiently investigated. Indirectly it can be estimated that for ions of stable structure the dependence of the reduced mobility on temperature can be characterized by a power with the absolute value below 1/2. The experimental data show that this dependence is considerably weaker. Proceeding from the data in the range 300-500 K, we obtain the relative change of the reduced mobility which does not exceed ±2% for 10% change of the absolute temperature [1,2].

We have carried out a systematic recording of the mobility spectra of small air ions (together with the small fraction of intermediate ions) in natural air [3]. Temperature, pressure, and relative humidity of the air were recorded at the same observation point. Below we will analyze the dependence

of the mobility spectrum of small air ions on temperature and pressure during a one-year observation period (10.06.1985 - 02.06.1986), and the dependence of the same on humidity during a three-month period (10.06.1985 - 15.09.1985).

Fig. 1 presents average spectra for different temperature ranges. The spectra have been created by plotting the fraction concentrations on a graph and connecting the respective points with a smooth curve. As spectral change at temperatures below -4°C is relatively weaker, we present an average spectrum for these temperatures, above these temperatures the intervals are 6°C.

As can be seen in Fig. 1 the rise of temperature is generally accompanied by the increase in the concentration of small air ions, whereas the mobility decreases. The form of the spectrum of negative air ions undergoes considerable changes. To clarify these conclusions Fig. 2 graphically presents the dependencies of the concentrations of n_- and n_+, average mobilities of small ions $\bar{k}_-$ and $\bar{k}_+$ and also the relative widths of the respective spectra s_- and s_+ on temperature. At first concentrations increase together with temperature and then, achieving a maximum at about 10-12°C, they start to decrease. The average mobilities are initially almost stable, later they start to decrease with temperature. The respective estimates of the coefficients of linear correlation are $r_{\bar{k}_- t} = -51\%$, $r_{\bar{k}_+ t} = -46\%$. According to Fig. 2 the average mobility of air ions decreases about 14% for the growth of temperature by 10%. This can be explained only by the rise of air ion clusters in proportion with the growth of temperature. The relative width of the spectrum of negative ions grows about 10% for the rise of temperature by 10%, in the case of positive ions it is almost stable.

The statistic correlation between the relative width of the spectrum and the average mobility is similarly asymmetrical ($r_{s_- \bar{k}_-} = -70\%$), in the case of positive ions there is no correlation ($r_{s_+ \bar{k}_+} = -4\%$).

A partial justification for reducing the mobilities to normal conditions with formula (1) is the fact that the right sides of the spectra on Fig. 1 coincide rather well. A similar justification was found also on the basis of the measurement of spectra of one-second air ions in natural air [4].

A comparison of the present results with the preliminary results of a three-months period of the same observation

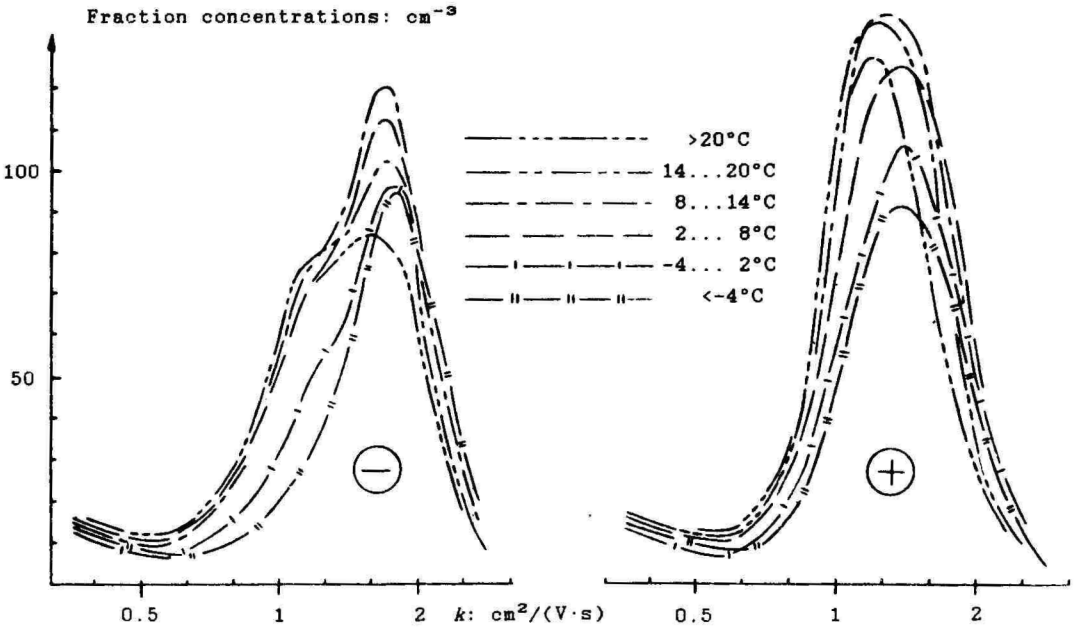

Fig. 1. Mobility spectra of air ions in different temperature ranges. Fraction boundaries are designated at the abscissa axis (10 fractions $k_{j+1}/k_j = \sqrt[3]{2}$).

series [3] shows that in summer in the temperature range of 0-30°C the reduced average mobility falls even more sharply with the growth of temperature, especially in the range of 0-15°C (see Fig. 2).

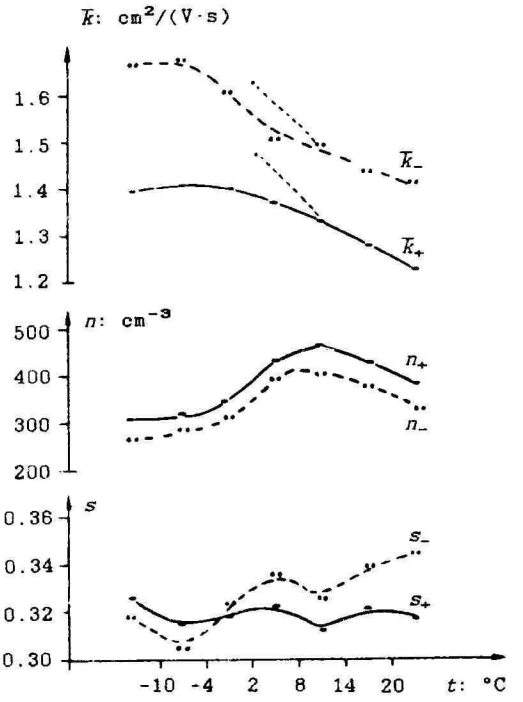

Fig. 2. The dependence of the parameters of air ion spectra on temperature. The dotted line designates the values of $\bar{k}$ in summer.

On the basis of the above material it can be concluded that air ion clusters grow in accordance with temperature. Growth accelerates when temperatures above 0°C are achieved, for negative air ions it happens sooner, for positive ions later. The reasons for this phenomenon have not yet been proposed. The role of air humidity seems negligible here. The coefficients of correlation with absolute humidity for average mobilities are $r_{\bar{k}_-A} = -18\%$ and $r_{\bar{k}_+A} = -11\%$. If to

eliminate the influence of temperature in linear regressions, the correlation coefficients will be positive $r_{\bar{k}\_A/t} = 0.15$, $r_{\bar{k}+A/t} = 0.25$. The coefficients of correlation for relative humidity are also positive ($r_{\bar{k}\_R} = 0.39$, $r_{\bar{k}+R} = 0.49$) which can easily be explained by the indirect influence of temperature.

It is likely that some kind of trace gases, the content of which in the air is correlated with temperature, may also play a role in cluster formation. Temperature, in its turn, is correlated with the intensity of solar radiation, and also with various biological processes and with the activity of man. These factors can hypothetically be viewed as supplementary in the change of the composition of the air. On the one hand, temperature is closely connected with the hours of the day, on the other hand, biological processes and human activity are also correlated with the hours of the day. It is known that the concentration of ozone and many other small components in the atmosphere have a strong daily variation which is correlated with temperature [5, 6].

During a one-year period temperature varied between 257.5 K and 296 K in 95% of the cases, i.e . ±7% in relation to the average. The variability of pressure is weaker: 985.5-1035.5 mbar, i.e. ±2.5%. The dependence of the mobility spectrum of small ions on pressure was studied with similar procedures as were applied in the case of temperature and it was found that the dependence was noticeably unmonotonous. Fig. 3 presents the dependence of the parameters of the spectra and averaged temperature on pressure.

The highest concentrations and the lowest average mobilities are located in the region of average values of pressure (about 1017 mbar). The concentration decreases and the average mobility increases almost symmetrically in accordance with the distance from the extreme. This dependence does not havw a direct physical explanation. However, during the considered one-year period there was a strong non-linear statistical dependence between pressure and temperature which can be a peculiarity of this particular period of observation. The average temperatures for the fixed pressure values are also presented in Fig. 3. It seems that the observed statistical dependence can be explained as a secondary effect due to a physical dependence of mobility on temperature and a statistical dependence of temperature on pressure.

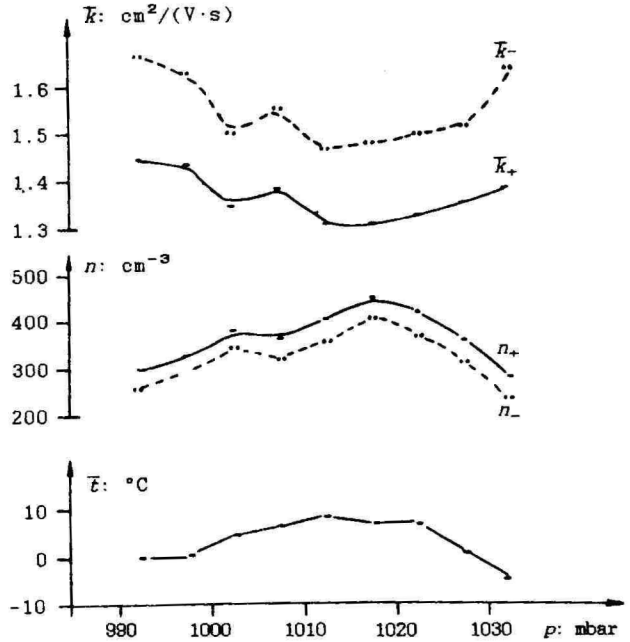

Fig. 3. The dependence of the parameters of the spectra and averaged temperature on pressure during the period of observations.

We can draw the following conclusions. The results of the observations coincide with the acknowledged statement that natural mobility of small air ions with stable structure is inversely proportional to the density of the air and the mobility reduced to normal conditions is independent of pressure and almost independent of the temperature of the air.

The spectrum of small air ions created on the basis of mobilities reduced to standard conditions is significantly dependent on the temperature of the air which can be explained by the dependence of the structure of air ions on temperature and on factors statistically dependent on temperature.

The average reduced mobility of small air ions decreases together with the rise of temperature which indicates the

growth of clusters together with temperature. The dependence of the concentration of small air ions on temperature is unmonotonous with a maximum at the temperature 10-12°C.

The dependence of average reduced mobility of air ions on temperature cannot be explained by the effect of air humidity. It can be assumed that the rise of temperature leads to the growth in the concentration of some kind of trace gases in the air, and this in its turn causes the formation of larger clusters.

The quantitative dependencies of the mobility spectra on temperature are significantly different for negative and positive ions.

References

1. McDaniel, E.W., Mason, E.A. The Mobility and Diffusion of Ions in Gases.- New York a.o.: John Wiley and Sons, 1973.

2. Ellis, H.W. et al. Transport properties of gaseous ions over a wide energy range. Part II // Atomic Data and Nuclear Data Tables.- 1978.- Vol. 22, N 3.- P. 179-217.

3. Таммет Х.Ф., Ихер Х.Р., Сальм Я.Й. Спектр атмосферных ионов в диапазоне подвижности 0,32-3,2 $см^2/(В·с)$ // Уч. зап. Тарт. ун-та.- 1987. - Вып. 755. - С. 29-46. (See this volume pp. 35-49).

4. Таммет Х.Ф., Ихер Х.П., Миллер Ф.Г. Спектр подвижностей односекундных легких аэроионов в природном воздухе // Уч. зап. Тарт. ун-та.- 1985.- Вып. 707.- С. 26-36.

5. Окабе Х. Фотохимия малых молекул.- М.: Мир, 1981.

6. Lopez, A., Lecouteux, G., Prieur, S., Fontan, J. Etude de la formation de particules à partir des hydrocarbures naturels dégagés par la végétation // J. Aerosol Sci.- 1983.- Vol. 14, N 2.- P. 99-111.

Translated from:

Сальм Я.Й., Таммет Х.Ф., Ихер Х.П., Хыррак У.Э. Зависимость спектра подвижности легких аэроионов в приземном слое атмосферы от температуры и давления воздуха // Уч. зап. Тарт. ун-та.- 1988.- Вып. 804.- С. 87-94.

ATMOSPHERIC ELECTRICITY AT THE PROSPECTIVE BOROVOYE BACKGROUND MONITORING STATION

M. Arold and R. Matisen

In the framework of the international program of environment pollution studies "Monitoring", a worldwide system of background stations is created. The concentration of pollutants at these stations should not depend on local sources, but rather reflect their global concentration, i.e. the background.

The authors of this paper have participated in pilot studies of atmospheric electricity at a background station.

The location of the background station is the conservation and hunting area at Borovoye, Kokchetavsky region, Kasakhstan. The height of the location of the station is about 300 m above the sea level.

Atmospheric electricity measurements were conducted with three air ion counters *UT-7502*. One device was used to measure the air ion spectrum, the two others were used for uninterrupted 24-hour measurements of the polar conductivity $\lambda_{\pm}$ (at the limiting mobility $k_0 = \pm 2.0$ cm^2/(V·s). The results were registered with automatic recorders.

The potential gradient of the electric field of the atmosphere dv/dh was measured with *S50* static voltmeter provided with a radioactive collector.

The measurement period was 16-31 August 1976.

As Borovoye is situated in a weakly polluted region of the subcontinent of Eurasia, a high conductivity of the air could be expected. This expectation was confirmed (see Table 1). As can be seen in the Table 1, the total electric conductivity of the air exceeds the mean for the Earth approximately 4 times. Accordingly, the potential gradient was found to be very low. It should be kept in mind that the mean value of dv/dh is taken to be 130 V/m. The content of Table 1 is obtained by the statistical processing of hourly means of the measurement results corresponding to fair weather.

The discovered positive correlation between small (n_+ + n_-) and large (N_+ + N_-) air ions is of special interest. The limiting mobility was 0.5 cm^2/(V·s) for the small ions, and 0.001 cm^2/(V·s) for the large ions. The correlation coefficient between these concentrations was +42%. The critical

Table 1

Local time	Positive mobility			Negative mobility			Mean value of the potential gradient
	No.of measurements	mean fS/m	standard deviation	No.of measurements	mean fS/m	standard deviation	V/m
0-1	4	89	7	5	78	8	42
1-2	5	88	5	5	79	2	-
2-3	5	91	5	5	79	3	23
3-4	4	92	7	5	83	8	21
4-5	3	89	2	5	80	6	-
5-6	3	83	1	5	77	8	-
6-7	4	82	6	4	81	11	15
7-8	6	81	21	5	68	16	-
8-9	8	58	19	6	52	21	-
9-10	8	31	5	7	27	7	64
10-11	8	25	4	7	21	3	48
11-12	7	23	4	7	20	3	58
12-13	6	23	4	6	20	3	-
13-14	7	23	5	7	21	5	69
14-15	7	23	5	7	21	4	68
15-16	7	22	5	7	21	4	68
16-17	7	23	4	7	22	5	60
17-18	8	25	4	8	23	4	58
18-19	6	27	3	8	27	5	57
19-20	7	43	11	7	40	8	41
20-21	4	62	11	4	50	13	36
21-22	7	72	14	8	60	12	-
22-23	7	75	11	7	68	13	24
23-24	7	83	13	7	73	10	22
Total:	145	51	29	149	46	26	46

value of the correlation coefficient for checking the hypothesis of independence against the bilateral alternative is 29% on a 95% level of reliability [1]. The other computed values included the correlation coefficients of the concentrations of air ions with the air pressure, with the relative humidity

of the air, with the temperature, with the solar irradiation (units were 0 or 1) and with the potential gradient; also all mutual correlation coefficients between all the above parameters. On the basis of these data the correlation of (n_++ + n_-) and (N_++ N_-) was found, whereas the influence of other listed meteorological parameters is excluded. In this case the correlation between small and large ions was low as expected. Consequently, these parameters are not connected causally, but are both dependent on the meteorological parameters. A possible explanation of the discovered phenomenon can be a hypothesis of positive correlation between the intensity of ion formation and the aerosol content of the air.

Let us try to explain this hypothesis. In the daytime convection mixes the lower layers of the air which have higher conductivities with the higher layers of lower conductivities. Assuming that in the nighttime the preterrestrial layer has an inverted or similar height distribution of the temperature, then the convection is either absent or negligible. Due to this (according to the known mechanism [2]) both, the electrical conductivity of the preterrestrial air and aerosol concentration in it, increase. This is completely understandable, but in all locations the authors have studied except Borovoye, the ion absorption by atmospheric particles dominates over the growth of conductivity.

Thus, from the point of view of atmospheric electricity, Borovoye is an exceptional place, and as any exception, is to be carefully studied on the basis of a special program.

References

1. Tammet, H. Statistikameetodid arvuti *NAIRII-2* kasutajale.- Tallinn: Valgus, 1976.

2. Тверской П.Н. Атмосферное электричество.- Л.- 1949.

Translated from:

Арольд М.У., Матизен Р.Л. Об атмосферном электричестве на планируемой фоновой станции Боровое // Уч. зап. Тарт. ун-та.- 1977.- Вып. 443.- С. 44-47.

AIR ION COUNTERS AND SPECTROMETERS DESIGNED IN TARTU UNIVERSITY

R. Matisen, F. Miller, H. Tammet and J. Salm

Counters

Air ion counters are used for measuring the concentrations of air ions in atmospheric physics research as well as for various applications of air electricity in medicine, industry etc. Air Electricity Laboratory of Tartu University has a long experience in the design and use of various air ion counters. The paper presents a short survey of the design of the counters.

The first counter designed and built in Tartu University was a stationary integral counter with a mechanical electrometer for the measurement of small and large air ions. The counter was built in university workshops by engineer A. Susi under the supervision of J. Reinet in 1950 [1]. In the end of the 1950s this counter was substantially developed by O. Saks who applied a vibrating reed electrometer for the measurement of low currents [2]. In the 1950s and at the beginning of the 1960s several portable integral air ion counters with a mechanical electrometer (model *SG-2M*) were designed [3].

In 1963 J. Salm designed the first portable integral counter with a vibrating reed electrometer [4]. Theoretical research connected with the design of air ion counters was started in 1956 by H.Tammet [5]. Development of portable air ion counters of the series *SAI-TGU* was started under his supervision in 1964 [5,6,7]. Universality and high sensitivity of these counters were achieved by the use of a vibrating reed electrometer. The counters were equipped with a measuring capacitor which took into account and minimized such distorting factors as turbulence, edge effect, and ion adsorption in the inlet device. The counters *SAI-TGU-66* were produced for about fifty research institutions in the Soviet Union and Eastern Europe.

In 1960-1980 research in air ion applications was highly active. This motivated the design of new air ion counters, whereas the increase of reliability was considered as the main aim of improvements. Several counters were designed according to special requirements. The examples are the counter *UT-7001* with a small-size probe-like measuring capacitor and

a low-inertia counter *UT-7004* with a measuring capacitor working at high pressures (up to 5 atm.)

With the air ion counter *UT-6914* an attempt was made to create a highly reliable device suitable for industrial production. In this counter, and later in *UT-7406*, ventilation of the inner volume with dried air while maintaining a low superpressure in the inside of the case was used [8]. An attempt was made to improve the electrometric commutator of the measurement ranges. In the counter *UT-6914* a needle switch was used, however, its design turned out to be unreliable. In the later developments *UT-7406* and *UT-7714* commercially manufactured magnetically controlled "hercon" contacts were used. They were abandoned due to the poor insulation properties of the glass shell, as even insignificant contamination brought about a large bias current.

Up to 1977 the laboratory-made dynamic capacitors [10] were used in all counters. The commercially made dynamic capacitor *DRK-3* was introduced only in the last counter of Tartu University *UT-7714* designed with the vibrating reed electrometer. The other improvements of this counter were a digital display and output to an automatic data acquisition system.

After 1977 solid state electrometric amplifiers were used in all new counters. This was facilitated by the appearance of new MOS-transistors with low bias currents. Due to the introduction of MOS-electrometers the design of counters was significantly simplified. In the case of selected MOS-transistors *KP-305* the guaranteed bias current is about 10^{-15} A. A necessary stability of zero level is ensured by thermo--compensatory elements of the circuit and by the use of the transistor near the thermo-stable point [11]. The first counters with MOS-electrometers were *UT-7905* and *UT-8217*.

The next model in the family of Tartu University air ion counters is *UT-8401*, designed to meet high technical requirements including maximum reliability, easy operability, minimum size and weight. The inner volume of the device is ventilated with dried air, a superpressure of 10-20 mm water column is maintained in it. The insulator of the measuring capacitor is protected by ventilation with dried air. Improvements are made in the commutation of measurement range and in switching on/off of the operation mode. A built-in flow-chart recorder or a pointer instrument is available as

indicator.

The main parameters of *UT-8401* are as follows.

1. The limiting mobility from $3.2 \cdot 10^{-4}$ to 2 $cm^2/(V \cdot s)$.
2. The range of concentration from 10^2 to $6.4 \cdot 10^6$ e/cm^3.
3. The size of the counter 250 x 335 x 525 mm.
4. The weight depending on the type of built-in recorder is 12-16 kg.
5. The power consumption is below 50 W.

The counter *UT-8401* was produced for over a hundred institutions in the Soviet Union.

All the above counters are designed to measure both small and large air ions. If to give up the measurement of large air ions, the design of the counter will be essentially simpler. Such counters will be described below. They are designed to indicate small air ion concentration and/or electrical conductivity of air, because the technical requirements at the measurement of small air ion concentration and air conductivity are identical.

Building and testing of an aspirational air conductivity measurement device with a modulating measuring capacitor was completed in 1980 [12]. Such a measuring capacitor is especially reliable in field conditions as its main insulator is not sensitive to humidity and contamination. Requirements set to the electrometric amplifier are relatively lax and there is no need for zero adjustment. One conductivity meter on such a principle was built in 1984 by the order of the Institute of Experimental Meteorology of the Soviet Committee of Hydrometeorology and for a long time it has been used for field measurements.

About 1980 a reliable conductivity meter making it possible to estimate also the concentrations of small air ions was built for a workshop of physics students [13].

F. Miller introduced an original measuring capacitor with an inner collector electrode and an electrometer inside the electrode [14]. The whole system requires only one high-ohmic insulator which can be optimized from the electrometric point of view and is sufficiently protected from pollution. The device consists of separate measurement and ventilation blocks. The measurement block consists of two measuring capacitors and a power source. The device makes possible simultaneous measurement of positive and negative conductivity. The size is 180 x 150 x 340 (measurement block) and 150 x 180 x 200 mm

(ventilation block). The total weight is less than 9 kg.

A small-size air ion meter for the measurement of air conductivity *UT-8510* was designed by H. Tammet [15]. The device is meant for conductivity measurements in the range 1-1000 fS/m and has an original construction of the sensor with a plane collector electrode. Automatic zero correction is used for the suppression of measurement errors. The air ion meter has a modular construction and consists of three blocks: sensor, fan, and controller. The modular principle makes it possible to use different sets of equipment, whereas the universal air ion sensor is not modified. The size of the sensor is 160 x 100 x 23 mm, weight 0.27 kg.

The latest development is a small air ion meter *UT-9007* with a digital display and remote control. The limiting mobility of the device is 0.5 $cm^2/(V \cdot s)$. The measuring capacitor and the electrometer of the air ion meter are similar to the construction described in [12]. The limits of the measurement of air ion concentrations are from 10 to $2 \cdot 10^5$ e/cm^3.

Spectrometers

In general air ion spectrometers are similar to air ion counters but they are specially adapted for getting more detailed information about the mobility spectrum of air ions. Therefore, as a rule, they also have a more complicated structure than the counters. All the ion spectrometers use a static or quasistatic electric field as a basic factor for air ion classification. They can be divided into two large groups: spectrometers with motionless (still) air called drift tubes [16] and spectrometers with flowing air (aspiration spectrometers) [5]. The choice of a drift tube is reasonable when:

- the volume of air under investigation is limited,
- there are only small ions to be measured,
- the concentration of air ions is sufficiently high.

The choice of an aspiration spectrometer, in its turn, is reasonable when the volume of air is not limited. Aspiration spectrometers can be used in the case of low air ion concentration and there are no limitations with regard to the region of mobilities.

Air Electricity Laboratory of Tartu University has a long experience in the study, design, and use of aspiration spectrometers. The basic principles of mobility spectrometry

have been published in the monograph [5]. Later the principle of multichannel spectrometry has been elaborated, the problems of resolution have been specified, the automation of operation and digital data processing have been introduced.

The first multichannel automatic air ion spectrometer (model *UT-7205*) was built in 1972 [17]. This spectrometer was designed on a parallel principle: all the spectral intervals in a wide mobility range were measured simultaneously. The spectrometer has two independent measuring capacitors, the outer cover of either is divided into 25 well insulated measuring electrodes. Adjusting properly the regime of operation, it is possible to measure the mobility spectrum simultaneously as maximum in 50 intervals which can cover up to three orders of magnitude of mobility. Using various regimes it is possible to expand the range from 0.0001 to 3.2 $cm^2/(V \cdot s)$. The spectrometer has a built-in automatic control unit: one has to choose the desirable regime on the keyboard and to push the starter button. After the selected measurement period the device puts out the measurement data on a punched tape, ready to be fed into a computer.

The shortcomings of the described spectrometer were mainly of technological origin and resulted often in technical failures of the instrument.

The further development of that same spectrometer was influenced by the problem of electrical analysis of aerosols. A special charging chamber for aerosols was joined with the intake of the spectrometer [18]. This chamber enabled to give definite charges to aerosol particles by means of an unipolar corona discharge. The mobility spectrum of the particles charged in this way was measured by means of the above spectrometer and after that the size spectrum of aerosol particles was calculated on the ground of the mobility spectrum. Further development of this principle resulted in the design of a special multichannel electrical aerosol spectrometer [19]. Aerosol spectrometry was established as a separate field of research in laboratory and it is not considered in the present paper.

The further development of air ion mobility spectrometers continued with the design of the multichannel spectrometer *UT-7914*. The control unit of this spectrometer was designed in a modern engineering level. The basic technical characteristics of the spectrometer *UT-7914* are as follows:

- mobility range 0.00048-0.48 $cm^2/(V \cdot s)$ is logarithmically divided into 9 main intervals and a supplementary interval 0.48-∞ $cm^2/(V \cdot s)$ provided for small ions;
- the spectrometer has two measuring capacitors each of them with 5 measuring electrodes; one capacitor is fitted for measurement of more mobile and the other for measurement of less mobile air ions;
- each measuring electrode is connected with an individual small-sized MOS-electrometer [11]. Such an electrometer in the structure of the spectrometer guarantees the measurement of concentrations of air ions beginning from about 10 cm^{-3} in intermediate ions mobility intervals and from 50 cm^{-3} in large ions mobility intervals.

The design of the spectrometer *UT-7914* was accomplished in 1987. Special preliminary capacitors for the realization of second-order apparatus differentiation have been installed on the intakes of the measuring capacitors [21]. In 1988 the spectrometer has been put into a continuous exploitation in the Air Ion Observatory Tahkuse.

An interest in the detailed study of the mobility spectrum of small air ions in natural conditions occasioned the design and building of a six-channel air ion spectrometer (model *UT-8415*) [22]. The measuring capacitor has a divided air flow and six outer measuring electrodes. By switching the voltage it is possible to measure mobility spectra in 10 logarithmically distributed mobility intervals in the range 0.32-3.16 $cm^2/(V \cdot s)$. The measurement of the mobility spectra at both polarities in this range takes as minimum a period of 5 min.

A particular class of spectrometers is represented by scanning-voltage one-channel air ion spectrometers, which are provided for investigations of the effect of chemical microadmixtures on mobility spectrum. The first spectrometer of this class (model *UT-7509*) was built in 1975 [23]. This spectrometer is equipped with a corona point for unipolar ionization of the air under investigation. The air flow passes the corona point, runs through a coaxial electrofilter and enters the measuring capacitor, which has one narrow (outer) measuring electrode. By scanning the voltage the mobility range 0.6-2.4 $cm^2/(V \cdot s)$ is run through in 75 s.

The next spectrometer of this class (model *UT-7801*) was finished in 1978. This spectrometer is similar to the above model *UT-7509*, but an extra effort has been made to raise the

spectral resolution [24,25]. The invention [26] was used to avoid the errors due to the incomplete sedimentation of air ions in the entrance filter.

References

1. Рейнет Я.Ю. Комбинированный счетчик атмосферных ионов // Труды ГГО им. И.А. Воейкова.- Л., 1956.- Вып. 58.- С. 23--30.

2. Прюллер П.К., Сакс О.В. Счетчик атмосферных ионов с автоматическим фоторегистратором // Уч. зап. Тарт. ун-та.- 1970.- Вып. 240.- С. 32-60.

3. Рейнет Я.Ю., Сальм Я.Й. Переносный счетчик атмосферных ионов // Уч. зап. Тарт. ун-та.- 1963.- Вып. 140.- С. 37-45.

4. Reinet, J., Tammet, H., Salm J. On the methods of counting air ions // Biometeorology.- 1967.- Vol. 2.- P.1037--1046.

5. Tammet, H. The aspiration method for the determination of atmospheric-ion spectra.- Jerusalem: Israel Program for Scientific Translations, 1970.- 200 p.

6. Tammet, H., Salm, J., Tamm, E. Measurement of air ions and aerosols // Bioclimatology, Biometeorology and Aeroionotherapy.- Milan: Carlo Erba Foundation Publ., 1968.- P. 54--56.

7. Таммет Х.Ф. Счетчик аэроионов *САИ-ТГУ-66* // Уч. зап. Тарт. ун-та 1970.- Вып. 240.- С. 157-163.

8. Матизен Р.Л., Ютс Э.Ю. Счетчики аэроионов *UT-6914* и *UT-7406* // Уч. зап. Тарт. ун-та.- 1975.- Вып. 348.- С. 24-29.

9. Матизен Р.Л., Ээвель Я.Р., Ютс Э.Ю., Якобсон А.Ф. Счетчик аэроионов с цифровой индикацией *UT-7714* // Уч. зап. Тарт. ун-та.- 1977.- Вып. 443.- С. 52-56.

10. Сакс О.В., Мадисе Т.В. Динамический конденцатор *ДК--64Т* // Уч. зап. Тарт. ун-та.- 1969.- Вып. 239.- С. 106-121.

11. Миллер Ф.Г. К разработке электрометров прямого усиления для многоканальных спектрометров аэроионов // Уч. зап. Тарт. ун-та.- 1981.- Вып. 588.- С. 124-132.

12. Леппик К.П., Таммет Х.Ф., Миллер Ф.Г., Сальм Я.Й. Полевой измеритель проводимости воздуха с модулирующим измерительным конденсатором // Уч. зап. Тарт. ун-та.- 1980.- Вып. 534.- С. 80-83.

13. Сальм Я.Й. Лабораторная работа "Измерение проводимости воздуха" в общем физическом практикуме // Методика преподава-

ния физики в вузе.- Тарту: Тарт. ун-т, 1983.- С. 51-53.

14. Миллер Ф.Г., Ээвель Я.Р. Новая конструкция измерительного конденсатора в измерителе электропроводности воздуха // Уч. зап. Тарт. ун-та.- 1984.- Вып. 669.- С. 69-71.

15. Таммет Х.Ф., Миллер Ф.Г., Матизен Р.Л., Ээвель Я.Р. Малогабаритный аэроионометр высокой предельной подвижности // Уч. зап. Тарт. ун-та.- 1988.- Вып. 809.- С. 95-102.

16. Mason, E.A., Mc Daniel, E.W. Transport Properties of Ions in Gases.- New York a.o.: John Wiley & Sons, 1988.

17. Таммет Х.Ф., Якобсон А.Ф., Сальм Я.Й. Многоканальный автоматический спектрометр аэроионов // Уч. зап. Тарт. ун-та.- 1973.- Вып. 330.- С. 48-75.

18. Мирме А.А., Сальм Я.Й., Тамм Э.И., Таммет Х.Ф. Гранулометр субмикронного аэрозоля // Методы и приборы контроля параметров окружающей среды. Межвуз. сб.- Л., 1979.- Вып. 1(136).- С. 64-67.

19. Mirme, A., Noppel, M., Peil, I., Salm, J., Tamm, E., Tammet, H. Multichannel electric aerosol spectrometer // Eleventh Int. Conf. on Atmospheric Aerosols, Condensation and Ice Nuclei.- Budapest, 1984.- Vol. 2.- P. 155-159.

20. Сальм Я.Й. Десятиканальный спектрометр аэроионов // Методы и приборы биоинформации и контроля параметров окружающей среды. Межвуз. сб.- Л., 1981.- Вып. 150.- С. 34-38.

21. Hõrrak, U., Miller, F., Mirme, A., Salm, J., Tammet,H. Air Ion Observatory at Tahkuse: instrumentation // Acta et comm. Univ. Tartuensis.- 1980.- Nr. 880.- P. 33-43.

22. Таммет Х.Ф., Миллер Ф.Г., Тамм Э.И., Бернотас Т.П., Мирме А.А., Сальм Я.Й. Аппаратура и методика спектрометрии подвижностей легких аэроионов // Уч. зап. Тарт. ун-та.- 1987.- Вып. 755.- С. 18-28.

23. Таммет Х.Ф., Хилпус А.О., Сальм Я.Й., Ютс Э.Ю. Спектрометр аэроионов для обнаружения некоторых примесей воздуха // Уч. зап. Тарт. ун-та.- 1977.- Вып. 409.- С. 84-88.

24. Сальм Я.Й. О повышении разрешающей способности спектрометра легких аэроионов // Уч. зап. Тарт. ун-та.- 1979.- Вып. 479.- С. 10-14.

25. Ихер Х.Р., Сальм Я.Й. Зависимость спектра подвижности легких аэроионов от их возраста // Уч. зап. Тарт. ун-та.- 1981.- Вып. 588.- С. 33-39.

26. Сальм Я.Й. Устройство для определения спектра аэроионов. А.с. 938336 СССР, H01J39/36. Заявл. 14.11.80, опубл. 23.06.82. Бюл. Но. 23.

UNIPOLAR CHARGING OF INITIALLY CHARGED AEROSOLS

J. Salm

The general pattern of unipolar charging has received a fairly detailed treatment already in [1]. For initially neutral aerosols the equations of kinetics are written as (with minor alterations in symbols):

$$\frac{dN_0}{dt} = - I_0 N_0 ,$$

$$\frac{dN_1}{dt} = I_0 N_0 - I_1 N_1 ,$$

$$\frac{dN_2}{dt} = I_1 N_1 - I_2 N_2 ,$$

$$\cdots\cdots\cdots\cdots\cdots$$

$$\frac{dN_q}{dt} = I_{q-1} N_{q-1} - I_q N_q ,$$

where N_q is the partial concentration of aerosol particles of a given radius and charge number q,

t is time,

I_q is air ion flux for a particle of a given charge number.

The initial conditions for charging of initially uncharged aerosol are:

$$N_0(t = 0) = a_0 ,$$
$$N_q(t = 0) = 0 , \quad q \geq 1 .$$

This system of differential equations is also known as the equations of generation. They can also be used for the description of radioactive transformations of elements [2].

The solution of the system is written as:

$$N_q(t) = a_0 \left(\prod_{k=0}^{q-1} I_k \right) \sum_{L=0}^{q} \frac{\exp(-I_L t)}{\prod_{m=0}^{q}{}^{*} (I_m - I_L)} ,$$

where 1) Π^* is product with one exception: in the case of equality of indexes the respective factor is always equal to unity;

2) in the case $q = 0$ the product

$$\prod_{k=0}^{q-1} I_k = 1.$$

Thus

$$N_0(t) = a_0 \exp(-I_0 t) ,$$

$$N_1(t) = a_0 I_0 \frac{\exp(-I_0 t)}{I_1 - I_0} + \frac{\exp(-I_1 t)}{I_0 - I_1} ,$$

$$N_2(t) = a_0 I_0 I_1 \frac{\exp(-I_0 t)}{(I_1-I_0)(I_2-I_0)} + \frac{\exp(-I_1 t)}{(I_0-I_1)(I_2-I_1)} + \frac{\exp(-I_2 t)}{(I_0-I_2)(I_1-I_2)} ,$$

.....

Actually atmospheric aerosol is never completely neutral, therefore it is better to allow for an initial charge distribution of partial concentrations. Let us suppose that in the initial moment we have both negatively and positively charged aerosol particles with the concentrations a_q , where q is the charge number.

In normal atmospheric conditions the charge distribution is probably close to the stationary distribution, i.e. a_q differs from zero in a certain interval $q_{min} \le q \le q_{max}$ symmetrically in relation to the point $q = 0$. For instance, in the case of the smallest particles only the initial concentrations a_{-1}, a_0, a_1 are taken into account. With the growth of the radius a_{-2}, a_2, etc. appear. In any case, there is some minimum charge number q_{min}, below which $a_q = 0$.

In such a case the system of equations of charge kinetics looks like as follows:

$$\frac{dN_{qmin}}{dt} = - I_{qmin} N_{qmin} ,$$

$$\frac{dN_{qmin+1}}{dt} = I_{qmin} N_{qmin} - I_{qmin+1} N_{qmin+1} ,$$

.

$$\frac{dN_{qmin+2}}{dt} = I_{qmin+1}N_{qmin+1} - I_{qmin+2}N_{qmin+2} ,$$

$$\cdots\cdots\cdots ,$$

$$\frac{dN_q}{dt} = I_{q-1}N_{q-1} - I_qN_q$$

with the initial conditions:

$$N_q(t = 0) = a_q , \qquad q_{min} \leq q \leq q_{max} ;$$
$$N_q(t = 0) = 0 , \qquad q_{min} > q > q_{max} .$$

This system of equations consists of linear differential equations in relation to time. The solution of the first equation can be found when the initial conditions are specified, and it is possible to try to write the solution in a general shape for an arbitrary equation:

1) $q = q_{min}$

$$N_{qmin} = a_{qmin}\exp(-I_{qmin}t).$$

2) $q = q_{min} + 1$

$$N_{qmin+1} = a_{qmin+1}\exp(-I_{qmin+1}t) + a_{qmin}I_{qmin}\sum_{L=q_{min}}^{q_{min}+1}\frac{\exp(-I_Lt)}{\prod_{m=q_{min}}^{q_{min}+1}{}^{*}(I_m-I_L)}.$$

3) $q = q_{min} + 2$

$$N_{qmin+2} = a_{qmin+2}\exp(-I_{qmin+2}t) + a_{qmin+1}I_{qmin+1}\sum_{L=q_{min}+1}^{q_{min}+2}\frac{\exp(-I_Lt)}{\prod_{m=q_{min}+1}^{q_{min}+2}{}^{*}(I_m-I_L)} +$$

$$+ a_{qmin}I_{qmin}I_{qmin+1}\sum_{L=q_{min}}^{q_{min}+2}\frac{\exp(-I_Lt)}{\prod_{m=q_{min}}^{q_{min}+2}{}^{*}(I_m-I_L)} .$$

Using mathematical induction the solution can be written for an arbitrary partial concentration

$$N_q(t) = \sum_{j=q_{min}}^{q} a_j\left(\prod_{k=j}^{q-1}I_k\right)\sum_{L=j}^{q}\frac{\exp(-I_Lt)}{\prod_{m=j}^{q}{}^{*}(I_m-I_L)} .$$

Analogously to what was presented above: 1) Π^* denotes the

product in which the factor with equal indexes is equal to unity,

2) the product $\prod_{k=j}^{q-1} I_k = 1$, if $q = q_{min}$.

Thus, proceeding from the initial distribution a_j and the air ion fluxes I_L, it is possible to find the distribution of partial concentrations at any arbitrary moment of time $N_q(t)$. To be more precise, an explicit two-dimensional distribution by charges and radii $N_{q,r}(t)$ is obtained proceeding from the initial distribution $a_{j,r}$ and the fluxes $I_{L,r}$. The radius r enters all the expressions as a supplementary argument (parameter).

According to the above suppositions it is necessary for the calculation of charge distributions to know the air ion fluxes for particles of different charges and radii.

References

1. Boisdron, M., Brock, J.R. On the stochastic nature of the acquisition of electric charge and radioactivity by aerosol particles // Atmos. Envir.- 1970.- V. 4.- P. 35-50.

2. Гольданский В.И., Куценко А.В., Подгорецкий М.И. Статистика отсчетов при регистрации ядерных частиц.- М., 1959.

Translated from:

Сальм Я.Й. Об униполярной зарядке первоначально заряженного аэрозоля // Уч.зап. Тарт. ун-та. - 1977. - Вып. 443. - С. 57-61.

GENERATION OF A NARROW BIPOLAR CHARGE DISTRIBUTION ON AEROSOL PARTICLES

I. Peil, E. Tamm and P. Zubchenko

Electrical classification. Requirements to input aerosol.

Monodisperse aerosols are necessary for the calibration of aerosol measurement devices as well as for experimental investigation of physical processes in aerosols. Currently, the method of electric separation is used for the generation of such aerosols, especially in the submicron range [1,2,9,10]. A narrow fraction is separated from particles which carry one elementary charge e (positive or negative). Multiply charged particles which are carried to the outlet of the separator widen the size spectrum of the separated aerosols. To estimate the suitability for electric separation of a particle charge distribution it is expedient to use two quality criteria.

$$\zeta = \frac{n_1}{\sum_{j=2}^{\infty} n_j} , \qquad (1)$$

$$\zeta_0 = n_1/N . \qquad (2)$$

Here n_j denotes the numeric concentrations of the particles carrying j elementary charges of one polarity, N - the total numeric concentration of particles. The growth of ζ is accompanied by a decrease of the risk of widening of the output aerosol spectrum on the account of multiply charged "alien" particles; the growth of ζ_0 leads to an increase of the concentration of the output aerosol. The criterion ζ is a reciprocal of an analogous criterion ξ proposed for the estimation of the quality of separated aerosol in [1].

For electrical separation usually aerosols with a stationary charge distribution are used, such a distribution occurs when the value of the charging parameter [3]

$$a_{(\pm)} = \frac{1}{\varepsilon_0} \int_0^{t_a} \lambda_{(\pm)}(t)\, dt \qquad (3)$$

is sufficiently large for the ions of both polarities. Here $\lambda_{(\pm)}$ is the polar conductivity of the air, t_a - the time the aerosol is in a bipolar ionic atmosphere, ε_0 - the electric constant. The stationary distribution arises independently of the initial state of the aerosol; for particles which are not very small (radius $r \geqslant 0.2$ μm) the stationary probability distribution is similar to the Boltzmann distribution [1].

The stationary distribution is rather wide and thus the values of the criteria ζ and ζ_0 are relatively small and decreasing with the increase of particle size. In an initially uncharged or weakly charged aerosol it is possible to obtain a narrower particle charge distribution. For this purpose it is necessary to guarantee small values of the parameters $a_+ \approx a_-$ in the charging device.This is possible in a charger with an ionizer which can be switched off. At some initial moment in such a charger an initial concentration ν_0 of ions of both signs is created. This concentration will then fade due to the recombination of ions of both signs with one another and with aerosol particles. After the consumption of all ions the elementary processes of charge exchange cease and the resulting charge distribution of aerosol particles will be maintained. We will call this distribution the output distribution of the charger.

Theory of the charging process

Following Fuchs [4] we will designate with p_j the probability that a particle which carries j elementary charges, catches one ion of the same sign in a unit of time at the unit concentration of these ions; q_j will be used to designate the probability of such a particle catching an ion of the opposite sign under the same conditions. Then, assuming that $p_j = p_{-j}$, $q_j = q_{-j}$ and that the initial concentrations of the ions of both signs are equal $\nu_0^+ = \nu_0^- = \nu_0$ which ensures the symmetry of the charge distribution of particles at any one moment, the process of particle charging can be described by the system (4) of kinetic equations. In this system n_j denotes the concentration of the particles carrying j elementary charges (according to the above assumption $n_j = n_{-j}$), α is the coefficient of mutual recombination of ions, and g is the aerosol electric density [5]. Theoretically $m \to \infty$, at practical solving of the system it is necessary to choose a sufficiently large value.

$$\left.\begin{aligned}
\frac{dn_0}{dt} &= \nu(2n_1q_1 - 2n_0p_0),\\
\frac{dn_j}{dt} &= \nu(n_{j-1}p_{j-1} - n_jp_j - n_jq_j + n_{j+1}q_{j+1}),\\
&\qquad j = 1, 2, \ldots, m-1,\\
\frac{dn_m}{dt} &= \nu(n_{m-1}p_{m-1} - n_mp_m - n_mq_m),\\
\frac{d\nu}{dt} &= -\alpha\nu^2 - g\nu.
\end{aligned}\right\} \qquad (4)$$

The aerosol electric density takes into account all processes of ion loss due to their adsorption to particles; it can be calculated by the equation

$$g = \sum_{j=1}^{m} n_j(p_j + q_j). \qquad (5)$$

The system (4) was solved numerically on a computer using the method of Runge-Kutta for the particle radius $r = 0.6$ μm. The values p_j , q_j were calculated according to the theory of Fuchs [4], the values $\alpha = 1.6\cdot10^{-12}$ m^3/s and $m = 5$ were used. The solution shows that the output distribution of the charger is fully determined by the ratio ν_0/N ; if $\nu_0/N \geq 50$, then this distribution is practically stationary. Table 1 compiled on the basis of the results of solving (4) presents the dependencies of the criteria ξ and ξ_0 on the ratio ν_0/N. The difference of the obtained final distribution from the Boltzmann distribution can be explained by the low selected value of $m = 5$.

Table 1

Dependence of the calculated values of ξ and ξ_0 on the ratio ν_0/N

ν_0/N	1.0	2.0	3.0	3.3	6.7	10.0	20.0	67	200	Boltzm.
ξ	5.66	2.63	1.71	1.54	0.85	0.68	0.56	0.53	0.53	0.42
ξ_0	0.18	0.22	0.22	0.21	0.18	0.17	0.15	0.15	0.15	0.14

The solution makes it possible to estimate the time t of

the formation of the output distribution of the charger. At $\nu_0/N < 50$ when this distribution is far from stationary, the above time is practically independent of ν_0 but is decreasing in inverse proportion to N. E.g. assuming the equality $\nu_0 = N$, the dependence of t on N can well be approximated with the equation

$$t/s/ = \frac{10^{11}}{N/m^{-3}/} . \qquad (6)$$

The formation time of the stationary distribution in the case of $\nu_0/N \geq 50$ is independent of N and decreases approximately in inverse proportion to ν_0. $a \geq 1.4$ was found to be the condition of the formation of the stationary distribution by the charging parameter a.

Experimental testing of the charging theory

The idea of experimental testing of the above theory can be described as follows. A symmetric bipolar ionic atmosphere with an adjustable initial ion concentration ν_0 is created in an aerosol with maximally monodisperse neutral particles of a known concentration N. The aerosol is given a relaxation time sufficient for the decrease of ion concentration to the natural level, and the charge distribution of aerosol particles at the outlet of the charger is measured. A detailed block-diagram of the experimental set-up is presented in Fig. 1. DOP aerosol from the condensation generator AG arrives at the inlet of the mixer-relaxer M-R with the flow rate Φ_2 through the electric filter EF (for the removal of charged particles). Ions from the corona ionizer CI are flown out by a sonic jet of filtered air flowing around a needle before the nozzle (flow rate Φ_1). A high mixed voltage is applied to the needle point relative to the nozzle from sequentially switched on sources of AC and DC.

Bipolarily ionized air comes into the mixer through the tube T of adjustable length L (for the adjustment of the initial concentration of ions ν_0 at the inlet of the mixer). CI, T, and M-R together form the charger with an ionizer that can be switched off.

The aerosol particle concentration N at the inlet to the mixer was determined with a photoelectric counter PEC model AZ-5. Due to the low dynamic range of PEC it was necessary to dilute the aerosol, for this purpose electric dilutors ED1

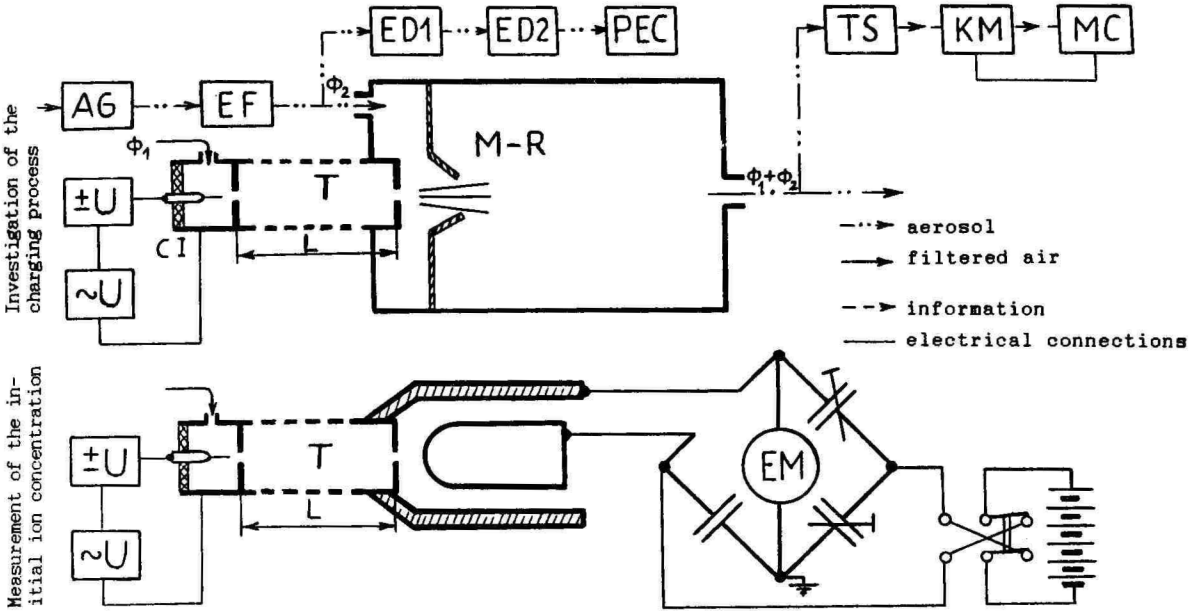

Fig. 1. Diagram of experimental set-up.

and ED2 [6] were used. Charge distributions of the particles were determined with a trajectory spectrometer TS [7]. Photos of the particle tracks were processed with a semi-automatic coordinate measurement device KM [8] operated on-line with an microcomputer MC (model *Elektronika D3-28*).

The device depicted in Fig. 1 (below) was used to determine the initial ion concentration ν_0 in dependence on the length L of the tube T where ion concentrations fall because of their mutual recombination. Bipolarily charged air from the tube T enters the measuring capacitor, in the electric field of the capacitor ions are separated according to their sign and precipitated to the covers. The polarity of the capacitor voltage is commutated and the electrometer EM is used alternately for the measurement of ion currents of both signs on the cover of the capacitor. ν_0 is calculated through the current and the flow rate Φ_1. To suppress noise ensuing from the instability of the power source the measuring capacitor was connected into a bridge circuit balanced by AC.

The constructional and regime parameters of the ionizer were selected so that by changing the length L from 0 to 430 mm, the initial concentrations of ions of both signs in M-R (taking into account the dilution by Φ_2) were adjusted in the limits $(1.0 \cdot 10^{11}$-$1.0 \cdot 10^{15})$ m^{-3}. The average error of the determination of ν_0 is 15%. The equality $\nu_0^+ = \nu_0^-$ is achieved by the selection of the direct component of the voltage on the point.

The experiments were conducted with DOP aerosol with an average particle radius of 0.6 μm , the particle concentration in M-R was kept constant: $N = (1.0 \pm 0.5) \cdot 10^{12}$ m^{-3}. The accuracy of the determination of N is low due to the low precision of PEC (the same PEC was used for the determination of dilution coefficients of ED1 and ED2).

The charge distribution of particles was measured for five values of the ratio ν_0/N . In every case tracks of 200-300 particles were processed. Fig. 2 graphically exemplifies some experimental distributions, as a comparison Fig. 2 presents theoretical curves for similar values of the relation ν_0/N and the curve of the Boltzmann distribution. The shift of the modes of the experimental curves towards negative charges can be explained by the fact that if $\nu_0^+ > \nu_0^-$, then, due to the inequality of the mobilities of ions of different signs,

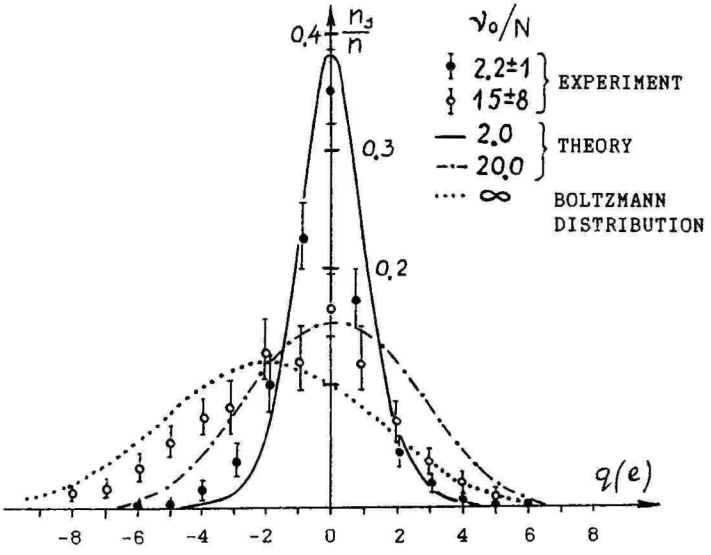

Fig. 2. Comparison of experimental and theoretical distributions. n_j - the number of particles with the charge je, n - the total number of particles.

the probability of a particle catching a negative ion is higher than the respective probability for a positive ion. To simplify the task this is disregarded in equations (4); in the Boltzmann equation [1] it is reflected in the inequality of polar conductivities. If to shift the theoretical curves so that the mode coincides with the mode of the respective experimental distribution, then the experimental points would coincide with the theoretical curves within the confidence limits. Confidence limits of relative frequencies n_j/n are calculated using unsymmetrical estimation formulas.

Conclusions

The satisfactory coincidence of experimental and theoretical distributions makes it possible to use the data in Table 1 for the selection of the operational regime of a charger with an ionizer that can be switched off. For particles with an average radius of 0.6 μm the optimum value of the ratio ν_0/N can be considered to be 2. The dependence

of the optimum value of this ratio on particle size needs further investigation.

References

1. Кикас Ю.Э., Сузи Р.Э., Тамм Э.И. К теории метода электрического сепарирования аэрозольных частиц // Уч. зап. Тарт. ун-та.- 1982.- Вып. 631.- С. 76-84.

2. Пейль И.А., Тамм Э.И. О получении монодисперсного аэрозоля методом электрического сепарирования // Уч. зап. Тарт. ун-та.- 1984.- Вып. 669.- С. 44-52.

3. Таммет Х.Ф. К технике электрической гранулометрии аэрозолей // Уч. зап. Тарт. ун-та.- 1980.- Вып. 534.- С. 55-78. (See this volume pp. 94-115).

4. Фукс Н.А. О величине зарядов на частицах атмосферных аэроколлоидов // Изв. АН СССР. Сер. геогр. и геофиз. - 1947.- No.4.- С. 341-348.

5. Таммет Х.Ф. Электрические параметры загрязненности воздуха // Уч. зап. Тарт. ун-та.- 1977.- Вып. 443.- С. 48-51.

6. Пейль И.А. Электростатический разбавитель аэрозоля // Уч. зап. Тарт. ун-та.- 1987.- Вып. 755.- С. 120-125.

7. Тамм Э.И., Фишер М.М. Определение размеров и зарядов аэрозольных частиц в пределах радиусов от 0.35 до 1.2 мкм ультрамикроскопическим (траекторным) методом // Уч. зап. Тарт. ун-та.- 1973.- Вып. 320.- С. 109-128.

8. Мирме А.А. и др. Полуавтоматический координатомер // Уч. зап. Тарт. ун-та.- Вып. 479.- С. 132-139.

9. Liu B.Y.H., Pui D.Y.H. A submicron aerosol standard and the primary, absolute calibration of the condensation nuclei counter // J. Coll. Interf. Sci.- 1974.- Vol.47, N 1.- P. 155-171.

10. Scheibel H.G., Porstendörfer J. Generation of monodisperse Ag- and NaCl-aerosols with particle diameters between 2 and 300 nm // J. Aeros. Sci.- 1983.- Vol. 14, N 2.- P. 113-126.

Translated from:

Пейль И.А. и др. Генерирование узкого биполярного распределения заряда на частицах аэрозоля // Уч. зап. Тарт. ун-та. - 1987.- Вып. 755.- С. 89-97.

CORONA DISCHARGE AS A GENERATOR OF NANOMETER-RANGE MONODISPERSE AEROSOL

E. Tamm, A. Mirme and Ü. Kikas

Introduction

The generation of aerosol particles in corona discharges has been known for a long time [1,2], but their size spectrum and physical-chemical nature have not been thoroughly studied. The reason is a low development of methods and equipment for the measurement of particle spectra at the beginning of the nanometer size range (particle diameter $D \approx 1$-20 nm) which includes particles generated in corona discharge. The aim of the present paper is the study of the regularities of the evolution of the spectrum of these particles. The paper also has an applied aim - to study the possibility to use "corona" aerosols as calibration aerosols in the above size range where to date such aerosols do not practically exist.

Design of the experiment

The experimental set-up is shown in Fig. 1.

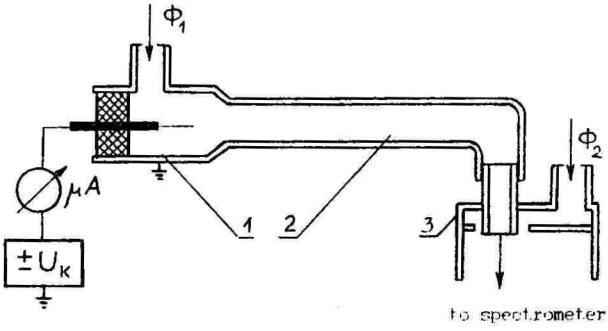

Fig. 1. Diagram of the experimental set-up.

An unipolar corona discharge is produced in the charger 1 in the point-to-cylinder discharge gap. In the present investigation Sn rod was used, but analogous results have been obtained with Pt and Fe rods. The corona current was varied in the limits 1-40 μA by the selection of voltage $U_к$, the

current was controlled with a micro-ampermeter.

The air (air flow Φ_1) filtered with a high efficiency fibre filter was blown through the charger. The air with the corona products was directed into a cylindrical relaxation chamber 2. Chambers of two different shapes were used (Table 1), the relaxation time was controlled by changing the air flow Φ_1.

Table 1

Configuration	Material of chamber walls	Diameter cm	Length cm	Volume cm^3
I	Al	2.4	60	280
II	PCV	0.6	200	60

Before injection into the spectrometer the aerosol was mixed with filtered air (air flow Φ_2) in the mixer 3, this was done to avoid further changes in the particle spectrum and to bring the general air flow rate to the value required by the spectrometer.

The measurement of the particle spectrum

To measure the nanometer-range spectrum of aerosol particles we used an electric aerosol spectrometer (*EAS*) of Tartu University [3]. *EAS* nominal measurement range (particle diameter 10 nm-10 μm) turned out to be unsuitable and the spectrometer had to be modified. We used only one measuring capacitor (with a diffusion charger). The measurement limits (2.4-17.8 nm and 0.7-5.6 nm) were achieved by decreasing the voltage on the acceleration electrode. In the *EAS* the aerosol particles were charged in the corona charger with small air ions. As the ions of the *EAS* charger fell into the first part of the range (0.7-5.6 nm), the real lower limit of the measurement was 1.8 nm. At this limit an empirical correction had to be introduced to eliminate the distorting influence of the ions.

The particle spectrum was computed using the least squares method [4]. The apparatus matrix was computed theoretically by the formula presented in [5]. The technical parameters of the *EAS* were considered to be known, the size and the electrical mobility of the particles were linked with Milliken's formula. It was assumed that in the *EAS* charger, the

particles obtain maximally one elementary charge, the probability of particle charging has been computed by M. Noppel on the basis of the theory by Fuchs [6] taking into account the equation of Salm [7] and using the ion parameters presented in [8].

The influence of the space charge of the ions of the charger was taken into account by the correction of the *EAS* technical parameters on the basis of an extension of the recording of charger ions in comparison with the recording of low concentration air ions injected from the outside in the case of a switched off charger. Diffusional particle losses on the walls of the inlet device of the spectrometer were not taken into account, as they only have a value of about 20% for the lower limit of the range, and quickly decrease with the growth of particle size.

A very strong dependence of particle mobility on their diameter in this size range made it possible to use a spectrometer with heightened resolution power. The above real measurement range was split into eight fractions uniformly in a logarithmic scale. The limits of the fractions were (in nm) 1.8; 2.4; 3.2; 4.2; 5.6; 7.5; 10; 13; 18.

The possible particle generation in the corona charger of the *EAS* was specially investigated. At the injection of filtered air to the inlet of the spectrometer, the numerical fraction concetrations in the calculated spectrum (100-200 cm^{-3}) were found to be in the limits of measurement interference. Only in the first fraction (1.8-2.4 nm dia) a heightened particle concentration was observed. This could be caused by shift in the regime of the charger (the absence of precipitation of ions to particles), or it could be a trace of very "young" particles of the charger.

Results

The aerosol generated by the system of discharge gap and chamber turned out to be monodisperse with a geometric standard deviation $\sigma_g \approx 1.2...1.3$. The other two parameters of the spectrum - the average diameter and the numeric particle concentration - are clearly dependent on the regime parameters of the system. Most illustrative was the presentation of the results as a dependence of the average diameter and the productivity (the total number of particles generated per second) on the corona current and relaxation

time (Table 2). The productivity was computed as a product of the sum of the measured fraction concentrations on the total air flow rate ($\Phi_1 + \Phi_2$).

Table 2

The dependence of the productivity N and the particle diameter D on the time of relaxation T (air flow rate Φ_1) and the corona current I

A. Negative corona, configuration I

Φ_1: cm^3s^{-1}	44		22		11	
T: s	6,3		12,5		25	
I: μA	$N\cdot10^{-7}$ s^{-1}	D nm	$N\cdot10^{-7}$ s^{-1}	D nm	$N\cdot10^{-7}$ s^{-1}	D nm
2	-	-	3,7	2,0	3,2	3,7
4	-	1,8	7,4	2,9	7,2	5,7
10	22	2,4	-	-	-	-
13	31	2,8	-	-	25	9,0
24	45	3,6	-	-	32	14,5
36	64	4,2	46	7,5	48	18,0

B. Negative corona, configuration II

Φ_1 = 44 $cm^3\cdot s^{-1}$ T = 1.35 s			Φ_1 = 11 $cm^3\cdot s^{-1}$ T = 5.4 s		
I: μA	$N\cdot10^{-7}$:s^{-1}	D: nm	I: μA	$N\cdot10^{-7}$:s^{-1}	D: nm
19	-	2	1	-	2
			2	1.7	3.5
30	19	3.0	4	5.6	4.9
			9	22	9.0
36	28	3.5	14	36	10.0
			25	48	11.0
41	36	3.9	30	48	12.5
			39	56	14.5

C. Positive corona, configuration II

Φ_1 = 11 cm^3s^{-1} T = 5.4 s		
I: μA	$N \cdot 10^{-8}$: s^{-1}	D: nm
4	1.0	2.9
9	6.1	4.1
14	18.4	8.5
19	36.0	10.0
24	52.0	13.0

The analysis of the data presented in Table 2 shows that in the case of a negative corona the productivity N is linearly dependent on the current I_- of the corona and nearly independent of the relaxation time:

$$N \sim I_- \ . \qquad (1)$$

Deviations from the law (1) are well explicable by diffusion losses on the walls of the chamber. The dependence of the particle diameter D on the regime parameters has a more complex character and is in good conformity with the law

$$D \sim T \sqrt{I_-} \ , \qquad (2)$$

where T is the average relaxation time. It appears that the coefficient of proportionality in (2) depends on the configuration of the chamber. In the present case for configurations I and II (Table 1) the difference is about fourfold.

There are less data from the experiments with positive corona (Table 2C), but even these are sufficient to show that here the dependencies are somewhat different:

$$N \sim I^2 \qquad (3)$$

and

$$D \sim T \cdot I_+ \ . \qquad (4)$$

In all the cases the percentage of charged particles turned out to be small and comparable with the percentage of charged particles at bipolar equilibrium charging.

A threshold of particle generation by the corona current was not detected. If the current was decreased, the average

particle size gradually faded out of the measurement range. No sharp changes were observed.

It is interesting to consider the results of the study of laboratory air. A minimum in the particle spectrum was observed near 5 nm (fraction concentrations of the order of 500 cm^{-3}). Large temporal aerosol concentration changes were observed, especially in the range of smallest sizes. These changes can probably be explained by fluctuational processes of the generation and coagulational particle growth.

The results of our experiments (in the limits of measurement error) confirmed the lack in the air of ions with mobilities higher than 2 $cm^2/(V \cdot s)$, though it is likely that there are neutral particles of equivalent sizes. This demonstrates a radical limitation of the electrical method of aerosol particle size measurement which presupposes an obligatory joining of a small ion to a particle. The resulting particle cannot be "smaller" than a small ion.

Discussion

We designed a model of the process on the basis of the established regularities (1), (2), (3) and (4).

The independence of the productivity on the relaxation time points to the condensation mechanism of particle growth. Also, a small width of the particle spectrum ($\sigma_g \approx 1.2$) is characteristic of a condensation aerosol.

Coagulation as the main mechanism of particle growth is rejected by the fact that this growth is not accompanied by a sharp decrease of the number of particles. Furthermore, small width of spectra is not characteristic of strongly coagulated aerosols.

It is known that the change of the diameter of particles at the condensation of vapour on them takes place according to the proportionality

$$\frac{dD}{dt} \sim \frac{A(t)}{D} \qquad (5)$$

Here it has been assumed that the pressure of the saturating vapour at the surface of a particle is zero, and that the pressure in the distance is proportional to the concentration of the vapour A. Let us assume that this concentration decreases according to the equation:

$$A(t) = A_0 \exp(-t/\tau), \qquad (6)$$

where τ is an equivalent time constant. Let the corona discharge produce B molecules of vapour in a unit of time, then $A_0 = B/\Phi_1$, where Φ_1 is the air flow rate, and

$$\frac{dD}{dt} \sim \frac{1}{D} \frac{B}{\Phi_1} \exp(-t/\tau). \qquad (7)$$

After integration and square rooting we obtain:

$$D(t) = \sqrt{K \frac{B}{\Phi_1} \tau \, [1 - \exp(-t/\tau)]}. \qquad (8)$$

Here it is assumed that $D(0) = 0$, and the coefficient of proportionality has been expressed through K . In the experiment the particle size was determined through the relaxation time T which is connected with Φ_1 by the relaxation volume V (see Table 1):

$$\Phi_1 = V/T \ .$$

We get:

$$D = \sqrt{K \frac{B}{V} \frac{\tau}{T} \, [1 - \exp(-T/\tau)]} \cdot T \ . \qquad (9)$$

For low T/τ the expression (9) can be written as:

$$D = \sqrt{K \frac{B}{V}} \cdot T \ . \qquad (10)$$

If to assume that the number of the nuclei of future particles and the mass of vapour produced in a unit of time are both proportional to the corona current, i.e.

$$N \sim I \quad \text{and} \quad B \sim I \ , \qquad (11)$$

then formula (10) agrees with the experimental relations (1) and (2) for negative corona. If to assume that

$$N \sim I^2 \quad \text{and} \quad B \sim I^2 \ , \qquad (12)$$

then the case of positive corona is described (experimental formulas (3), (4)).

The dependence of the shapes of the functions $N = N(I)$ and $B = B(I)$ on the polarity of the corona can be explained by the difference of the physical nature of the discharge for

different polarities. Negative corona has pulse character with a nearly constant amplitude and duration of current pulse. An increase of the average value of the current is achieved by a proportional increase of the frequency of pulses. This explains the proportionality of the vapour production rate to the average current. Positive corona has a continuous character. A detailed explanation of the shape of function (12), as well as of the dependence of the production of vapour on the pulse amplitude at negative corona, are out of the scope of the present investigation.

Comparing Table 2B with Table 2C at the same air velocity it can be seen that a relation between the productivity and the diameter is evident. This is possible if $N \sim B$, i.e. the sign of the corona does not influence the proportionality between the number of nuclei and the amount of vapour. This indicates that the nuclei are formed together with the vapour generated by the corona discharge.

Now we will consider the influence of the shape of the relaxation chamber on the proportionality coefficient in formula (2) for average particle diameter. Formula (10) shows that the relation of the values of this coefficient for two shapes is to be equal to the square root of the relaxation volumes. From Table 1 we obtain: $\sqrt{V_I / V_{II}} = 2.16$. The difference between the obtained estimate of the relation of coefficients and the experimental value cannot be explained by experimental errors. Also it was not possible to get the estimate of τ which would have made it possible to estimate the diffusion coefficient of the particles of the postulated vapours and thus to decide about its nature. The above facts point to the necessity of further development of the model and of further experimental investigations.

Conclusions

The proposed model of the generation of aerosol particles in the corona discharge adequately describes the experimentally established general properties of the phenomenon. A number of details require further investigation.

Simple adjustment of the average size and good replicability of the particle spectrum makes it possible to use the corona discharge as a generator of a nanometer range calibration aerosol.

References

1. Nolan, P.J., O'Toole, C.P.J. The condensation nuclei produced by point discharge // Geofisica pura e applicata. - 1958. - Vol. 42. - Pp. 117-126.

2. Загайнов В.А. и др. Исследование образования высокодисперсных аэрозольных частиц в коронном разряде // Тез. докл. V всесоюз. конф. "Аэрозоли и их применение в народном хозяйстве". - М., 1987. - Т. I. - С. 37.

3. Мирме А.А., Тамм Э.И., Таммет Х.Ф. Электрогранулометр аэрозольных частиц с широким пределом измерения // Уч. зап. Тарт. ун-та. - 1981. - Вып. 588. - С. 84-92.

4. Таммет Х.Ф., Мирме А.А., Тамм Э.И. К проблеме электрического анализа аэрозолей // Труды ИЭМ. - М., 1983. - Вып. 30 (104). - С. 122-136.

5. Таммет Х.Ф. Об электрической гранулометрии аэрозолей // Уч. зап. Тарт. ун-та. - 1975. - Вып. 348. - С. 30-33.

6. Фукс Н.А. О стационарном распределении зарядов аэрозольных частиц в биполярно ионизированной атмосфере // Изв. АН СССР. Сер. геофиз. - 1964. - Но. 4. - С. 579-586.

7. Сальм Я.Й. Об униполярной зарядке первоначально заряженного аэрозоля // Уч. зап. Тарт. ун-та. - 1977. - Вып.443. - С. 57-61. (See this volume pp. 68-71).

8. Hussin, A. et al. Bipolar diffusion charging of aerosol particles. I : Experimental results within the diameter range 4-30 nm // J. Aerosol Sci. - 1983. - Vol. 14, N 5.- - Pp. 671-677.

Translated from:

Тамм Э.И., Мирме А.А., Кикас Ю.Э. Коронный раэряд как генератор монодисперсного аэрозоля нанометрового диапазона // Уч. зап. Тарт. ун-та. - 1988. - Вып. 824. - С. 123-131.

DISPERSION OF DROPLET STREAM IN VIBRATING ORIFICE AEROSOL GENERATOR

V. Tamme

Berglund-Liu vibrating orifice aerosol generator is a suitable device for generating liquid and solid aerosols in the size range 0.5-50 μm.

This generator has been used for thorough investigation of the conditions for generating monodisperse droplets. These investigations have been based on the theory of break-up of cylindrical liquid jets and experimental data [1,2].

By direct microscopic measurement of several thousands of droplets and statistical analysis it has been proved that the size distribution of primary droplets is very narrow (geometrical standard deviation σ_g is below 1.01) [3,4].

On the basis of the experimental data of Berglund and Liu, Wedding et al., and Tamme and Koppelmaa [1,2,4] it can be claimed that a correct choice of the dispersion parameters makes it possible to completely exclude the generation of the so-called satellite droplets which are smaller than the primary droplets, however, it is not possible to rule out the generation of the so-called multiplets which are larger than primary droplets.

The multiplets can be defined as compound-droplets formed in the coagulation of two or more droplets, the diameter of such compound-droplets can exceed that of a primary droplet 1.26; 1.59; etc. times. In the best dispersion mode the main droplets are accompanied only by doublets formed in the coagulation of two primary droplets [4].

Statistical processing which, in addition to the primary droplets, takes into account the multiplets yields a wider size distribution and σ_g is in the range 1.038-1.1 [4,5].

Using an optical aerosol counter Berglund and Liu [1] have studied the relative multiplet content of aerosols in dependence on the consumption of dispersion airflow. They demonstrate that the content of multiplets in the output aerosol depends strongly on the consumption of dispersion air, but it is not indicated, how it would be possible to choose the optimal consumption which would ensure maximum quality of the output aerosol (minimal multiplet content).

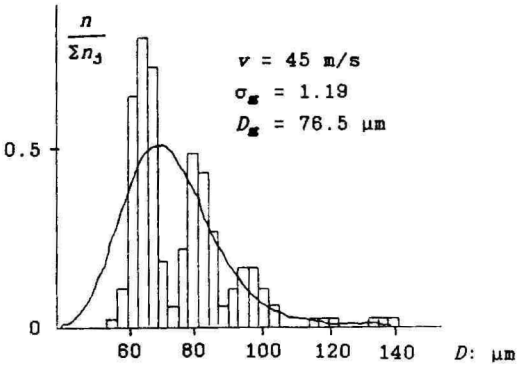

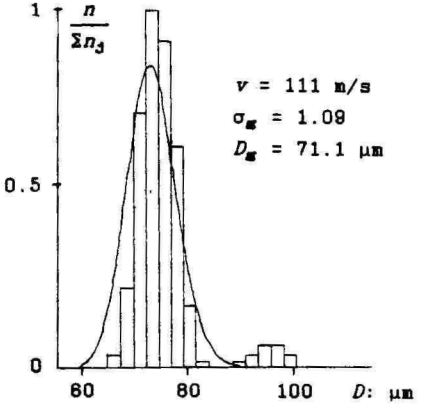

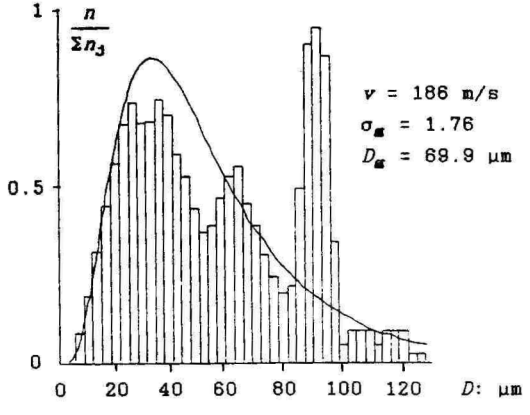

Fig. 1, 2 and 3. Droplet size distribution. v = 45 cm/s, 111 cm/s and 186 cm/s.

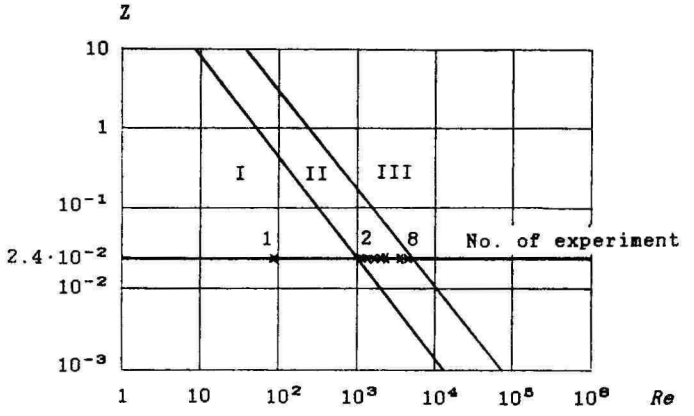

Fig. 4. Graphic dependence of the disintegration of the jet on the Reynolds number.

Tamme and Koppelmaa [4] have made an experimental study of the change of spontaneous jet dispersion, if the jet is submitted to low-amplitude axis-symmetrical mechanical vibrations. This investigation was based on the study by Ohnesorge [6] and showed that the use of mechanical vibrations turns the size spectrum into a discrete entity, i.e. there are separate peaks for primary droplets, doublets, and triplets (see Figs. 1 and 2). This made it possible to connect the peculiarity of the droplet spectrum with the hydrodynamic and geometrical parameters of the dispersion process (e.g. the Reynolds number Re and the jet diameter D_j).

In the experiments an aerosol generator with vibrating orifice designed at Tartu University was used to study the influence of the relative speed of the dispersion air and the jet (distilled water) on the percentage of multiplets in the stream of monodisperse droplets. The jet diameter D_j = 25 μm, the voltage on piezoelectric ceramic U_c = 20 V and 50 V, the relation of the disturbance wavelength and the jet diameter was $\lambda/D_j = 4.5$. In these conditions a stream of monodisperse droplets was produced.

In the experiments the droplets were collected on Petri's disks covered with a thin layer of vaseline oil, shortly after that the disks were photographed. The measurement and

counting of the droplets was done on a film using a semi-automatic coordinate digitizer *UT-7603* [7].

The speed of the air in the nozzle was computed according to the classical method [8] using the measurement of static and total pressures in the atomizing air. The results of the experiments are summarized in Table 1.

Table 1

Comparison of U_c (ceramic voltage), v , Re, σ_g and the relative multiplet content for different velocities of atomization air.

No. of experiment	U_c V	v m/s	Re	Multiplets %	σ_g	D_g mm	No.of figure
1	50	4	94	-	1.26	104.1	
2	50	45	1090	-	1.19	76.5	Fig.1
3	50	70	1688	2.5	1.04	66.6	
4	20	108	2586	11.1	1.10	69.8	
5	50	111	2660	5.6	1.09	71.1	Fig.2
6	50	114	2729	6.7	1.09	68.1	
7	20	152	3645	6.9	1.22	62.7	
8	20	186	4455	-	1.76	69.9	Fig.3

For some dispersion modes figures depicting the size distributions of droplets are added.

Conclusions

From Table 1 the results of the experiment have been transferred to Ohnesorge's graph [6] (Fig. 4). For the liquid used (distilled water) and the jet diameter D_J a line parallel to the abscissa is formed. The discrete change of the size distribution of the droplets makes it possible to observe clearly the transition from region II to the region of complete dispersion (III) (see Fig. 3). The most monodisperse dispersion mode is in region II.

Consequently, it can be said that Ohnesorge's graph makes it possible to determine optimal linear velocities of the atomizing air in a Berglund-Liu type device for several dispersed agents and orifice apertures D_A.

The ratios of D_A/D_J are linear and range from about 0.84-0.96 for jet velocity range of 7 m/s to 25 m/s [3].

Thus in addition to the parameters λ, D_j, U_c [1] the region of monodisperse dispersion is determined by the parameters

$$Re = \frac{vD_j\rho}{\mu} \quad \text{and} \quad Z = \frac{\mu}{\sqrt{\rho\sigma D_j}},$$ where v - relative speed of liquid and air jet, D_j - jet diameter, ρ - liquid density, μ - dynamic viscosity of the liquid, σ - surface tension of the liquid.

References

1. Berglund, R.N., Liu, I.H. Generation of monodisperse aerosol standards // Env. Sci. & Techn.- 1973.- Vol. 7.- P. 147-153.

2. Wedding J.B., Stukel J.J. Operation limits of vibrating orifice aerosol generator // Env. Sci. & Techn.- 1974.- Vol. 8.- P. 456-457.

3. Wedding J.B. Operational characteristics of the vibrating orifice aerosol generator // Env. Sci. & Techn.- 1975.- Vol. 9.- P. 673-674.

4. Тамме В.Б., Коппелмаа И.В. Вибрационный генератор монодисперсных аэрозолей // Уч. зап. Тарт. ун-та.- 1987.- Вып. 755.- С. 113-119.

5. Boyd, J.V. The commissioning of a commercially available vibrating orifice aerosol generator // J. Aerosol Sci.- 1982.- Vol. 13.- P. 221.

6. Ohnesorge, V. Die Bildung und die Auflösung flüssiger Strahlen // Z. angew. Math. u. Mech.- 1936.- B. 16., H.6.- S. 23-26.

7. Мирме А.А. и др. Полуавтоматический координатомер // Уч. зап. Тарт. ун-та.- 1984.- Вып. 479.- С. 132-139.

8. Абрамович Г.Н. Прикладная газовая динамика // М.: Наука, 1969.- 824 с.

ON THE TECHNIQUES OF AEROSOL ELECTRICAL GRANULOMETRY

H. Tammet

Symbols and units

All equations in the paper are in SI. Alongside with the units of SI, also practical measurement units, which are multiples of SI units, are used. Below, the symbols of physical quantities are followed by a practical measurement unit or a SI unit.

d - particle diameter, 1 nm = 10^{-9} m, (d_c - critical diameter, d_D - characteristic diffusion diameter, d_E - characteristic field diameter),

e - $1.602 \cdot 10^{-19}$ C - elementary charge,

h - thickness of the charging layer, 1 cm = 10^{-2} m,

k - air ion mobility, 1 $cm^2/(V \cdot s)$ = 10^{-4} $m^2/(V \cdot s)$,

k_{st} = 1.5 $cm^2/(V \cdot s)$ - conventional standard mobility of small air ions,

n - concentration of small air ions, 1 cm^{-3} = 10^6 m^{-3},

r - particle radius, 1 nm = 10^{-9} m,

t - time, s , (t_q - particle charging time),

q - particle charge, C ,

A - dimensionless coefficient of relaxation of diffusion charging,

C - electric capacitance, F ,

E - electric field, 1 V/cm = 100 V/m (E_c characteristic field of particle charging),

F - air flow rate 1 cm^3/s = 10^{-6} m^3/s.

K = $1.38 \cdot 10^{-23}$ J/K - Boltzmann's constant,

R - electric resistance, Ω ,

T - temperature, K ,

U - electric voltage, V ,

α - dimensionless coefficient of charging intensity,

β - coefficient of nonuniformity of charging conditions, 1 cm/s = 10^{-2} m/s,

$\gamma = q/e$ - dimensionless particle charge,

ϑ - dimensionless coefficient of nonuniformity of charging level,

ε - dimensionless relative permittivity of aerosol particles,

ε_0 - 8.86 pF/m = $8.86 \cdot 10^{-12}$ F/m - absolute permittivity of the air,

τ - RC - time constant, s ,

ω - dimensionless electrostatic coefficient,

θ - dimensionless coefficient of nonuniformity of the charging process,

Introduction

Electrical aerosol granulometry is proved to be a promising technique of aerosol analysis in practice. The most important contributions to the field have been made by the laboratory of aerosol technology of the University of Minnesota [1]. Despite the practical success it should be said that the technique of electrical granulometry is but at the start of its development and far from perfect.

The process of electrical granulometry can be divided into three stages :

- charging of aerosol particles,
- separation and registration of the particles,
- calculation of size spectrum of the particles.

All three stages are equally responsible for the correctness of the results and the efficiency of the measurement method. Different methods can be used at every stage. Therefore the technology of the process as a whole makes possible numerous modifications.

The present paper will deal only with two first stages of the process of electrical granulometry. Some considerations of the author concerning the third stage can be found in [2]. Of the numerous possible methods, the paper will consider only the unipolar charging of particles in a flow of small air ions, and particle registration by the electric current in the same measurement capacitor where particles are separated. The paper does not attempt to develop the charging theory of aerosol particles, it concentrates on the technique of granulometry, whereas the mathematical model of particle charging is considered only with the narrow aim of establishing the dependence of granulometer properties on the charger. The treatment is limited to a fairly rough mathematical model proposed by Mirzabekyan [3]; new improvements in the theory of particle charging have not been taken into account. It is assumed that the particles are spherical. Only the average charge of a particle is estimated and the statistical dispersion of the charges is ignored. This does not mean that the mathematical model simplified to such an

extent is taken to be sufficient at the stage of calculation of particle size spectra. Here, evidently, none of the known theories of particle charging can be viewed as totally reliable. It is better to describe particle charging with a semi-empirical formula which would take into account the statistical dispersion and loss of charged particles in the charger. Semi-empirical formulas contain theoretically indeterminate constants which should be determined by calibration of the granulometer by test aerosols having known particle size distributions.

Mathematical models of particle charging

The charging parameter α

The traditional parameter of diffusion charging of aerosol particles is the product of small air ion concentration and the time of charging. It arises from the assumption that small air ions have fixed mobilities. In the opposite case the intensity of charging is proportional also to the average mobility of the air ions. Sometimes also the change of small air ion concentration over time is to be taken into account. In view of the above, instead of the traditional product nt_q, the charging parameter

$$\alpha = \frac{1}{\varepsilon_o} \int_{t_q} \lambda \, dt \qquad (1)$$

is introduced, where $\lambda = ekn$ - conductivity caused by small air ions. Permittivity of the air is included in order to obtain a dimensionless quantity.

For air ions with a conventional standard mobility of 1.5 $cm^2/(V \cdot s)$ and a steady concentration over time, we have

$$\alpha = 2.71 \frac{nt_q}{10^6 \ cm^{-3}s} \ . \qquad (2)$$

Electrostatic dispersion of air ions

Let us consider air containing monomobile small air ions of only one polarity, and follow a point moving along the trajectory of an air ion. In such a point the space charge density decreases according to the law of electrostatic dispersion

$$\frac{d\varrho}{dt} = -\frac{k\varrho^2}{\varepsilon_o}, \qquad (3)$$

which is valid also in external electrostatic field and in moving air [4]. A general solution of the equation can be written as

$$\lambda = \frac{\varepsilon_o}{t - t_o}, \qquad (4)$$

where the moment t_o is determined by the initial conditions.

Let us henceforth agree to take into account time in accordance to concrete conditions starting from the moment t_o. Then $t_o = 0$ and

$$\lambda = \frac{\varepsilon_o}{t}. \qquad (5)$$

For $t \to 0$, we have $\lambda \to \infty$. $t = 0$ can be assumed at the beginning of an air ion trajectory on the point of the corona discharger. The time counted from the moment t_o is henceforth called the conventional age of small air ions.

For small air ions with standard mobility $t = 1$ s gives us $n = 369000$ cm^{-3}.

An ideal transversal charger

The design of the charger is schematically depicted in Fig. 1.

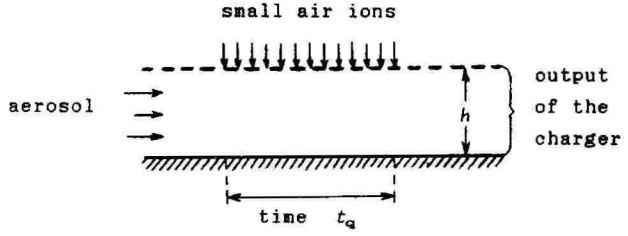

Fig. 1. Longitudinal section of an ideal transversal charger.

A uniform flow of air passes through the charger from left to right. An air layer of a certain limited thickness h is used as the output of the charger. Influenced by the external electric field, the small air ions move approximately cross-wise to the air flow. Compared to h, the charging zone is

relatively long, the time of air flow through this zone is t_q. Due to electrostatic dispersion, the conductivity is better in the layers which are nearer to the air ion source and worse at the bottom side of the charger. Let us denote the values of the parameter α on the upper and lower limit of the charging zone with α_{max} and α_{min}. Non-uniformity of the charging process can be described with the parameter

$$\theta = \frac{\alpha_{max} - \alpha_{min}}{\bar{\alpha}} , \qquad (6)$$

where

$$\bar{\alpha} = \sqrt{\alpha_{max}\alpha_{min}} \qquad (7)$$

is the average value of the charging parameter α.

The electric field in an transversal charger

A certain aerosol particle passes through the charger at a certain height where the conductivity has a certain value. Then $\alpha = \lambda t_q / t_o$ and according to (5) we have

$$\alpha = t_q / t , \qquad (8)$$

where t - the conventional age of air ions at the considered height. Using (6), it is easy to find that

$$\theta = \delta t / t , \qquad (9)$$

where $\delta t = t_{max} - t_{min}$ - the time of the flow of small air ions through the charging zone, and $\bar{t} = \sqrt{t_{max} t_{min}}$ - the average age of small air ions in the charging zone. Let us now determine the average intensity of the electric field in the charging zone so that

$$\frac{h}{\delta t} = \bar{E} k . \qquad (10)$$

Now it is possible to write the basic relation

$$\bar{E} = \frac{h}{\theta t_q} \frac{\bar{\alpha}}{k} . \qquad (11)$$

From this result it follows that the average intensity of the electric field in a transversal charger is limited from below by the permitted non-uniformity of the charging process.

The parameter of charger β

If to fix the parameter α and the mobility k, then, according to formula (11), the field intensity in the charger depends on the design of the charger only through the factor $h/\theta t_q$. This factor is denoted by β:

$$\beta = \frac{h}{\theta t_q} \tag{12}$$

and viewed as the second basic parameter of the charger. The parameter β has a dimension of velocity. It is proportional to the average velocity of small air ions in the charger.

$$\beta = \frac{1}{\bar{\alpha}} \bar{E} k. \tag{13}$$

The larger the parameter β, the stronger is the influence of the mechanism of field charging of aerosol particles in the electric field.

Example

Let an ideal transversal charger have the following characteristics :

$n = 3 \cdot 10^8$ cm^{-3}, $k = k_{st}$, $t_q = 1$ s, $h = 1$ cm, $\theta = 20\%$.

These data unambiguously determine the intensity of the electric field in the charger. Using the above formulas, we obtain

$$\alpha = 8.14 \ , \quad \beta = 5 \text{ cm/s} \ , \quad E = 27 \text{ V/cm} \ .$$

If to decrease the electric field, then the parameter of non-uniformity β will correspondingly grow.

Non-uniformity of the charging in a real transversal charger

As a rule, the parameters of a real device are worse than those of an ideal device. In the case of transversal charger there are exceptions to the above regularity. An ideal transversal charger presupposes a uniform profile of the air flow. If the air enters a real charger through a long channel, then the profile will be close to parabolic. Then the time t_q is longer in lower and shorter in higher layers of the air in the charger. This compensates for the non-uniformity of conductivity and lessens the value of the parameter θ in comparison with an ideal charger. This effect can be fairly

significant. In devices with relatively short inlet channels the profile of air flow velocities is close to uniform and the above effect is weak.

In relatively short chargers a phenomenon of longitudinal widening of the air ion flow from the top to the bottom is observed. This also compensates for the non-uniformity of conductivity.

There can also be some deviations from the ideal conditions which cause the deterioration of the parameters of the charger. The biggest danger is spatial non-uniformity of the source of small air ions. However, a good design makes it possible to reduce the non-uniformity of charging when compared with the theory of ideal transversal charger.

Mirzabekyan's model

Mirzabekyan [3] demonstrated that the charge of the particle q_D , acquired on the account of the diffusion mechanism, and the charge of the particle q_E , acquired on the account of the field mechanism, are simply added in the first approximation and the particle charge is

$$q = q_D + q_E \ . \qquad (14)$$

To calculate the charge q_D , Mirzabekyan proposes the equation

$$\frac{\varepsilon_o}{ek}\left[\mathrm{Ei}\left(\frac{q_D e}{4\pi\varepsilon_o rKT}\right) - \ln\left(\frac{q_D e}{4\pi\varepsilon_o rKT}\right) - 0{,}5772\right] = nt_q \ , \qquad (15)$$

and for the charge q_E , he proposes the Pauthenier equation

$$q_E = 4\pi\varepsilon_o\left(1 + 2\,\frac{\varepsilon - 1}{\varepsilon + 2}\right) Er^2\,\frac{\pi kent_q}{4\pi\varepsilon_o + \pi kent_q} \ . \qquad (16)$$

Below Mirzabekyan's model will be presented in a shape which is easier to interpret. For this purpose it is necessary to determine certain supplementary quantities.

The relaxation coefficient and electrostatic coefficient

Equation (15) can be written as:

$$\sum_{m=1}^{\infty}\frac{A^m}{m\cdot m!} = \alpha \ . \qquad (17)$$

The quantity

$$A = \frac{q_D e}{4\pi\varepsilon_o r K T} \qquad (18)$$

is considered as a dimensionless coefficient of the relaxation of diffusion charging.

In the interval $\alpha = 3...300$ with an error less than 0.1, the approximate equation is valid

$$A \approx \ln(1 + \alpha^{4/3}). \qquad (19)$$

To keep the Pauthenier formula short we will use a special denotation for the electrostatic coefficient

$$\omega = \frac{1}{2} + \frac{\varepsilon - 1}{\varepsilon - 2} . \qquad (20)$$

The values of this coefficient are in the interval 1 ± 0.5 . In the examples $\omega = 1$ will be considered as the standard value, the corresponding permittivity $\varepsilon = 4$.

Characteristic sizes and electric field

Let us determine the characteristic size of diffusion charging

$$d_D = \frac{e^2}{2\pi\varepsilon_o K T} , \qquad (21)$$

the characteristic size of field charging

$$d_E = \sqrt{\frac{k}{\omega\beta}\,\frac{e}{2\pi\varepsilon_o}} = \sqrt{\frac{\bar{\alpha}}{\omega\bar{F}}\,\frac{e}{2\pi\varepsilon_o}} \qquad (22)$$

and the characteristic intensity of the electric field

$$E_o = KT/d_D e . \qquad (23)$$

At a temperature of 18°C we have:

$$d_D = 115 \text{ nm} , \quad E_o = 2185 \text{ V/cm}.$$

If to assume $k = k_{mt}$ and $\omega = 1$, then

$$d_E = \frac{6570 \text{ nm}}{\sqrt{\beta : (\text{cm/s})}} .$$

The equation of particle charging

The above characteristic quantities allow us to describe Mirzabekyan's model using the expressive equation

$$\bar{\gamma} = \frac{\bar{q}}{e} = A\frac{d}{d_D} + \frac{\alpha}{1 + 4/\alpha}\left(\frac{d}{d_E}\right)^2 \qquad (24)$$

or an equivalent equation

$$\bar{\gamma} = A\frac{d}{d_D} + \frac{\omega}{1 + 4/\alpha}\frac{E}{E_o}\left(\frac{d}{d_D}\right)^2 . \qquad (25)$$

In the case of small particles $\bar{\gamma} < 1$, this indicates that many particles are uncharged. The electric mobility of the particles is dependent not on the average charge of all particles $\bar{\gamma}$, but on the average charge of charged particles γ . Evidently γ is never less than a unit. For obtaining the first approximation the following equation can be proposed

$$\gamma \approx \sqrt{1 + \bar{\gamma}^2} . \qquad (26)$$

The electric mobility of particles

At the description of the movement of spherical particles the well-known Millikan equation is acknowledged to be sufficiently precise over the size range we are concerned with. Let us express the numeric value of the diameter in nm through d', then the Millikan equation will acquire the shape

$$k = (8.44/d')\ 1+(165/d')(1+0.336\exp(-d'/153))\cdot 10^{-3}\ \frac{cm^2}{V\cdot s}. \qquad (27)$$

Here it has been assumed that the temperature is 18°C and the atmospheric pressure is 1000 mb .

The dependence of particle mobility on the size is illustrated in Fig.2. The four upper curves correspond to four typical combination of charger parameters α and β . The fifth curve will be explained in the second part of the paper.

Critical particle diameter

We will call the diameter at which particle mobility is minimal the critical diameter. Usually the critical diameter is of an order of μm . In the case of micrometric particles the exponential member of the Millikan formula may be ignored and $\gamma = \bar{\gamma}$ can be assumed. Let us assume that the mobility of small air ions is k_{st} and $\omega = 1$. Then

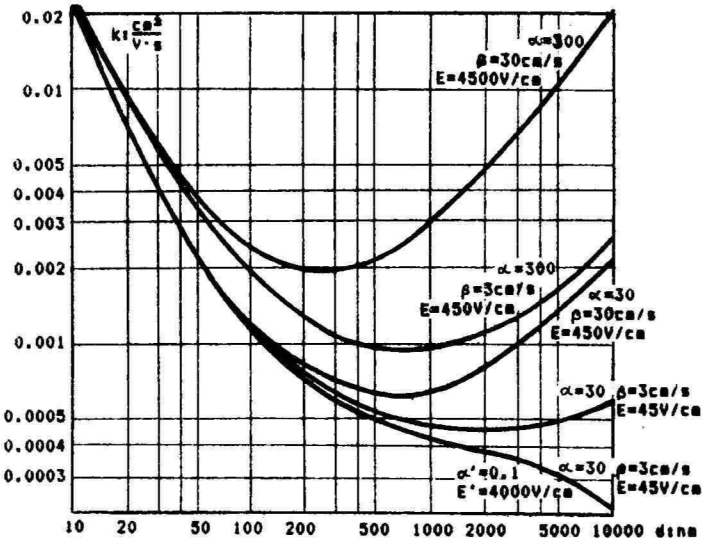

Fig. 2. The dependence of the mobility on particle diameter and charger parameters.

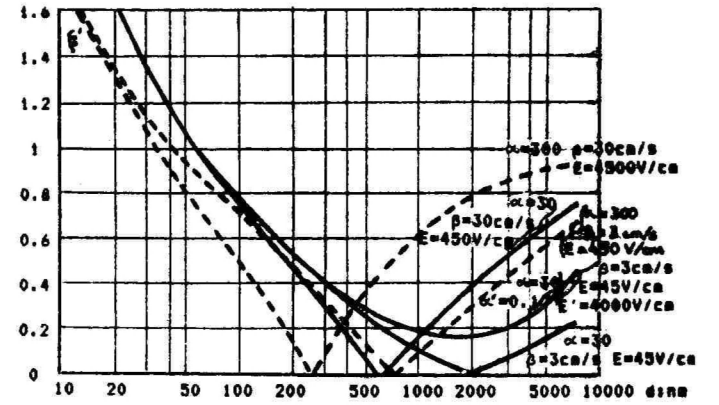

Fig. 3. The dependence of the criterion of quality of the charging law on particle diameter and charger parameters.

$$k \sim \left(\frac{A}{115} + \frac{\alpha\beta:(cm/s)}{(1+4/\alpha)6570^2}\, d'\right)\left(1 + \frac{165}{d'}\right). \qquad (28)$$

This expression achieves a minimum at the diameter

$$d_c = \sqrt{\frac{(1+4/\alpha)\ \ln(1+\alpha^{4/3})}{\alpha\beta:(cm/s)}} \cdot 7870 \text{ nm} . \qquad (29)$$

Some values of the critical diameter are presented in Table 1.

Table 1

Critical diameter in nm for different values of the parameters α and β:(cm/s), according to formula (29)

$\alpha \setminus \beta$	1	3	10	30
10	5200	3000	1640	950
30	3260	1880	1030	600
100	1990	1150	630	360
300	1260	730	400	230

Near the critical diameter granulometers lose the ability to discriminate particles by size. In the case of large values of d_c we will speak of a regime of dominant diffusion charging; in the case of small values, of a regime of dominant field charging.

Criterion of the quality of the charging law

Tamm [5] has proposed the following criterion of the quality of analytic particle charging

$$\xi = \frac{r}{\sigma_r}, \qquad (30)$$

where σ_r - the standard deviation of radii at the mobility considered. The criterion ξ depends on the coefficient of variation of the mobility of particles of one and the same size and on the law of average charging. These factors can be taken into account separately

$$\xi = \varkappa \xi' . \qquad (31)$$

Here $\varkappa = k/\sigma_k$ - the criterion of the quality of monodisperse particle charging and

$$\xi' = \frac{r}{k}\left|\frac{dk}{dr}\right| \qquad (32)$$

is the criterion of the quality of the charging law.

The paper [5] contains also a graphic analysis of the dependence of the criterion of the quality of the charging law on particle size and charging regime. In Fig.3 this analysis is repeated for our system of charger parameters. The curves in Fig.3 exactly correspond to the curves in Fig.2. Similarly to Fig.2, the fifth curve will be explained below.

Spatial non-uniformity of the aerosol charge

The criterion θ describes the non-uniformity of the charging process. In practice, the most interesting is the regime of dominant diffusion charging where the non-uniformity is levelled out due to the effect of saturation. Therefore other criteria should be determined for the description of the non-uniformity of the result of diffusion charging

$$\vartheta = \frac{\delta A}{A} . \qquad (33)$$

In the first approximation

$$\frac{\vartheta}{\theta} = \frac{\alpha}{A}\frac{dA}{d\alpha} . \qquad (34)$$

Using the approximation (19) , we get

$$\vartheta \approx \frac{4}{3(1+\alpha^{-4/3})\ln(1+\alpha^{4/3})}\,\theta . \qquad (35)$$

In the regime of practically interesting values of the parameter α , the criterion ϑ is 25...50% of the criterion θ .

Devices for particle charging

The Whitby charger

Let us evaluate the features of the most well-known granulometric aerosol charger described in [6]. It is a typical transversal charger where the air ions are let in through a grid maintained at a certain potential. The authors of the charger present the following data :

height	h	1.43 cm
length		0.95 cm
time	t_q	0.21 s
voltage		100 V
nt_q		10^7 $cm^{-3}s$.

On the basis of these data it is easy to calculate :

$$\alpha = 27$$
$$\beta = 4 \text{ cm/s}$$
$$\theta = 1.75$$
$$\vartheta = 50\%$$
$$d_c = 1.8 \text{ μm}$$

These values enable us to doubt the ability of the device to discriminate fractions in the size range in the neighbourhood of 1 μm. Our calculation points out the simplest way to improve the parameters of the charger - the length of the charger and charging time should be increased. Then θ and ϑ are proportionally decreased. After the achievement of a sufficiently low value of the criterion θ , voltage can be decreased on the account of further increase of the time t_q; this makes it possible to increase the critical particle size.

We do not have sufficient data to evaluate modifications of the Whitby charger built after the device [6].

The ways of widening the size range

The range of particle size for a granulometer using a regime of dominant diffusion charging is limited from above. The only effective way to expand the measurement range towards large sizes is the use of the regime of dominant field charging. Two chargers are necessary : one with a high value of critical size, and the other with a low critical size Three basic technical solutions can be pointed out :

1. Design a "double" device with parallel measuring capacitors, whereas one capacitor is used in the regime of dominant diffusion charging and the other in the regime of dominant field charging.

2. Make the granulometer to alternate the regimes of dominant diffusion and dominant field charging.

3. Provide the granulometer with a double charger so that the main charger would work in the dominant diffusion regime and the subsidiary charger in the dominant field regime with polarity opposite to the one of the main charger.

The method of compensation charging

The third technical solution could be called the method of compensation charging. There is no correct and rigorous theory of charging compensation. Rough estimates can be obtained by adding the charges taken into account separately for main and subsidiary chargers. In such an approximation the lowest curve in Fig. 2 is taken into account; this curve provides a good illustration of the practical effect achieved by the method of compensation. The symbols with apostrophes at the curves indicate the parameters of the subsidiary charger. Fig. 3 also includes the curve of the quality of average charging for the compensation method. As can be seen, the criterion of the quality of average charging still has a rather deep minimum in the neighbourhood of one-micrometer sizes.

If the electric field strength in the subsidiary charger exceeds the critical value

$$E'_c = \frac{1 + 4/\alpha'}{1 + 4/\alpha} \frac{\alpha\beta}{k}, \qquad (36)$$

then large particles are recharged to the other polarity. In the formula the symbols without apostrophes refer to the main charger and the symbols with apostrophes to the subsidiary charger.

In practice slight exceeding of the critical field strength is permissible, as the recharging of particles whose sizes are beyond the measurement range does not have negative consequences. The curves illustrating the compensation charging in Fig. 2 and 3 are drawn for a charger with parameters E'_c = 2200 V/cm and E' = 4000 V/cm .

A shortcoming of the compensation method is the low mobility of large particles which significantly complicates their registration. Technical difficulties may also be caused by the necessity to ensure extremely high stability of the chargers.

Deactivation of the air by opposite charging

As a rule, the differential method of mobility spectrum measurement is used in granulometers. Then the air flow entering the measuring capacitor is divided into two parts. One part with the air flow δF contains the investigated aerosol. The other part with the air flow $F - \delta F$ should be

inactive. This inactivity means that the air does not contain particles which would cause signal at the outlet of the granulometer. Usually, the air is deactivated by conducting it through a mechanical or electric filter. A significant technical difficulty at this point is sufficient filtering of the air. Instead of filtering, deactivation could be carried out by unipolar charging to the polarity opposite of the polarities of the measured particles. This simplifies the design of the granulometer. During deactivation with opposite charging, it should be carefully checked, if the space charge of the oppositely charged aerosol does not cause interference in the measuring capacitor. If necessary, the space charge could be suppressed using an electric filter.

The effect of focussing

In the granulometers of the University of Minnesota the geometrical position of the layers of the air is not retained during the passage from the charger to the measuring capacitor. In this case the non-uniformity of charge indubitably causes deterioration of the discrimination power of the granulometer.

However, the geometrical position of the air layers can be retained during the passage from the charger to the measuring capacitor. In this case the mutual relations of the processes in the charger and the measuring capacitor become essential. If charging is absolutely uniform ($\vartheta = 0$), then the places of precipitation of the particles of the same size are scattered to the extent determined by the relation of air flows $\delta F/F$. If $\vartheta \neq 0$ and the position of layers is retained, then the effects of the scattering caused by non-uniformity of charging and the final relation of the air flows interfere with each other. If the particles, entering nearer to the collector electrode of the measuring capacitor are charged more strongly, then the interference increases the scattering. If the particles, entering nearer to the collector electrode are charged more weakly, then the interference weakens the scattering. In the latter case charging non-uniformity is useful. This effect, though described already in [7], has been somewhat forgotten.

We can imagine a charging non-uniformity where the distance of the spot of precipitation from the inlet of the measuring capacitor is absolutely independent of the point of

entrance of the particle into the granulometer. Then we can speak of perfect focussing of particles.

The use of the effect of focussing makes it possible to select the ratio $\delta F/F$ in the measuring capacitor to be 50%, and simultaneously to guarantee an apparatus function of the granulometer which would be characteristic of a good differential spectrometer. This means a combination of the high sensitivity on integral measuring capacitor and the high discrimination of a differential measuring capacitor.

An inner charger for a measurement capacitor with an inner collector electrode

Fig. 4 presents a diagram of one of the possible designs of an axial charger

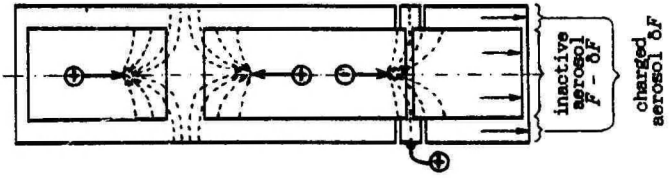

Fig. 4. Diagram of an axial inner charger for a measuring capacitor with an inner collector electrode.

A corona discharge is used for generation of small air ions. Special design makes it possible not to use a partition grid. The field strength and air ion flow are controlled by the depth of insertion of the positive corona points into the inner tube. A subsidiary charger of negative polarity makes it possible to carry out compensation charging. The intensity of compensation charging is adjusted by the width of the slit. Opposite the slit is an electrode which gets voltage to achieve sufficient field strength. At the same time the negative charger has the function of the deactivation of the air passing through the inner tube with the rate $F - \delta F$.

In a device of this type the non-uniformity of the charge increases the scattering of the particles on the collector electrode in the measuring capacitor.

An outer charger for a measuring capacitor with an inner collector electrode.

To achieve the effect of focussing in the case of an inner collector electrode it is necessary to direct the movement of small air ions towards the axis of the charger. A possible design of such a charger is presented in Fig. 5. It is more

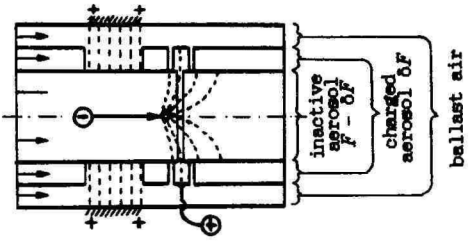

Fig. 5. Diagram of an axial outer charger for measuring capacitor with an inner collector electrode.

complicated to ensure the independence of local charge intensity from the angular coordinate. It is also complicated to use corona discharge as a source of small ions. A compact design can be achieved by the use of α-rays or weak β-rays for the generation of small air ions.

The radioactive preparation should be uniformly spread on the inner surface of a cylindrical electrode. In the described charger a method of deactivation of the air by opposite charging is applied, an inner corona charger is used for it. Compensation charging is carried out similarly to the charging in Fig. 4. An outer ballast layer of air flowing past the measuring capacitor serves to insulate the radioactive preparation and to improve the parameters of the charger.

An inner charger for a measuring capacitor with an outer collector electrode

The arrangement "inner charger and outer collector electrode" does not ensure good discrimination of the granulometer. The arrangement "outer charger and inner collector electrode" should theoretically ensure high discrimination and sensitivity, but the design of an actual granulometer according to this arrangement would run into serious difficulties. High discrimination can be combined with constructional simplicity as shown in Fig. 6. Here the outer cover of

the measurement capacitor serves as the collector electrode which is reasonable, if it is necessary to divide the elec trode into several rings insulated from one another.

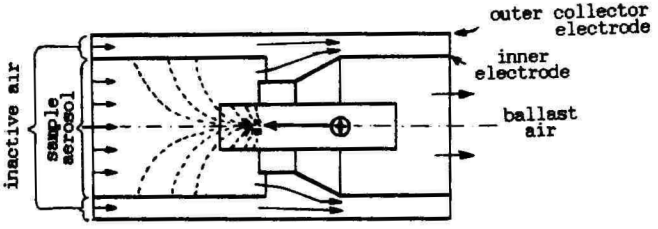

Fig. 6. Diagram of axial inner charger for a measuring capacitor with an outer collector electrode.

Fig. 6 does not include the device for the deactivation of the air and the subsidiary charger for compensation charging. In the case of this arrangement compensation charging is more complicated than in the two preceding cases. Therefore the arrangement "inner charger and outer collector electrode" is most suitable for two-capacitor systems where one measuring capacitor has the regime of dominant diffusion charging, and the other has the regime of dominant field charging.

The modulation method in aerosol granulometry

Numeric synchronous detection and the nature of the modulation method

We speak of the modulation method when the transformation coefficient of the measured signal undergoes periodic variation and the output signal of the device is formed as a result of detection, most frequently synchronous detection. In aerosol measurements it is reasonable to carry out modulation by periodic switching on/off of the measured signal. Here we will not to consider the method of signal modulation inside the amplification circuit.

The optimum period of modulation depends both, on the frequency characteristics of the noises of the measurement system, and on the transition characteristics of the modulator of the air ion flow and the measuring capacitor. For the measurement of small air ions it is useful to have a modulation period ranging from some tenths of a second to

some seconds. In aerosol granulometry air ions of low mobilities are recorded and the measuring capacitor has a long transition time. A modulation period of some tens of a second or longer may be optimal. Certain difficulties occur in the application of traditional analog equipment of synchronous detection.

In the range of low modulation frequencies it is possible to digitize the signal in each half-period of modulation. Detection is then executed with a computer. Numerical processing of the signal is carried out on-line. In this case the process of measurement is outwardly rather similar to the process of measurement with an analog synchronous detector. If it is not possible to use the computer on line, the signal of every half-period can be recorded on magnetic or punched tape, or other storage media, and the computations can be executed later. Then the procedure of measurement is outwardly different from the usual procedure with an analog synchronous detector. It could be argued that this is not the modulation method, but a periodic zero correction to obtain data for the correction of results during the processing of measurement data. This argument gets further support, if for technical reasons an amplifier of direct current is used for the amplification of the signal. However, there is a deeper difference between the methods of modulation and periodic zero correction. In the modulation method the period of modulation is at the same time also the minimum period of measurement. In the periodic zero correction method, the period of measurement is shorter than the period of zero correction, whereas the ratio of the periods can be rather large. Therefore we consider it appropriate to speak of the modulation method, if the signal is amplified with an amplifier of direct current, the period of modulation lasts several minutes, and synchronous detection is postponed until the phase of data processing.

Modulation with a charger

In air ion measurement devices modulation is executed by the switching of the air flow, the voltage of the measuring capacitor, or the voltage on a special preliminary capacitor. All these methods can be used in aerosol granulometry. However, there is a simpler method of modulation through periodic switching on/off of a unipolar aerosol charger.

The method of modulation with a charger has all the advantages of the method of modulation with a preliminary capacitor. Special attention should be paid to an advantage specific for granulometry. In charger modulation the flow of residual air ions in the air which should be inactive is not modulated. This suppresses measurement errors connected with possible imperfection of the device of air deactivation making it possible to simplify the design of this device and there appears a possibility to realize the differential measurement method without the device of air deactivation. For instance, in the device depicted in Fig. 6, the inactive air could be replaced by an uncharged variant of the aerosol which is being analyzed. Modulation here is carried out by periodic switching on/off of high voltage on the corona point.

RC-regime of the measurement of current strength

Let us consider the task of measuring the strength of direct current of air ions in a measuring capacitor and denote the duration of the measurement cycle through δ . Let the transition process of the measuring device be a simple exponential process with the time constant τ

Two measurement regimes are widely spread :

- the regime of measurement of the voltage drop on the resistance or R-regime where $\tau \ll \delta$,
- the regime of charge cumulation on the capacitance or C-regime where $\tau \gg \delta$ is assumed.

As is known, R-regime is characterized by a lowered sensitivity, and C-regime requires periodic commutation of the input circuit of the electrometric amplifier. Two variants of C-regime are known:

- the variant of fixed zero,
- the variant of floating zero.

In the case of fixed zero the charge generated by the electrometric commutator will be included in the measurement result as noise. Therefore the electrometric commutator should meet rigorous requirements, and the sensitivity of the electrometer will not be significantly higher than in R-regime. Floating zero makes it possible to realize the highest theoretically possible sensitivity. However, complicated equipment for signal commutation and registration would be necessary in this case.

In practice, for reasons of technical simplicity, R--regime is the most wide-spread one. Therefore the improvement of the sensitivity of R-regime is especially significant. The sensitivity of the electrometer in R-regime to current strength is growing together with the ratio τ/δ . At $\tau/\delta \gg 1$ the sensitivity is approaching that of the electrometer in C-regime. However, a systematic measurement error called the error of inertia occurs, if the condition $\tau \gg \delta$ is not satisfied. The error of inertia depends on the voltage on the electrometer at the end of the previous cycle. If this voltage is known, then the error of inertia can be unambiguously established and the measurement results can be corrected computationally. In the case of computational correction of the error of inertia, a measurement regime with $\tau \approx \delta$ is quite acceptable. This regime might be called RC-regime.

The correction of the inertia

Let us consider the measurement of the strength of the current in a modulating granulometer. The process in an electrometer with RC-regime is illustrated in Fig.7.

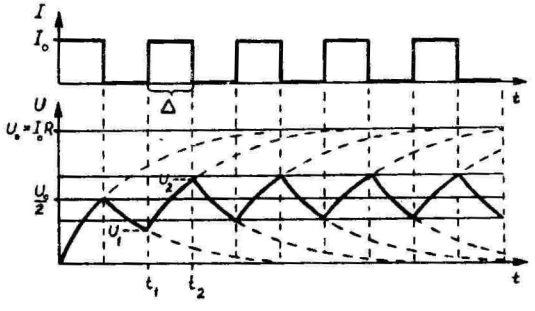

Fig. 7. The process in an electrometer with RC-regime at a rectangular modulation of the measured current.

Let δ , τ , U_1 , and U_2 be known. For the correction of the measurement error we need a computation formula for the level of U_0 which would be valid for any period of modulation, independently of the history of the process. It is easy to derive such a formula from the equation of the transition process, according to which

$$U_o - U_2 = (U_o - U_1) \exp(- \frac{t_2 - t_1}{\tau}) . \qquad (37)$$

The correction formula will be

$$U_o = U_2 + \frac{\exp(-\delta/\tau)}{1 - \exp(-\delta/\tau)} (U_2 - U_1). \qquad (38)$$

It is expedient to carry out the correction together with synchronous detection. As the factor in formula (38) is an apparatus constant, the correction is simple to execute also if analog synchronous detection is used.

References

1. Whitby, K.T. Electrical measurement of aerosols // Fine particles. Aerosol generation, measurement, sampling and analysis.- New York - San Francisco - London, 1976.- P. 581-624.

2. Таммет Х.Ф. Об электрической гранулометрии аэрозолей. // Уч. зап. Тарт. ун-та, 1975.- Вып. 348.- С. 30-34.

3. Мирзабекян Г.З. Зарядка аэрозолей в поле коронного разряда // Сильные электрические поля в технологических процессах.- М., 1969.- С. 20-39.

4. Таммет Х.Ф. Аспирационный метод измерения спектра аэроионов // Уч. зап. Тарт. ун-та.- 1967.- Вып. 195.- 234 с.

5. Тамм Э.И. О функциональной зарядке аэрозольных частиц. // Уч. зап. Тарт. ун-та, 1975.- Вып. 348.- С. 35-55.

6. Liu, B.Y.H., Whitby, K.T., Pui, D.Y.H. A portable electrical analyser for size distribution measurement of submicron aerosols // APCA Journal.- 1974.- Vol. 24, No. 11.- P. 1067-1072.

7. Yosikawa, H.H. et al. Electrostatic particle size analyser // Rev. Sci. Instr.- 1956.- Vol. 27, No 6.- P. 359-362.

Translated from:

Таммет Х.Ф. К технике электрической гранулометрии аэрозолей // Уч. зап. Тарт. ун-та.- 1980.- Вып. 534.- С. 55-79.

PRINCIPLES OF THE GRADUATION OF AN ELECTRIC AEROSOL GRANULOMETER

H. Tammet and M. Noppel

The measuring block of a granulometer or an electric analyser of aerosols gives direct information about the particle size spectrum in the form of a set of channel signals $\psi = \{\psi_1, \psi_2, \ldots, \psi_n\}$. The particle size spectrum is also described by a set of numbers $\varphi = \{\varphi_1, \varphi_2, \ldots, \varphi_n\}$ (e.g. fraction concentrations of particles). For a measurement method based on the primitive mathematical model of the measurement process, the estimate of the spectrum is obtained through the scale transformation

$$\varphi_j = a_j \psi_j \qquad (1)$$

and graduation is reduced to determining the constants of a_j.

If a modified primitive mathematical model is used, then a preliminary transformation of the primary channel signals ψ' to secondary ψ'' is admissible (e.g. using the formula $\psi_j'' = \psi'_j - \psi'_{j-1}$). This mathematical model is used as the data processing basis of the well-known device *TSI-3030*, however, the use of the primitive model sets strict requirements to the design of the granulometer, whereas these requirements can be met only approximately.

According to the general linear mathematical model the channel signals are dependent on the size spectrum according to the linear apparatus equation $\psi_j = \sum_k H_{jk}\varphi_k$ or

$$\psi = H\varphi, \qquad (2)$$

where the table of coefficients H is called the apparatus matrix.

The size spectrum of particles is calculated by solving the apparatus equation using the least squares method.

The general linear mathematical model excludes strict requirements to the equipment and makes it possible to avoid simplifications and approximations which cannot be avoided in the case of the primitive mathematical model. The primitive model is a special case of the general model and it demands a diagonal structure of the apparatus matrix. If the general linear mathematical model is used, then the graduation of the granulometer is reduced to the determination of the elements

of the apparatus matrix H_{jk}.

For the graduation of the granulometer information from various sources may be used. We will consider four methods of graduation different in the kind of information used: absolute, etalon aerosols, analysis of aerosol deposit, and complex methods.

In absolute graduation the granulometer is viewed as an absolute measuring device which is graduated by theoretical calculation on the basis of the measurement of geometrical and electrical parameters of the device. A general outline of absolute graduation is presented in [1].

The apparatus matrix is calculated according to the formula

$$H_{jk} = \frac{e}{\int_{r_{k-1}}^{r_k} f^{(k)}(r)\mathrm{d}r} \int_{r_{k-1}}^{r_k} f^{(k)}(r) \sum_{\delta} \gamma_\delta P_\delta(r) G_j(k_\delta(r))\mathrm{d}r, \qquad (3)$$

where e - the elementary charge; G_j - the apparatus function of the measuring capacitor; index j - the channel number; $P_\delta(r)$ - the probability of getting into the capacitor of particles with the size r and charge γe; $k_\delta(r)$ - the mobility of a γ-times charged particle calculated by the Stokes-Millikan formula.

In formula (3) for the sake of simplicity the fraction model of the particle size spectrum has been adopted

$$f(r) = \sum_k \varphi_k f^{(k)}(r) / \int_{r_{k-1}}^{r_k} f^{(k)}(r)\mathrm{d}r, \qquad (4)$$

whereas the function $f^{(k)}(r)$ is considered to be defined, and the experiment is to determine only the value of φ. If under the integral sign in equation (3) the function is smooth and the fractions narrow, then the apparatus matrix is practically independent of the concrete shape of the function $f^{(k)}(r)$ and those functions can be chosen arbitrarily. In the general case the values of φ_k are viewed as the coordinates of linear expansion of the particle size spectrum by elementary spectra $f^{(k)}(r)$

$$f(r) = \sum_k \varphi_k f^{(k)}(r). \qquad (5)$$

Electric aerosol granulometer can be viewed as an absolute device only if the function $P_\delta(r)$ is known. In practice, the

function of particle charging $P_\gamma(r)$ is sufficiently well known only in the case of a steady bipolar particle charging. The latter gives the devices with a bipolar charging a certain advantage. However, those devices are significantly less sensitive than devices with unipolar particle charging.

The research in the charging of aerosol particles shows that the charge distribution of particles depends on the field strength E_o and the quantity $kn_o t$ in the charging zone, where n_o - the ion concentration; k - the ion mobility; and t - the time the particles stay in the charging zone. The above distribution depends also on the initial distribution the influence of which decreases with the increase of $kn_o t$. Let us denote this distribution, normed to a unity, through $P_{1\gamma}(r/kn_o t, E_o)$. This function describes aerosol charging in an ideal charger which guarantees identical values of E_o and $kn_o t$ for all aerosol particles. In real chargers aerosol particles pass through zones with different values of E_o and $kn_o t$. Particles may also be precipitated in the inlet of device and the charger. Let us denote the probability of a particle passing through the inlet of device and the charger in the zone with a known value of E_o and $kn_o t$ through $P_2(kn_o t, E_o, r)$. Then

$$P_\gamma(r) = P_{1\gamma}(r/kn_o t, E_o) P_2(kn_o t, E_o, r). \qquad (6)$$

If the ion flows onto a particle are known, then $P_{1\gamma}(r/kn_o t, E_o)$ are determined by an equation proposed in [2]. Application of this formula for the range of large sizes causes substantial difficulties [3]. Therefore an approximate method for the determination of $P_{1\gamma}$ has been proposed for aerosol particles which are much larger than the mean free path of air ions [4]. In this case $P_{1\gamma}$ is described by the following equation

$$P_{1\gamma} = \frac{1}{\sigma_\gamma \sqrt{2\pi}} \exp\left(-\frac{x^2}{2}\right)\left\{1 + \frac{\nu_1}{6}(x^3 - 3x) + \right.$$

$$\left. + \frac{\nu_2}{24}(x^4 - 6x^2 + 3) + \frac{\nu_1^2}{72}(x^8 - 15x^4 + 45x^2 - 15)\right\}, \qquad (7)$$

$$x = \frac{\gamma - \bar{\gamma}}{\sigma_\gamma},$$

where $\bar{\gamma}$ - the average particle charge, σ_γ - the standard de-

viation, ν_1 - the coefficient of asymmetry and ν_2 - the coefficient of excess. On the basis of this formula a system of four differential equations has been formulated, there dependencies of $\bar{\gamma}$, σ_γ, ν_1 , ν_2 on $kn_o t$ are wanted. This system of differential equations was solved with the method of Runge -Kutta for diffusion charging taking into account the ion flow onto a particle (formula in [5]). The dependencies $\bar{\gamma}(r,\ kn_o t)$, $\sigma_\gamma(r,\ kn_o t)$, $\nu_1(r,\ kn_o t)$, $\nu_2(r,\ kn_o t)$ are represented as polynomials. Using the above methods for the determination of $P_{1\gamma}(r/kn_o t, E_o)$ for charging in the electric field, the ion flow onto a particle is to be determined. For this purpose it is necessary to solve the differential equation of charging which simultaneously takes into account the diffusion of ions and their directed movement in the summary electric field created by external surface charges and the charged and polarized particle itself. On the basis of numeric solution of this equation approximate formulas of the ion flow to conductive particles have been found. For instance, for $7 \le W \le 130$ and $0 \le \mu \le 2.4W + 3.87$ the following formula can be used

$$\frac{d\mu}{d\tau} = 3W\left(1 - \frac{\mu}{3W}\right)^2 +$$

$$+ \exp\left[-4.567\{\sqrt{\left(1 - \frac{\mu}{3W}\right)^2 + 0.01159\cdot\ln(3W) + 0.02806} + \right. \quad (8)$$

$$\left. + \left(\frac{\mu}{3W} - 1\right)\} - 0.04182\cdot\ln(3W) + 1.198\right],$$

where $W = \dfrac{eE_o r}{KT}$ - the non-dimensional strength of the electric field, $\mu = \dfrac{\gamma e^2}{4\pi\varepsilon_o r KT}$ - the non-dimensional charge; $\tau = \dfrac{ekn_o t}{4\varepsilon_o}$ - the nondimensional time, ε_o - the electric constant, T - the absolute temperature, K - the Boltzmann constant. To determine $P_{1\gamma}(r)$ for particles with radii coinciding with or less than the mean free path of air ions, the above-mentioned equation [2] can be used and the necessary

values of the ion flow can be calculated according to the theory of Fuchs [6].

The shape of the function $P_2(kn_o t, E_o, r)$ depends on the design of the charger and is to be determined for every particular case. Charging conditions in effective unipolar chargers are non-uniform and there are no sufficiently precise methods to establish the field distribution in a real charger. Theoretical calculations do not ensure the precision necessary for calibration, therefore in making up an apparatus matrix some free parameters connected with constructional and physical parameters of the device are left into the matrix; these parameters are to be established empirically.

Theoretically the most simple is a calibration method which is based on the use of test aerosols with spectra proportional to separate elementary spectra of expansion (5). Then an element of the apparatus matrix H_{jk} is determined directly as the signal of the j-th channel at the k-th separate elementary spectrum. However, practical difficulties occur here, connected with the generation and attestation of the test-aerosols for the whole range of particle sizes covered by the electric granulometer.

Calibration of an electric granulometer by the distribution of precipitated particles has been proposed in [7]. It is assumed that

- the precipitation coefficients of the particles of each group in the analyzer η_I were determined independently of the described procedure of calibration;
- the particles precipitated in the analyzer stick to the electrodes and could be measured with an electron or optical microscope separately in each measurement channel;
- the electric mobilities of the particles precipitated in each measurement channel are limited to certain intervals, and their means k_j^* are known.

There are two possibilities for the calibration: firstly, a polydisperse aerosol with approximately spherical particles the sizes of which cover the whole calibrated range is sucked through the granulometer, or, secondly, only an aerosol covering one sub-interval of the size range is used, and subsequently aerosols covering the next subintervals are used in a successive order. The precise size distribution of the particles may be unknown. At the stage of preliminary analysis of the calibration observations, the sizes

of the particles gathered on the electrodes of different channels are measured, then, on the basis of the initial size table, particle size spectra by channels $f_j(r)$ are calculated. These functions $f_j(r)$ may be approximated by expanding them by the elementary spectra of the adopted model of the spectrum:

$$f_j(r) = \sum_I f_{jI} f^{(I)}(r). \qquad (9)$$

Information presented in the table of coefficients f_{jI} is sufficient for the calibration of the granulometer.

Elements of the apparatus matrix are calculated according to the equation

$$H_{jI} = eF\xi_j \eta_I f_{jI} k_j^{*} \Big(\int f^{(I)}(r)dr \Big) / (k_I \sum_k f_{kI}), \qquad (10)$$

where F - the aerosol flow, k_I - the average particle mobility, ξ_j - the channel sensitivities, i.e. $\psi_j = \xi_j I_j$, I_j - the current of charged aerosol particles in the j-th channel.

The most exact results are ensured by a complex calibration of the granulometer. In this case all sources of information are used, i.e. the theoretical model, the measurement results of etalon aerosols, and the analysis of the precipitation gathered on the channel electrodes. Let us consider one possible method of complex graduation. In this method the theoretical model is used, first and foremost, for the parametrization of the apparatus matrix. Let us denote the parameters of the apparatus matrix with $(h)_1$, $(h)_2$, ..., $(h)_m$. On the basis of the results of the measurement of geometrical and electrical parameters of the measuring capacitor and the chargers, absolute estimates of the parameters of the apparatus matrix are calculated; these estimates make up the vector h_A. In order to use this particular estimate for complex graduation, it is then necessary to estimate the standard deviations of possible errors of these estimates $(\sigma_A)_j$, and also the correlation between the errors $(\varrho_A)_{jk}$. On the basis of these data a covariation matrix of absolute graduation C_A with the elements $(C_A)_{jk} = (\sigma_A)_j (\sigma_A)_k (\varrho_A)_{jk}$ is set up. The vector h_A and the matrix C_A contain the whole information about absolute calibration.

By the results of the measurement of the etalon aerosols an independant estimate is made of the parameters of the same theoretically founded model of the apparatus matrix. The result is formulated as some other vector of the estimate of

parameters h_L and as the respective covariation matrix of estimate errors C_L. The same course of action is followed in the case of the data obtained in the analysis of the precipitation of particles by channels. The respective estimate is denoted with h_d and C_d. Let us suppose that the estimate errors of the parameters of the apparatus matrix have a normal distribution, and that h_A , h_L , h_d are particular estimates of maximum probability. Then the particular functions of probability are written as

$$L_\xi(h/h_\xi) = \text{const}_\xi \exp(-\tfrac{1}{2}(h - h_\xi)^T C^{-1}(h - h_\xi)), \qquad (11)$$

where ξ denotes the index A , L , or d . As all the information sources are independent, the joint probability function is

$$L_o = L_A\, L_L\, L_d.$$

This function is described with the vector h_o which is the most probable complex estimate of the parameters of the apparatus matrix, and the covariation matrix C_o which describes the precision of the estimate. It can be simply shown that

$$C_o = (C_A^{-1} + C_L^{-1} + C_d^{-1})^{-1}, \qquad (12)$$
$$h_o = C_o\,(C_A^{-1}h_A + C_L^{-1}h_L + C_d^{-1}h_d).$$

The above method, despite its apparent complexity of realization guarantees maximum reliability in the graduation of electric aerosol granulometers.

Translated from:

Таммет Х.Ф, Ноппель М.Г. Принципы градуирования электрического гранулометра аэрозолей // Методы и приборы контроля параметров биосферы. Межвуз. сб..- Л., 1984.- С. 21-28.

References see below.

APPENDIX

to the article translated above

As was pointed out in the article, direct empirical graduation of an electric granulometer directly on the basis of test aerosols is a technically complicated task. Despite that, a modified version of direct empirical graduation was

carried out by Mirme [8]. In Mirme's paper the spectra of the test aerosols did not coincide with the elementary spectra but were expanded by the elementary spectra. A sophisticated test aerosol generation equipment [8] made it possible to get experimental information sufficient to obtain an acceptable condition number of the equation system connecting the set of granulometer records with the known spectra of the test aerosols. This makes it possible to calculate the unknown elements of the apparatus matrix from the system.

A detailed algorithm for one method of complex graduation of a granulometer is presented in [10]. According to this algorithm the parameters of a theoretical model of the electric spectrometer are determined by the fitting of theoretically calculated quantities to the respective empirical quantities obtained in the measurement of etalon aerosols and the analysis of aerosol precipitation gathered on the channel electrodes. A necessary precondition here was the formulation of a preliminary algorithm for a quick computation of particle charge distribution in any condition of unipolar charging [4, 11, 12].

The approach to the graduation of aerosol granulometers described in the above article was also used for the analysis of the properties of the well known *TSI-3030* [13, 14]. The apparatus matrix of the device was calculated according to the above-mentioned algorithm from the data of test aerosol measurement. Mathematical modeling demonstrated that traditional processing (the scale transformation method) of the *TSI-3030* records of a unimodal spectrum of atmospheric aerosol leads to the appearance of two peaks. This points to a danger of considerable misinterpretations of measurement results. This danger can be avoided if the results are processed in accordance with the principles presented in the above article.

References

1. Таммет Х.Ф. Об электрической гранулометрии аэрозолей // Уч. зап. Тарт. ун-та.- 1975.- Вып. 348.- С. 30-34.

2. Сальм Я.Й. Об униполярной зарядке первоначально заряженного аэрозоля // Уч. зап. Тарт. ун-та.- 1977.- Вып. 443.- С. 57-61. (See this volume pp. 68-71).

3. Ноппель М.Г. О распределении зарядов на аэрозольных частицах при зарядке их легкими аэроионами // Уч. зап. Тарт. ун-та.- 1982.- Вып. 631.- С. 85-93.

4. Ноппель М.Г. О распределении зарядов на аэрозольных частицах при униполярной зарядке их легкими аэроионами // Уч. зап. Тарт. ун-та.- 1983.- Вып. 648.- С. 32-40.

5. Фукс Н.А. О величине зарядов на частицах атмосферных аэроколлоидов // Изв. АН СССР.- Сер. геогр. и геофиз.- 1947.- No. 4.- С. 341-348.

6. Fuchs, N.A. On the stationary charge distribution on aerosol particles in a bipolar ionic atmosphere // Geofisica pura e applicata. - 1963.- Vol. 56, No. 3.- P. 185-193.

7. Таммет Х. Ф. Калибровка электрического гранулометра аэрозолей по распределению осажденных часиц // Уч. зап. Тарт. ун-та.- 1983.- Вып. 648.- С. 52-58.

8. Мирме А.А. О калибровке электрического спектрометра аэрозолей // Уч. зап. Тарт. ун-та.- 1987.- Вып. 755.- С. 71--79.

9. Тамм Э.И., Тамме В.Б., Кикас Ю.Э., Пейль И.А., Мирме А.А., Лангус Л.Э. Система получения эталонных аэрозолей с размерами от 0.1 нм до 10 мкм // Тез. докл. XIV Всес. конф. "Актуальные вопросы физики аэродисперсных систем".- Одесса, 1986.- Т.2.- С. 102.

10. Ноппель М.Г., Таммет Х.Ф. Метод и алгоритм вычисления аппаратной матрицы электрического спектрометра аэрозолей // Уч. зап. Тарту. ун-та.- 1987.- Вып. 755.- С. 62-70.

11. Noppel, M. Algorithm for rapid approximate calculation of the charge distribution of conductive aerosol particles charged in a strong electric field // Acta et comm. Universitatis Tartuensis.- 1985.- N 707.- P. 84-93.

12. Ноппель М.Г. О зарядке и разядке аэрозольных частиц в сильных электрических полях // Уч. зап. Тарт. ун-та.- 1984.- Вып. 669.- С. 25-30.

13. Мирме А.А. и др. Измерение спектров калибровочных аэрозолей. Сравнение анализатора TSI со спектрометром ТГУ // Уч. зап. Тарт. ун-та.- 1987.- Вып. 755.- С. 80-88.

14. Noppel, M. Analysis of measurement methods of aerosol size spectrum with electrical analyzer TSI-3030 // Acta et comm. Universitatis Tartuensis.- 1990.- N 880.- P. 67-83.

SPECTRA OF NEAR-GROUND ATMOSPHERIC AEROSOLS

Ü. Kikas, V. Kimmel and A. Mirme

Introduction

Aerosol particles cover a wide size range from a couple of nanometers to some tens of micrometers. Their size distribution is one of the most important characteristics of atmospheric aerosols. The spectra of number, surface or mass concentrations contribute significant information about the character of processes in the aerosol.

Various shapes of particle number distributions are encountered in measurements. A monomodal spectrum is characteristic of stratospheric aerosol but it has also frequently been measured in near-ground unpolluted air [1, 2, 3]. Since Whitby [4] many authors support the multimodal model of number distribution of atmospheric aerosols. According to Jaenicke [5] a multimodal distribution is typical of both countryside aerosol and tropospheric background aerosol. The measurements of Hoppel [3] in the central part of the Atlantic Ocean showed clearly bimodal distribution functions of marine aerosol. A dropping spectrum with monotonously descending number concentrations towards larger particles is mainly described for urban areas [6].

The identification of different types of spectra in natural measurements is connected with the variety and peculiarities of atmospheric processes during measurement. Partially, as suggested by M. Noppel [7], it may be conditioned by the use of different equipment and methods by different authors.

The present paper gives a survey of atmospheric aerosol spectra measured at different locations of Baltic region in different conditions, but with the same equipment. The paper focuses on the density functions of the distribution of the number concentration.

Models of atmospheric aerosol spectra

Classically, the number distribution of over 0.1 μm dia particles is described by Junge's formula

$$N(r) \sim r^{-b}. \qquad (1)$$

Most measurement results in the atmosphere have agreed with the formula satisfactorily, whereas the power b is about 4 .

V.I. Smirnov [8] has specified the distribution function of the particles of 0.1-20 μm radius. As a result of an analytical solution of the coagulation problem he has obtained a distribution function which can be presented by two power functions.

$$f(r)=\begin{cases} f_B(r) = C_B r^{-2.5}, & r_o \le r \le r^* \\ f_g(r) = C_g r^{-4.5}, & r^* \le r \le r_{max} \end{cases} \qquad (2)$$

where r^* is the transition radius between two functions. For normal atmospheric conditions $r^* \approx 1.01$ μm . Unfortunately, relevant literature does not contain data on the comparison of measurement data with formula (2).

The picture of the distribution of particle sizes below 0.1 μm is considerably less clear. Junge's and Smirnov's formulas are not suitable for the description of the spectrum in the region below 0.1 μm. They yield an unlimited growth of the number of particles when the sizes of the particles decrease. The measurements, however, show a decrease or only a slight increase of the number concentration towards finer particles.

Several empirical distribution functions have been proposed for the description of the spectrum of the number concentration in a wide size range from 0.01 to 20 μm. A good survey of the models can be found in H. Tammet [9] who also proposes a new 4-parameter KL model distribution:

$$n_1(r) = \frac{A}{(r/r_x)^K + (r_x/r)^L}, \qquad (3)$$

where $n_1(r) = dN(r)/d(\ln r)$. One of advantages of this distribution is a good physical interpretability of the parameters: K and L, respectively, are the slopes of the right and the left asymptotes of the distribution, whereas r_x and A are the coordinates of the intersection of the asymptotes. Depending on whether $L < 0$ or $L > 0$, the KL formula describes a monomodal or a dropping spectrum.

The multimodal spectrum is usually described by means of the sum of the log-normal distributions.

The measurement conditions

The analysed spectra have been obtained as a result of 4 measurement series carried out in the Baltic region. The measurement locations are: the city of Tartu, Estonia (July 1987 and January 1989 - Tartu.JU, Tartu.JA), the clean air field station at Voore in Estonian inland (August 1987), the coastal field station of Preila on the Kura Peninsula, Lithuania (August 1989). The measurements were carried out round the clock with intervals 5 min (15 min at Preila). Most of the spectra are those of a fair weather; rain, thunderstorm, fog, haze or snow were observed in about 20% of the measurement time. The height of the measurement place from the ground varied between 3 m and 6 m. The length of a series of measurements did not exceed 11 days, thus the seasonal changes are not represented in the data. Total of about 5400 spectra has been analysed.

The diversity of the measurement conditions makes it possible to conjecture that the analysis gives a picture of the aerosol spectra occurring in the Baltic region.

In all series a Tartu University electrical aerosol spectrometer *EAS* was used. The spectrometer gives a 12-fraction representation of the spectrum in the region 0.01-10 μm.

The frequency of occurrence of different types of spectra

All three above-mentioned shapes of spectra were present in the analysed spectra. Fig. 1 presents examples of types of spectra.

The frequencies of occurrence of spectra of different shapes are presented in Table 1. Those differ strongly at different locations.

Table 1

Frequencies of occurrence of different types of spectra in %

Location	No. of spectra	dropping	monomodal	bimodal
Voore	1612	7.8	85.9	6.3
Preila	861	6.7	49.6	43.9
Tartu.JU	1695	38.5	61.4	0.1
Tartu.JA	1228	12.8	86.7	0.5

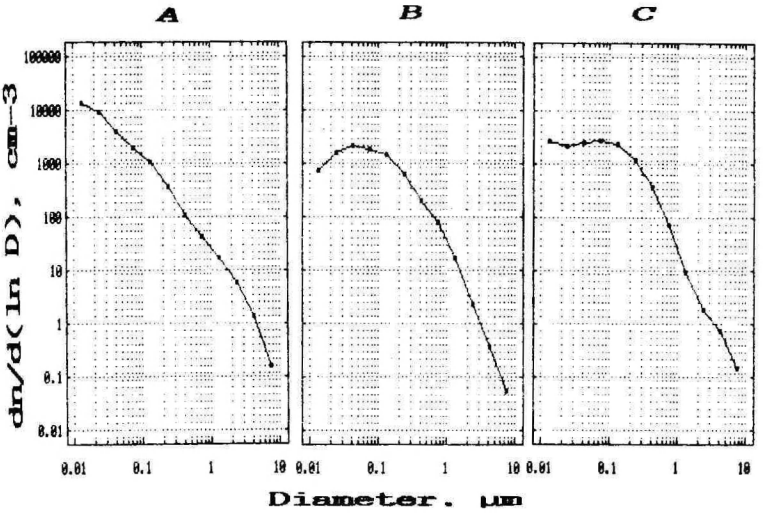

Fig. 1. a - dropping spectrum (Tartu, July 10, 8:30-9:30 (the mean of 12 spectra)
b - monomodal spectrum (Voore, August, average of nighttime (603 spectra)
c - bimodal spectrum (Preila, August 20-21, 23:00-16:00 (the mean of 64 spectra).

It can be seen that the dominant spectrum is monomodal one at all the measurement locations. It is explained by the case when the generation of small particles from the gaseous state does not fully compensate their transformation into larger fractions.

Numerous bimodal spectra were observed only at Preila. It may be a general property of the coastal aerosol, or a peculiarity of the weather during the measurement period. The data do not enable to unambiguously decide for either of the explanations. At Preila, the occurrence of the bimodal spectra was connected with haze (Fig. 2). On four days when the hollow spectrum occurred almost throughout the whole sunny period, haze or low fog clouds were observed. On the other hand, only few bimodal spectra occurred in clear sunny days when the UV-radiation of the sun contained a high proportion of shortwave radiation. The clear peak of bimodal spectra was present in fractions 3, 4, or 5, i.e. in the diameter range 0.03-0.2 µm and the fine particles peak below 0.01 µm.

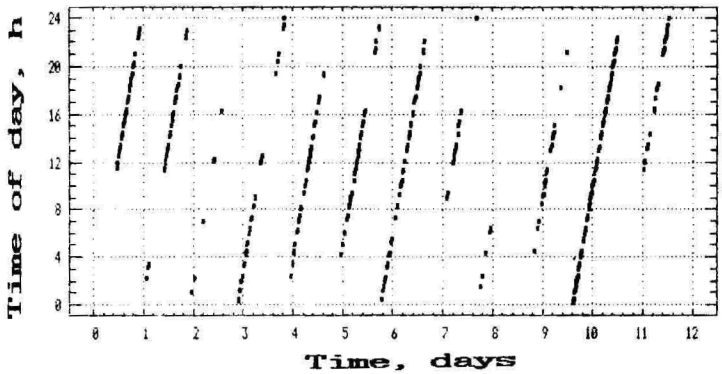

Fig. 2. The time of day of the occurrence of the bimodal spectra at Preila.

Dropping spectra were in significant amounts observed only in urban air in summer. The formation conditions of this kind of spectrum are an intense generation of fine particles on the one hand, and their relatively slow passage into the larger fractions on the other hand. The results of Tartu.JU confirm the hypothesis that the intensity of particle generation is determined by the amount of polluting gases and by the photochemical processes in these gases: the frequency of occurrence of dropping spectra (Fig. 3.1) corresponds to the daily variations of solar irradiation (Moscow time two hours ahead the local time is used) and to the life rhythm of city.

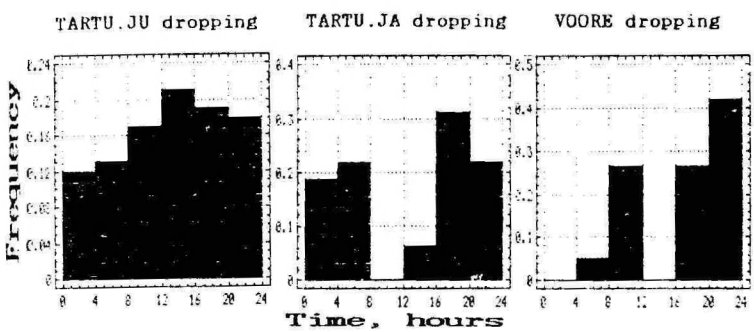

Fig. 3. Daily frequencies of occurrence of dropping spectrum: 1. Tartu, July; 2. Tartu, January; 3. Voore, August.

Somewhat unexpectedly, in winter Tartu.JA series, there are few dropping spectra and their daily frequency variation (Fig. 3.2.) does not correspond to the variation of solar irradiation. Rather, it is similar to the frequency distribution at Voore (Fig. 3.3) where dropping spectra occur mainly in the evening or at night. In most cases their appearance is connected with increased air humidity. The high concentration level on the one hand and the dominance of the monomodal spectra shape on the other hand can be explained by the intensive precipitation of fine particles to submicron and coarse particles which occur more often in the winter spectrum (Table 2).

The average spectra, total number, and mass concentration are presented in Table 2.

The dominance of monomodal spectra at Voore can be expected. At a location investigated with an aim of setting up a regional background station we really observed a low intensity of the generation of new particles, the monomodal shape of the spectrum and generally low particle concentration.

Table 2

Average number concentration spectra

Frac. No.	Limits μm	Tartu.JU cm^{-3}	Tartu.JA cm^{-3}	Voore cm^{-3}	Preila cm^{-3}
1	.010-.018	3688	2685	625	1520
2	.018-.032	3584	3852	1144	1420
3	.032-.056	2074	2405	1191	1321
4	.056-.10	1210	1345	985	1229
5	.10-.18	600	731	763	1028
6	.18-.32	217	295	327	552
7	.32-.56	62	112	102	194
8	.56-1.0	23	40	35	46
9	1.0-1.8	9.8	13	8.7	6.8
10	1.8-3.2	2.7	3.1	1.4	1.1
11	3.2-5.6	.55	.61	.27	.35
12	5.6-10.0	0.5	.06	.03	.08
Total number cm^{-3}		11600	11500	5207	7318
Total mass $\mu g \cdot cm^{-3}$.		67	87	48	63

The mean spectra are not in all locations of the monomodal type: in summer in Tartu, July and at Preila they are dropping. At Preila this effect is created by the simultaneous influence of the dropping and bimodal spectra, in Tartu, July the reason is the influence of relatively few spectra with very high concentrations of fine particles.

Approximation of atmospheric aerosol spectra with model spectra

An aerosol spectrum obtained with an electrical spectrometer is actually a 13-parameter model of the real spectrum, whereas the spectrum is described as a superposition of 13 triangular elementary spectra. In many cases the description of the spectrum in such detail is not necessary and a model with a smaller number of parameters may be used. To study the use of model spectra, the average spectra of measurement series have been compared with above described models.

Table 3 presents the powers of the power function approxi-

Table 3

Approximation parameters of average spectra for a power function or the KL-function

Approx. func.	$rf(r)=r^{b_j}$			$rf(r) = \frac{A}{(r/r_x)^K + (r_x/r)^L}$
Approx.limits:μm	.1-10	.1-1	1-10	.01 - 10
Parameter / Location	b_1	b_2	b_3	K
Voore	-2.5	-1.8	-3.2	2.2
Tartu. JU	-2.2	-1.9	-3.0	2.0
Tartu. JA	-2.2	-1.7	-3.1	1.7
Preila	-2.5	-1.8	-2.5	3.2
Junge (1)	-3*	-	-	-3
Smirnov (2)		-1.5*	-3.5*	

* The powers in formulae (1,2) and in the Table 5 are different by 1 because different representations are used.

mations of average spectra and K-parameter of the KL-approximation, comparing them to the parameters of the respective Junge's (1) or Smirnov's (2) formulas. It can be seen that in the region 0.1-10 μm the approximation of the spectrum with two power functions according to (2) is fully justified. Selecting $r^* \approx 1$ μm we obtain a good agreement with the parameters of Smirnov's formula.

An exception among the agreeing parameters b_2 and b_3 is b_3 at Preila. Also correlation analysis for Preila showed that the range of particles over 1 μm behaved practically independently of the rest of the spectrum. Supposedly an independent source of large particles formed by seaspray was active there. As can be seen in Table 3, Junge's two-parameter model does not make it possible to identify such peculiarity in the spectrum.

In Table 3 the parameter K of the KL-model fluctuates more than Junge's or Smirnov's parameters. This is caused by the dependence of K on the position of the maximum of the spectrum. Thus, the KL-approximation is not useful when only description of the spectra of large particles is needed.

The KL-model makes it possible to approximate monomodal and dropping spectra in a wide size range. Thus, bimodal spectra (in the present case about 13% of all spectra) were left out of the description. Table 4 presents the parameters of the KL-model of the average spectra of the measurement locations. An original computer program compiled by H. Tammet was used for the approximation.

Table 4

Parameters of the KL-approximation of average spectra

Parameter / Location	A	r_x	K	L
Voore	4068	47	2.2	0.6
Tartu, JU	9394	19	2.0	-0.2
Tartu, JA	12259	17	1.7	0.8
Preila	1935	134	3.2	-0.1

Generally, the KL-parameters describe spectra in correspondence with the 13-parameter model. To demonstrate that,

the pairwise comparison of the daily variations of the parameters of two models was done. Some more pronounced examples are presented in Fig. 4.

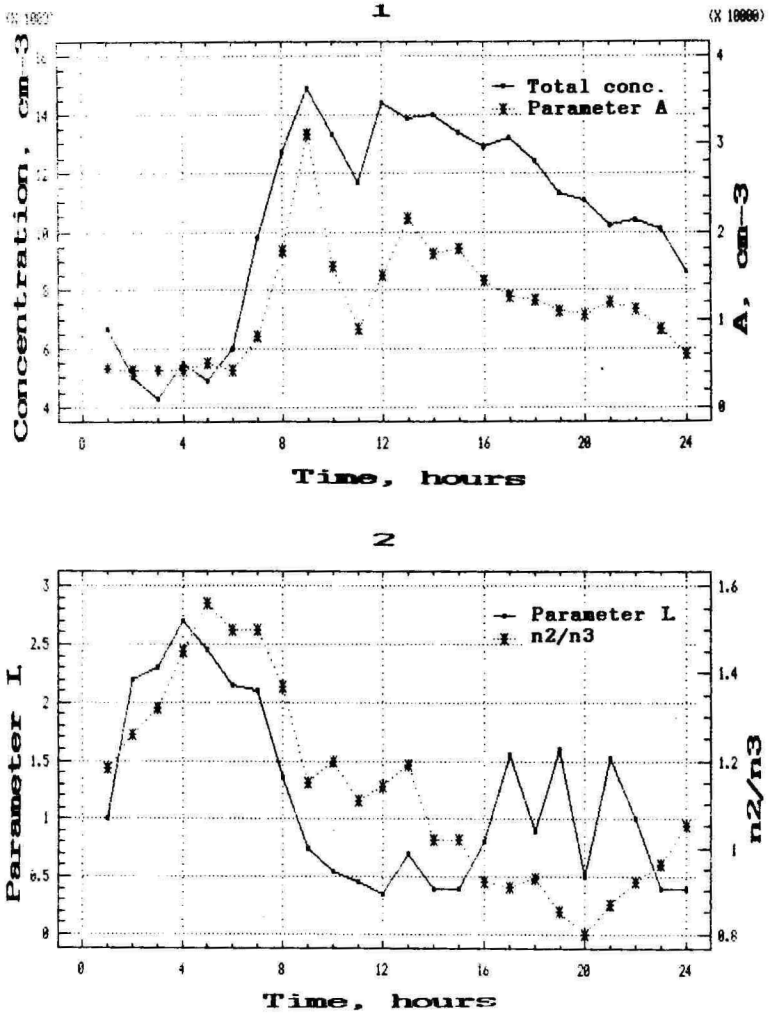

Fig. 4. Daily variations of the KL-model and the measured spectrum parameters: 1. KL-parameter A and the total particle concentration S, 2. KL-parameter L and the ratio of fine particle fraction concentrations N_3/N_2, Voore.

It can be seen that the average daily variations of KL-parameter A and of the total particle concentration N (Fig. 4.1) have quite similar walks.

The parameter L and the ratio of fraction concentrations N_3/N_2 describe the slope of the left wing of spectra and characterize the rate of particle generation: the higher L and N_3/N_2 the smaller the generation rate of fine particles. The average daily walks (Fig. 4.2) of the above parameters are similar before 16.00. The oscillation of the parameter L in the evening-time can be explained by its dependence on the spectral mode, which changes together with relative humidity of air.

Conclusions

Analysing the number concentration spectra of atmospheric aerosol measured during about 900 hrs at different times and at different locations, we met spectra of three different shapes: dropping (16.4% of the cases), monomodal (71.1%), and bimodal (12.7%). The frequency of occurrence of different types was significantly dependent on the measurement location.

The appearance of the spectrum of a certain type was not connected with quick fluctuations of the aerosol. Once arisen, a spectral type was usually maintained over several hours. The monomodal spectrum was more likely in regions with cleaner air, at night and in winter. The dropping spectrum was more likely in polluted air, in daytime and in summer. The bimodal spectra were frequent among the spectra of coastal aerosol on days with haze.

In the approximation of the coarse part (d > 0.1 μm) of the average spectra in representation $rf(r)$ with power functions we obtained Junge's constant between -2.2 and 2.5, Smirnov's formula (3) constants between 1.7 and 1.9; -2.5 and -3.2, respectively. For the description of spectra the use of the Smirnov's formula is preferable, especially, when the independent coarse particle sources are acting.

The fitting of atmospheric aerosol spectra by KL-model gives a good agreement with 13-parameter model for the dropping and monomodal spectra types.

References

1. Lopez, A., Lecouteux, G., Prieur, S., Fontan, J. Etude de la formation de particules à partir des hydrocarbures naturels dégagés par la végétation // J. Aerosol Sci. - 1983. - Vol. 14, No. 2.- P. 99-111.

2. Kikas, Ü., Mirme, A., Tamm, E. Size distribution dynamics of rural and urban aerosols. // Acta et comm. Universitatis Tartuensis.- 1990.- N 880.- P. 84-93.

3. Hoppel, W.A. et al. Atmospheric aerosol size distributions and optical properties found in the marine boundary layer over the Atlantic Ocean. / Washington, 1989.- Naval Research Laboratory Report 9188.- 73 p.

4. Whitby, K.T., Husar, R.B., Liu, B.Y.H. The aerosol size distribution of Los Angeles Smog // J. Colloid Interface Sci.- 1972.- Vol. 39, A61.- P. 179-204.

5. Янике П. Проблемы распределения глобального аэрозоля // Успехи химии.- 1990.- Т. 59.- С. 1654-1675.

6. Pill-Soo Kim. Size distribution of Atmospheric Aerosols in Seoul // Atmos. Envir.- 1986.- Vol. 20, No. 10.- - Pp. 1837-1845.

7. Noppel, M. Analysis of measurement methodes of aerosol size spectrum with electrical analyzer TSI 3030 // Acta et comm. Universitatis Tartuensis.- 1990.- N 880.- P. 67-64.

8. Смирнов В.И. Решения семейства уравнений стационарной коагуляции и модель спектра размеров частиц атмосферного аэрозоля // Изв. АН СССР ФАО.- 1977.- Т. 13, N 3.- С. 274- -287.

9. Таммет Х.Ф. Сравнение модельных распределений аэрозольных частиц по размерам // Уч зап. Тарт. ун-та.- 1988.- Вып. 824.- С. 92-108. (See this volume pp. 136-149).

COMPARISON OF MODEL DISTRIBUTIONS OF AEROSOL PARTICLE SIZES

H. Tammet

Introduction

A model distribution is described by a mathematical expression containing free parameters which are used for fitting the empirical data. These parameters may be related in more or less complex way with common physical entities, e.g., average particle size, etc. A multiplier depending on integral particle concentration is considered as one of the parameters of the model distribution.

In this paper the problem of creating model distributions will be considered without an emphasis on the physical theory of phenomena. It is presumed that the model will be used as a tool for the description of empirical data, and its main criteria of quality are the precision of fitting the data, interpretational simplicity, and mathematical convenience.

Mathematical structure makes it possible to distinguish simple and compound model distributions. Distributions which cannot be reduced to a sum of independently analysable component distributions are called simple. Compound distributions are sums of various simple distributions. The number of parameters of a compound distribution is the sum of the numbers of parameters of its component distributions. The following theoretical considerations are general and concern both, simple and compound distributions. However, the examples deal only with simple distributions.

As a rule, a model distribution with a large number of free parameters, guaranteeing a high precision of curve fitting, is not distinguished by other criteria of quality. Practically, atmospheric physicists have been using simple models with one (distribution a/r^3 of Junge) to six (Smerkalov's distribution [1]) parameters. For different practical tasks there are different optimum model distributions depending on the subset of observations, on the requirements of precision, interpretability, and mathematical convenience. The present paper will study the criteria of quality of model distributions and the application of these criteria in the comparison of some well-known model distributions meant for the description of tropospheric aerosols. A new model distribution (KL-distribution) will be described and investigated.

List of symbols

Continuous distributions will be described using the following symbols:

r - effective, e.g. hydrodynamic, particle radius,

$N(r)$ - concentration of particles with radii below r ,

$n_0(r) = dN(r)/dr$ - function of distribution or spectrum of zero order,

$n_p(r) = r^p n_0(r)$ - spectrum of the p-th order,

$M_q(r) = r^q n_0(r)dr$ - $(q-p)$-th moment of the spectrum of the p-th order, e.g., q-th moment of the spectrum of zero order,

$\tilde{r}_p = (M_p/M_0)^{1/p}$ - average radius of the p-th order,

$\hat{r}_p$ - modal radius of the p-th order, $n_p(\hat{r}_p) = \max(n_p(r))$.

The most popular tool for the representation of spectra is the function $n_1(r)$, as $n_1(r) = dN(r)/d(\ln r)$.

The model distributions considered

The present paper will investigate only those model distributions which are meant for the description of tropospheric aerosol spectra in wide size range. Expressions of the function $n_1(r)$ are presented in Table 1. For the sake of shortness abbreviations will be used to denote distributions.

Table 1

Model distribution for tropospheric aerosol

Abbreviation	Expression	No of parameters
MG	$ar^{\alpha}\exp(-br^{\beta})$	4
S1A	$ar^{-k}\exp(-br^{-s})$	4
S1B	$a_1(\hat{r}_1/r)^k \exp((k/s)(1-(\hat{r}_1/r)^s))$	4
S2	$ar^{-k}\exp(-b/r - cr)$	4
KLO	$a/((r/r_x)^K + (r_x/r)^L)$	4
KL1	$a_1(K+L)/(L(r/r_1)^K + K(r_1/r)^L)$	4
SME	$a(\exp(-k(\lvert r-\hat{r}_1\rvert/r)^{\nu}))/(\hat{r}_1^{\nu} + \lvert r-\hat{r}_1\rvert^{\nu^*})$	6

Table 1 does not include the log-normal distribution and Junge's one-wing distribution a/r^k, as they are used for the description of tropospheric aerosol only in a limited size range.

An analysis of a model distribution usually starts with

the study of its asymptotes, whereas, certain theoretical and empirical premises are taken into account. For instance, according to Smoluchowski's theory of coagulation growth of particles in the conditions of uniform nucleation the left asymptote (small sizes) conforms to the power law. On the other hand, Junge's empirical law points to the power dependence for the right asymptote.

Short comments to the distributions presented in Table 1 are as follows.

MG - well-known modified γ-distribution with power asymptote on the left strongly deviates from Junge's law on the right wing.

S1A - thoroughly described and analysed in [2] by V.I. Smirnov.

S1B - obtained from S1A by elementary transformation of the set of parameters :

$$\hat{r}_1 = (bs/k)^{1/m}, \quad a_1 = a\hat{r}_1^{-k} \exp(-k/s). \qquad (1)$$

The shape of curve and fitting precision by S1A is the same as by S1B and both distributions are called S1. The difference between the two variants becomes evident only in the analysis of stability.

S1 is obtained from MG by inversion of signs of the powers. Therefore the powers in the expressions of MG and S1 are to be considered to be non-negative by definition. S1 has a power asymptote on the right wing which makes it possible to consider S1 as a generalization of Junge's law.

Distributions MG and S1 as special cases of one general distribution were defined by K.S. Shifrin [3].

S2 has been proposed by V.I. Smirnov [4] as a component of a compound distribution.

Distributions KL0 and KL1 are related to each other similarly to the relation of S1A and S1B. Their common denotation in KL. The transformation of the set of parameters is as follows :

$$\hat{r}_1 = (L/K)^{1/(K+L)} r_x, \quad a_1 = aL^{L/(K+L)} K^{K/(K+L)}/(K+L). \qquad (2)$$

L.G. Makhotkin [5] proposed the following estimate of the average spectrum of tropospheric aerosol :

$$n_1(r) = \frac{r^{0.5}}{1 + br^{3.5}}. \qquad (3)$$

This is a good approximation to V.A. Smerkalov's estimate which has been presented in a more complicated form [1]. KL - distribution may be regarded as a generalization of distribution (3).

Model distribution SME has been introduced in [1]. The expression of average spectrum of tropospheric aerosol proposed in the presentation of SME found recognition, but there have been no applications of the distribution itself as a tool of curve fitting. The reason is its evident mathematical inconvenience.

Geometric and analytical properties of KL-model

KL-distribution has power asymptotes both on the left and the right wing. All the parameters of the distribution have a simple interpretation at graphic depiction curve $n_1(r)$ in the logarithmic coordinate grid, presented in Fig. 1.

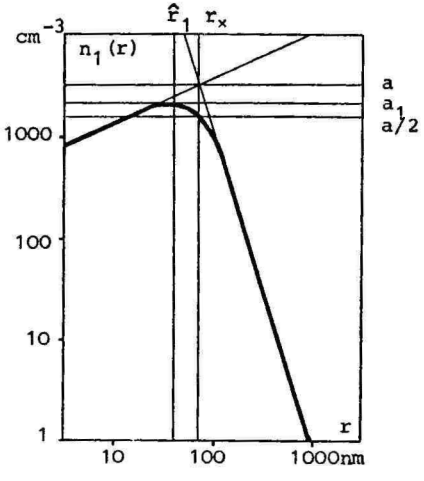

Fig. 1. KL-distribution. a, r_x - coordinates of the intersection point of the asymptotes, a_1, $\hat{f}_1$ - coordinates of the maximum point, L - ascent of the left asymptote, K - descent of the right asymptote. The values of the parameters correspond to Table 2.

Moments of distribution exist when $-L < q < K$ and are expressed in elementary functions :

$$M_q = a\pi r_x^q \;/\; \{(K+L)\,\sin(\pi\frac{L+q}{K+L})\}. \qquad (4)$$

Integral particle concentration:

$$M_0 = a\pi \;/\; \{(K+L)\,\sin(\pi\frac{L}{K+L})\}, \qquad (5)$$

average radii:

$$\bar{r}_p = \{\sin(\pi\frac{L}{K+L}) \;/\; \sin(\pi\frac{L+p}{K+L})\}^{1/p} r_x, \qquad (6)$$

modal radii:

$$\hat{r}_p = \left(\frac{L - 1 + p}{K + 1 - p}\right)^{1/(K+L)} r_x. \qquad (7)$$

Distribution KL1 is definite when $K > 0$ and $L > 0$. The scope of KL0 is limited only by the condition $K + L > 0$. Practically this is a considerable advantage of KL0 as one often has to deal with empirical distributions which can be well approximated by KL at negative values of the parameter L.

In atmospheric physics KL-distribution may be used in the size range from some nanometers to the upper limit of the applicability of Junge´s law.

Description of the precision of a model

The precision of a model is determined by error of fitting of given spectra using the model. Let us describe a given spectrum with a column vector n which consists of the values of the function $n_p(r)$ over a finite set of radii r_1, r_2... . If the approximation of this spectrum with the model is m , then the error of the approximation is expressed by the vector $e = m - n$. The most natural scalar measure of approximation error is the probabilistic norm

$$\delta^2 = e^T D^{-1} e \ , \qquad (8)$$

where D is the covariation matrix of the errors of measured points of the spectrum curve.

Matrix D is to be given together with the test spectrum n. In the case of description of the precision of the model as

such, it is necessary to determine the conditional standard form of the matrix D. The simplest way is to presume the independence of measurement errors of various points of the spectrum curve and proportionality of errors to the quantities measured. The coefficient of proportionality can have an arbitrary value. Let it be chosen so that $D_{ii} = n_i^2/k$, where k is the number of the values of radii in the representation of the spectrum. Then

$$\delta^2 = \frac{1}{k} \sum_{i=1}^{k} \left(\frac{m_i - n_i}{n_i} \right)^2 , \qquad (9)$$

and δ is interpreted as a quadratic mean relative error of approximation.

In the case of the set of l test-spectra, we denote the approximation error of the j-th spectrum through δ_j. If the weights of all test-spectra are the same, then the total estimate of the error will be

$$E^2 = \frac{1}{l} \sum_{j=1}^{l} \delta_j^2 . \qquad (10)$$

This quantity is used as an "inverse" measure of the precision of the model.

Loss of measurement information in the interpretation of measurement results

It is said that the aim of measurement is not numbers, but understanding. The part of measurement information used in this understanding could be called useful information while the unused part could be called lost information. The cognitive role of a model in data analysis consists in its power to yield meaningful interpretations of the values of the parameters of the model. In a model representation the measurement information is given by:

- values of the parameters,
- estimates of measurement errors of these values,
- estimates of correlation between measurement errors of the values of different parameters.

A meaningful interpretation uses information given by the values and estimates of measurement errors of the parameters, whereas the information given by the estimates of correlation of errors is, as a rule, lost. This is illustrated by the example in Fig. 2.

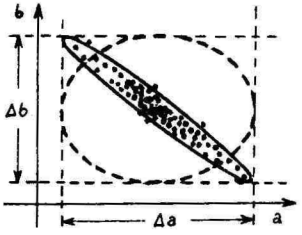

Fig. 2. Results of repeated measurements of the parameters (a, b) of the same spectrum in a bi-parametrical model.

Every dot in Fig. 2 depicts the results of one measurement, the scatter of dots shows measurement errors. Fig. 2 presents simultaneously the ellipse of scattering at a certain confidence level for a two-dimensional measurement result, and the intervals of scattering Δa and Δb separately for every parameter. In the interpretation of measurement results the parameters are considered separately in accordance with their physical content. For instance, parameter a can be the concentration and b - the particle mean radius. The uncertainty of the results is described by the values Δa and Δb ,and the information given by the narrow diagonal form of the ellipse of scattering is lost. This is equal to the replacement of the real ellipse of scattering in Fig. 2 by a wide ellipse shown in Fig. 2 by the indented line. The amount of lost information equals

$$\Delta I = \log \frac{S_2}{S_1} , \qquad (11)$$

where S_2 and S_1 are the areas of the wide and the narrow ellipse. It is easy to demonstrate that

$$\Delta I = \frac{1}{2} \log \frac{1}{1 - R^2} , \qquad (12)$$

where R is the coefficient of correlation between the measurement errors of the parameters a and b .

The same amount of information will be lost, if we increase by K times the measurement errors of every parameter where

$$K = \sqrt{\frac{S_2}{S_1}} . \qquad (13)$$

The quantities ΔI and K are formally equivalent and in practice the one giving a more comprehensible description of the loss of information should be preferred.

Description of the stability of the model

It is said that a model has a poor fitting stability if small disturbances in the approximated spectrum cause large disturbances in the values of the parameters guaranteeing the best approximation. In such cases the ellipse of the scatter of parameter values is strongly elongated, whereas its area may be small. Therefore poor stability is accompanied by large information loss in the interpretation of parameter values. In computational mathematics stability is described by the condition number of the matrix of fitting problem. There are different definitions of the condition number. As there is no expressive interpretation, the use of this concept in our problem is limited. This paper proposes to describe the level of model instability by the amount of information lost in interpretation or by the coefficient of equivalent amplification of measurement errors which are more expressive parameters in our problem.

To generalize the results obtained in the preceding section, let us consider a problem of fitting the spectrum n using the model $m(p)$, where n and m are finite vectors determined on the set of radii r_1 , r_2 , ..., and p is a vector whose elements are the scalar parameters of the model. The dependence of the deviation vector $e = m - n$ on the parameters p could be non-linear. Therefore stability is viewed as a local property depending on the spectrum.

Let us study stability in the neighbourhood of the spectrum $m(p^\circ)$ which is given by certain values of parameters p° . Linear approximation of errors in the neighbourhood of this spectrum is

$$e = B\,(p - p^\circ)\ , \tag{14}$$

where B - is the Jacobi matrix whose elements

$$B_{ji} = \frac{\partial m_j}{\partial p_i} \tag{15}$$

are calculated in the point p°. Here the index i counts the radii and the index j scalar parameters. The fitting problem is reduced to the task of minimizing the error δ^2 , represented by formula (8) , and it is solved by the well-known methods of the theory of least squares. The solution can be written as:

$$C = (B^T D^{-1} B)^{-1}$$
$$p = p^o + CB^T D^{-1} (n - m(p^o)) \quad . \tag{16}$$

Here C - the covariation matrix of parameter values if the spectrum n varies in accordance with the covariation matrix D.

The size of the region of scattering of parameter values calculated by (16), is proportional to det C, which is juxtaposed with the area of the narrow ellipse in Fig. 2. The interval of scattering of the j-th parameter is proportional to C_{jj}. If to ignore the correlations, the size of the scattering region of the parameters will be determined by the product $\prod_j \sqrt{C_{jj}}$ juxtaposed with the area of the wide ellipse in Fig. 2. The respective amount of lost information is

$$\Delta I = \frac{1}{2} \log \frac{\prod_j C_{jj}}{\det C} \tag{17}$$

and the coefficient of equivalent amplification of errors is

$$K = \left(\frac{\prod_j C_{jj}}{\det C} \right)^{1/(2h)} , \tag{18}$$

where h - number of scalar parameters.

Other characteristics of the quality of a model

The most important factor of the quality of a model is the cognitive value of its parameters. Unfortunately, there is no way of measuring this factor, and thus expert opinions are decisive.

Practical use of the model depends also on its mathematical convenience. Here three aspects can be mentioned :

1) analytical complexity of the model,
2) complexity and laboriousness of curve fitting using graphic procedures and simple calculations,
3) complexity and laboriousness of a more precise curve fitting usually done by the method of least squares.

There are, again, no exact criteria for the description of mathematical convenience. In this case, however, expert opinions can be supported by some procedures. To estimate analytical complexity, it is necessary to present the expressions of the moments of distributions and characteristic radii. To estimate complexity and laboriousness of an approximation, it is necessary to describe or point out the re-

spective methods and to determine the amount of computation on a standard set of test spectra.

Test spectra for checking the precision and stability of the model

Below in the examples of comparison of model distribution two sets of test spectra are used. The first consists of one spectrum

$$n_1(r) = \frac{a \exp(-0.42\,|1 - 30\text{nm}/r|^{0.47})}{0.000416 + 10^{-6}|r/\text{nm} - 30|^3}, \qquad (18)$$

which is proposed in [1] as the average spectrum of tropospheric aerosols. The second consists of 271 spectra and is obtained as follows. A. Mirme et al. [6] recorded 1661 spectra of tropospheric aerosol near Zvenigorod in the summer 1986. This set has been taken as a basis. All the spectra are presented in a seven-point grid of radii 5, 9, 16, 28, 50, 89, and 158 nm, in the range of this grid the relative measurement error in nearly uniform. 306 spectra turned out to be polymodal and were discarded. The rest were averaged by sets of 5 successively measured spectra. As a result, a set of 207 spectra was obtained, whereas most of them are averages over time interval of about 20 min.

Comparison of the precision of model distributions

The test spectrum (18) has exact presentation in terms of the model SME. The error of fitting of this spectrum with other models is described by Table 2.

Table 2

Model	Approximation of spectrum (18) at $a = 1$	Average relative error
S1A	$2.67\ 10^{15} r^{-4.54} \exp(-36.1 r^{-0.315})$	36%
S1B	$2660(18.4/r)^{4.54} \exp(-36.1 r^{-0.315})$	36%
S2	$3.06\ 10^{7}\ r^{-2.4} \exp(-36.1/r - 0.00049 r)$	70%
KL0	$3100/((r/72)^{3.15} + (72/r)^{0.44})$	7%
KL1	$2140\ 3.59/(0.44(r/42)^{3.15} + 3.15(42/r)^{0.44}$	7%

Table 2 does not contain the model MG which in approximating spectrum (18) is inferior to the model S1. The formal procedure minimizing the error of MG-approximation approaches

the point of inversion where the distribution is not determined and will be transformed into S1.

The results of the comparison of models in the fitting of 271 empirical test spectra are presented in Table 3.

Table 3

Precision of model distributions in the fitting of 271 empirical spectra on a 7-point logarithmic grid of radii from 5 to 158 nm

Model	Relative error average	Relative error maximum	Frequency of turning out as best of compared models
MG	12%	48%	22%
S1	16%	40%	10%
S2	13%	36%	19%
KL	8%	18%	48%

In the execution of computations for Table 3 with MG the limitations $\beta > 0.1$, and with S1 $s > 0.1$, were set up. Without limiting the polarity, the procedure of searching the best fit would "step over" the inversion, and reach S1 in 1/3 of cases, and MG in 2/3 of cases. The limitation of the absolute value was used to avoid losses of computational precision due to the instability of absolute values of the parameter below 0.1.

Comparison of the stability of model distributions

Stability has been studied in the neighbourhood of the best approximations of test spectra (19) described in Table 2. In contrast to precision (which does not change in reversible transformations of the set of parameters of the model) stability is significantly dependent on the representation of the set. Stability is also dependent on the covariation matrix of the disturbances of the spectrum D. Computations have been executed on the assumption of a diagonal structure of the matrix. Let us consider two variants :

- variant of a constant absolute error D_{jj} = const,
- variant of a constant relative error D_{jj} = const$\cdot n_1^2(r_j)$.

The second variant is closer to real situations. Computation results are brought in Table 4.

Table 4

Stability characteristics of the model distributions in the neighbourhood of the average spectrum of tropospheric aerosols according to V.A. Smerkalov, computed on a 13-point logarithmic grid of radii from 5 to 5000 nm.

Model	Constant absolute error ΔI:bit	ΔI:digits	K	Constant relative error ΔI:bit	ΔI:digits	K
SШ	11.7	3.5	3.8	8.9	2.7	2.8
S1A	20	6	32	12.6	3.8	8.9
S1B	4.3	1.3	2.1	4.0	1.2	2.0
S1	10.0	3.0	5.6	4.7	1.4	2.2
KL0	3.2	1.0	1.7	3.2	1.0	1.7
KL1	2.0	0.5	1.4	2.2	0.7	1.5

The reasons for poor stability can be studied by analysing the structure of the Jacobi matrix. For instance, in the case of the distribution S1A, the angle between the row vectors, corresponding to the parameters a and s is below 2°. The analysis of the structure of the Jacobi matrix also helps to make proposals for the transformation of the set of parameters in order to build more stable variants of model distributions.

Comparison of computational complexity of model distributions

Methods for the simplified fitting of spectra with the distributions MG and S1 are described in [3] and [2], respectively.

The simplified fitting using the model KL0 can be carried out graphically on a logarithmic coordinate grid (see Fig.1). Straight linear asymptotes are easy to estimate with a transparent ruler. On the condition of uniform relative error the precision of this method is close to that of the numerical method of least squares. An additional guideline to prove the asymptotes is the condition $n_1(r_x) = a/2$. The parameters could be measured as is shown in Fig. 1.

For an exact approximation by the method of least squares the models MG, S1, and S2 are considered on a logarithmic scale, whereas S2 will be linear in reference to all para-

meters, and MG and S1 retain non-linear dependencies on one parameter. The model KL gets the form :

$$1/n_1(r) = pr^K + qr^{-L}, \qquad (20)$$

which retains a non-linear dependence on two parameters. A necessary additional transformation is:

$$r_x = (q/p)^{1/(K+L)}, \quad a = 1/pr_x^K. \qquad (21)$$

The spectrum is to be transformed simultaneously with the estimates of measurement errors or the weights of points of the spectrum by the method of least squares.

In the case of the linear parameters of the transformed model, the computational procedure uses the standard linear algorithm of the least squares method. In the case of the rest of the parameters, methods of the extreme problems are to be used; this takes a considerably greater computational effort. The productivity of an approximation of spectra given in 7 points was empirically determined by means of an Iskra-226 personal computer using a Basic interpreter. The results are presented in Table 5.

Table 5

Productivity of approximation on PC Iskra-226

Model	Spectra per min.
MG	4
S1	4
S2	25
KL	2

The computational complexity of SME is significantly higher than that of the other considered models.

Conclusions

For a comparison of different model distributions it is necessary, on the level of expert decision:

- to estimate the cognitive value of every model which is expressed in the interpretation of parameters;
- to estimate the mathematical convenience of every model;
- to determine the set of test spectra for the calculation of quantitative characteristics of the performance of models.

Characteristics of precision and stability of the model and of laboriousness of the approximation of empirical spectra could be determined on the level of quantitative calculations.

Special attention in the comparison of models should be paid to the estimate of stability, as poor stability brings along not only computational difficulties but, more importantly, large losses of measurement information at the stage of interpretation of results.

A comparison of model distributions of tropospheric aerosols shows that KL-distribution suggested in this paper has the best quantitative characteristics among the considered models.

References

1. Смеркалов Б.А. Аппроксимация среднего распределения аэрозольных частиц по размерам // Изв. АН СССР, ФАО.- 1984.- Т.20, No.4. - С.317-320.

2. Смирнов В.И. Об аппроксимации эмпирических разпределений по размерам облачных капель и других аэрозольных частиц // Изв. АН СССР, ФАО.- 1973.- Т.9, No.1.- С.54-65.

3. Шифрин К.С. О вычислении радиационных свойств облаков // Тр. ГГО.- 1955.- Вып.46 (108).- С.5-33.

4. Smirnov V.I. On the mechanisms responsible for the formation of typical size spectra and vertical distribution of tropospheric aerosol particles // Eleventh International Conf. on Atmospheric Aerosols, Condensation and Ice Nuclei.- Budapest, 1984. Vol.1.- P.82-86.

5. Махоткин Л.Г. Многолетний ход величин атмосферного электричества по наблюдениям ГГО // Тр. ГГО.- 1990.- Вып.527.- С.3-7.

6. Мирме А.А., Кикас Ю.Э., Тамм Э.И. Динамика спектра атмосферного аэрозоля приземного слоя // Уч. зап. Тарт. ун-та.- 1988.- Вып.842.- С.109-122.

Translated from:

Таммет Х.Ф. Сравнение модельных распределений аэрозольных частиц по размерам // Уч. зап. Тарт. ун-та.- 1988.- Вып.824.- С.82-108.

ELECTRICAL PARAMETERS OF AIR POLLUTION

H. Tammet

Electrical parameters of the air

In the theory of electrical conductivity of the air, the electrical condition of the air is described by means of the distribution function or the spectrum of charge density by air ion mobility. The distribution function can be perfectly described only through an infinite table of values. Full determination of a function by measurement is impossible.

In practical measurements we are to be satisfied with a finite-dimensional description of the electrical condition of the air. Sophisticated equipment used for laboratory investigations makes it possible to measure partial charge densities for about ten mobility fractions. In ordinary geophysical observations it is possible to measure only few integral parameters.

A question arises as to which integral air electricity parameters should be measured. Below it will be assumed that the parameters to be measured are to:

1) give a maximum information useful in applications,
2) measurable with simple and reliable equipment.

Factors of the electrical condition of the air

The average time of existence of a small air ion is only about one minute. Therefore the electrical condition of the air is in a dynamic balance and depends on some primary factors. The main factors are:

1) ionizing radiation,
2) aerosol composition of the air.

The electrical condition of the air is somewhat dependent on the chemical composition of its gaseous phase. This, however, is reflected only in fine effects and will not be considered below.

The primary factors of the electrical condition of the air are directly connected with air pollution, and therefore the electrical condition of the air can be considered as a pollution indicator. This points to an important application of air electricity measurements and is to be taken into account already in the stage of the determination of the main integral electrical parameters of the air.

Small air ions

Small air ions make up an isolated group in the air ion mobility spectrum. Due to their high mobility they determine the main part of the conductivity of the air. The measurement of small air ions is easier than the measurement of other fractions in the air ion mobility spectrum.

Above the zone of the ground-layer electrode effect the concentrations of negative and positive air ions are nearly equal. Small air ions have relatively stable average mobilities and the concentrations of small air ions are in a nearly functional manner connected with the polar conductivities of the air.

Let us assume that the concentration of both negative and positive small air ions is n. Then the rate of small air ion loss on the account of recombination is αn^2 where α is the relatively stable coefficient of recombination. The rate of small air ion loss on the account of collisions with neutral and charged aerosol particles is gn, where the coefficient of adsorption g depends only on the aerosol composition of the air. As a rule gn is considerably larger than αn^2. If ionizing radiations generate small air ions with the rate q, then

$$\frac{dn}{dt} = q(t) - \alpha n^2 - gn. \qquad (1)$$

This differential equation determines the function $n(t)$. The solution of the equation depends on the function $q(t)$ and on the coefficient g. If the ion generation is constant, the balance $q = \alpha n^2 + gn$ is obtained.

The ionization rate

The ionization rate is determined by the intensity of ionizing radiations. A part of air ions, usually 10-20%, are generated by cosmic radiation, the rest are generated by radioactivity. As cosmic radiation is a stable factor, the ionization rate can be considered as an integral characteristic of radioactive pollution of the environment.

The traditional measurement unit of the ionization rate 1J means that one pair of elementary charges is formed in 1 s in 1 cm^3. The unit in SI is 1 $A/m^3 = 6.24 \cdot 10^{12}$ J. As a practical unit 1 pA/m^3 is acceptable.

The ionization rate is the first integral air electricity

parameter that can be considered as an indicator of atmospheric pollution.

Aerosol electrical density

Integral aerosol density is defined by the equation

$$\nu_p = \int p(r)f(r)dr, \qquad (2)$$

where $f(r)dr$ is the numeric density or the concentration of aerosol particles with radii from r to $r+dr$, and $p(r)$ is the weight function. When $p(r)\equiv 1$ we get the numeric density, when $p(r) = r^2$ - the surface density, when $p(r) = r^3$ - the volume density. A special weight function in equation (2) describes the optical density of aerosol. It is possible to determine a special weight function so that $\nu_p = g$. Therefore the adsorption coefficient of small air ions g can be considered as aerosol electrical density.

In comparison with other integral parameters, aerosol electrical density more completely characterizes the effect of aerosol in electrical processes. Supposedly, aerosol electrical density is correlated with the effect of aerosol in some other processes. The range of application of the concept of aerosol electrical density expands over the limits of specific electrical phenomena.

The measurement unit of aerosol electrical density is s^{-1}. Aerosol electrical density is the second integral air electricity parameter that can be considered as a characteristic of atmospheric pollution.

Measurement methods

The classical method of ionization rate measurement by means of an ionization chamber does not make it possible to create a simple and reliable measurement equipment. It is evident that for this reason in the practice of atmospheric electricity research the ionization rate is dealt with relatively seldom.

Equation (1) points to a possibility of simultaneous measurement of ionization rate and aerosol electrical density using a simple device - a counter of small air ions. For this purpose the counter is to be supplemented by a generator of small air ions having a reasonable constant ionization rate.

The concentration of small air ions n_1 is measured at a switched-off and n_2 at a switched-on air ion generator. Both

measured variables are dependent on the arguments q and g:

$$n_1 = f_1(q,g) \qquad (3)$$
$$n_2 = f_2(q,g)$$

The parameters of the air ion generator are taken into account in the expression of the function f_2. The system of equations (3) is solved in relation to the unknown members q and g. The function f_2 is weakly dependent on the argument q. This ensures a well-conditioned system of equations and quick convergence of the iterations by numerical solution.

Translated from:

Таммет Х.Ф. Электрические параметры загрязненности воздуха // Уч. зап. Тарт. ун-та.- 1977.- Вып. 443.- С. 48-51.

NOTES ON THE INTERPRETATION OF AEROSOL ELECTRICAL DENSITY

H. Tammet

Concept of aerosol electrical density

The term "aerosol electrical density" has been proposed in [1] to denote the coefficient g in the balance equation of small air ions

$$\frac{dn}{dt} = q - \alpha n^2 - gn, \qquad (1)$$

where n - the concentration of small air ions,

q - the ionization rate, and

α - the coefficient of recombination of small air ions.

Equation (1) is written on the assumption of charge symmetry $n_+ = n_- = n$.

The unit of measurement of aerosol electrical density is s^{-1}. For the ground layer of the atmosphere the typical values are $g = 0.01\text{-}0.1\ s^{-1}$. In tabulating measurements it is useful to apply the unit ks^{-1}, then the typical numerical values will be 10-100 and can be written as integers.

The interpretation of aerosol electrical density from the point of view of atmospheric electricity and the study of electrical processes in the air is given directly by the determination of this value. Aerosol electrical density is the measure of adsorption of small air ions by the aerosol. For the interpretation of aerosol electrical density from the point of view of other possible applications of the notion, it is necessary to determine the weight function $w_g(r)$ that would make it possible to define aerosol electrical density as a particular case of the generalised aerosol density

$$g = \int w_g(r) f(r) dr, \qquad (2)$$

where $f(r)$ is the size distribution function of particles normed to the number concentration of aerosol particles $N = f(r)dr$.

Equation of the weight function of aerosol electrical density

To calculate the function $w_g(r)$ the summand gn in equation (1) is to be expressed through the coefficients of attachment of small air ions by particles of a certain size and preliminary charge.

Let us use $\beta_q(r)$ to denote the partial attachment coefficient of a positive small air ion to a particle with the radius r and charge qe, where e is the elementary charge. On the assumption of charge symmetry, the coefficients of the attachment of a negative small air ion by a positively charged particle, and of a positive small air ion by a negatively charged particle $\beta_{-q}(r)$ are equal. The attachment coefficients are determined so that the flow of positive small air ions to a particle with the charge qe is $\beta_q n$.

Let us use $p_q(r)$ to denote the probability of the charge qe on a particle with the radius r.

The concentration of particles with the charge qe and the radius $r \ldots r + dr$ will be $p_q(r)f(r)dr$. The adsorption of small air ions by these particles is $n\beta_q(r)p_q(r)f(r)dr$. To find total adsorption gn, the resulting expression is to be summarized by all charges and integrated over all sizes: $gn = \int \sum n\beta_q(r)p_q(r)f(r)dr$. Cancelling n, we obtain the equation for calculating g. Comparing this equation with the expression of generalised aerosol density (2) it can be noticed that

$$w_g(r) = \sum_q \beta_q(r)p_q(r). \qquad (3)$$

Approximation of the function β (r)

In the region of Knudsen small numbers (r>100nm) the first formula of Fuchs [2] has a good theoretical and experimental foundation

$$\beta_q(r) = 4\pi r D \frac{\varkappa}{e^{\varkappa}-1}, \qquad (4)$$

where

$$\varkappa = q\frac{e^2}{4\pi\varepsilon_0 rKT},$$

K - the Boltzmann constant and T - the temperature. The diffusion coefficient of small air ions is calculated by the Einstein formula

$$D = \frac{KTk}{e}, \qquad (5)$$

where k - air ion mobility. At $k = 1.2 \cdot 10^{-4}$ m^2/V·s and T = 290 K we have $\varkappa = q(57.6 \text{ nm} / r)$.

The inadequacy of formula (4) in the region of Knudsen large numbers is demonstrated by the fact that instead of the experimentally confirmed limiting value $\beta_{-1}(0) = \alpha =$

= 1.4-1.6·10^{-12} m^3/s, it gives a higher value 2.2·10^{-12} m^3/s. The simplified molecular kinetic theory of White also gives an incorrect limit $\beta_{-1}(0) = 0$. Pui's well-known semi-empirical formula is at $r \to 0$ reduced to White's formula and gives the same result.

A correct molecular kinetic adsorption theory has been proposed by Natanson [5]. Unfortunately, Natanson has not specified the methods of calculating certain variables, the values of which are necessary for concrete calculations. This gap in Natanson's theory was filled by Hoppel [6] who also carried out concrete numerical calculations. Due to the amount of computations involved the results are limited to a table of four coefficients β_1, β_0, β_{-1}, β_{-2} for a certain set of sizes. On a different basis, the adsorption theory was developed by Fuchs [7] who proposed another fairly complex formula. Kojima [8] demonstrated that the discrepancy between Hoppel's results and the second formula of Fuchs does not exceed experimental error, and that experiment agrees with general theoretical results. He also proposed a simplified empirical formula which sufficiently well approximates experimental data of measuring $p_1(r)$. However, it is not satisfactory for approximating the function $\beta_\delta(r)$ in the whole region of definition. In fact, Kojima's improvement strengthens, rather than weakens the conflict of formula (4) with experiment in the case of determining $\beta_{-1}(0)$.

Computerized search yielded a simple empirical formula which at r<100 nm satisfaciorily approximates Hoppel's table and at r>100 nm is quickly reduced to the first formula of Fuchs:

$$\beta_\delta(r) = 4\pi r D \frac{\varkappa}{e^{\varkappa}-1} \left(1 - \frac{7}{7+10\delta^2+r:\text{nm}}\right). \qquad (6)$$

Here $\varkappa$ is determined by formula (4) and r:nm denotes the numerical value of the radius in nm.

Calculation of the weight function of aerosol electrical density

If the function $\beta_\delta(r)$ is known, then the function $p_\delta(r)$ for uniform distribution can be calculated according to the known procedure. Let us denote partial concentrations of particles with the charge δe and the radius $r \ldots r + \Delta r$ with N_δ. The sum of flows proceeding from a fraction as a result of

air ion adsorption is equal to the sum of flows entering this fraction. The balance of the zero fraction gives $\beta_0 N_0 = \beta_{-1} N_1$ and makes it possible to express N_1 through N_0. The balance of the i-th fraction makes it possible to express N_{i+1} through N_i. In practical calculations it is necessary to select an arbitrary value of N_0, to calculate recurrently all significant

$$N_i = \frac{\beta_{i-1}}{\beta_{-i}} N_{i-1}$$

and then

$$p_i(r) = N_i / (N_0 + 2 \sum_{i=1}^{\infty} N_i). \qquad (7)$$

The results of concrete calculations are depicted in the Figure by dots.

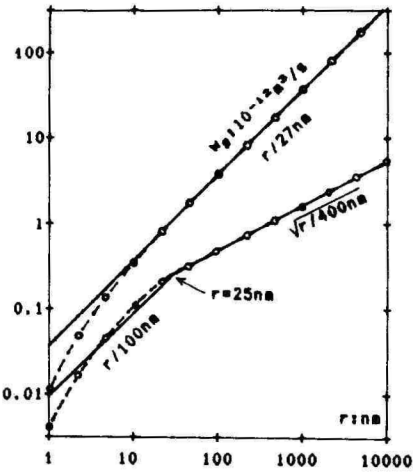

Fig. Approximation of the functions $w_g(r)$ and $w_*(r)$.

The function $w_g(r)$ in the region of large values of the radius approaches the straight line $w_g(r) = (r / 27\ \text{nm}) \cdot 10^{-12}\ \text{m}^3/\text{s}$. This follows from the fact that all significant coefficients β_i are simultaneously approaching the diffusion limit $\beta = 4\pi r D$ which is independent of i, and that the value w_g in accordance to formula (3) is viewed as a weighted average of β_i by i. In the region $r<10$ nm, w_g is approximately proportional to $r^{1.15}$. If the particles with $r<5$ nm are negligible, then the function is approximated by the formula

$$w_g(r) \approx \frac{r}{27\ \text{nm}}\ 10^{-12}\ \text{m}^3/\text{s}, \qquad (8)$$

where the value of the coefficient 27 corresponds to the assumption $k = 1.2 \cdot 10^{-4}\ \text{m}^2/\text{V}\cdot\text{s}$.

Comparative interpretation of large ion concentration

An effective concentration of large air ions N_* where every particle is taken into account γ times can also be represented as a generalised aerosol density:

$$N_* = \int w_*(r) f(r) \mathrm{d}r. \qquad (9)$$

As $N_* = \int \sum \gamma p_\gamma(r) f(r) \mathrm{d}r$, then

$$w_*(r) = \sum_{\gamma=1}^{\infty} \gamma p_\gamma(r). \qquad (10)$$

Results of the calculations carried out according to formula (10) are also presented in the Figure. This function cannot be approximated as simply as the function w_g. The simplest approximation is as follows

$$w(r) = \begin{cases} \dfrac{r}{100\ \text{nm}} & \text{at } r \le 25\ \text{nm} \\ \sqrt{\dfrac{r}{400\ \text{nm}}} & \text{at } r \ge 25\ \text{nm}. \end{cases} \qquad (11)$$

This approximation does not ensure a simple mechanical interpretation of the concentration of large air ions as an integral characteristic of aerosol.

Mechanical interpretation of aerosol electrical density

In approximation (8) aerosol electrical density is proportional to size concentration of aerosol particles. The size concentration ν_d is determined as a generalised aerosol density at the weight function $w = 2r$. It has an imaginable mechanical interpretation - the value of ν_d indicates the length of the chain composed of all particles in a volume unit. In approximation (8) we obtain the conversion formulae

$$g \approx \left(0.0185\ \frac{\text{m}^2}{\text{ks}}\right) \nu_d, \qquad \nu_d \approx \left(54\ \frac{\text{ks}}{\text{m}^2}\right) g. \qquad (12)$$

The values of ν_d = 540-5400 m^{-2} correspond to the values g = = 10-100 ks^{-1} typical for the ground layer atmospheric air. ν_d = 1000 m^{-2} means that the length of the chain composed of particles in 1 m^3 will be 1 km.

The concepts of particle size concentration and aerosol electrical density are useful everywhere where the effect of aerosol particles is approximately proportional to their size.

References

1. Таммет Х.Ф. Электрические параметры загрязненности воздуха // Уч. зап. Тарт. ун-та.- 1977.- Вып. 443.- С. 48-51.

2. Фукс Н.А. О величине зарядов на частицах атмосферных аэроколлоидов // Изв. АН СССР. Сер. геогр. и геофиз..- 1947.- Т. 11, N. 4.- С. 341-348.

3. White, J.H.J. Particle charging in electrostatic precipitatiton // AIEE Trans.- 1951.- Vol. 70.- P. 1186-1191.

4. Pui, D.Y.H. Experimental study of diffusion charging of aerosols // University of Minnesota Particle Technology Laboratory Publication N 288.- Minneapolis, 1976.- 213 p.

5. Натансон Г.Л. К теории зарядки амикроскопических аэрозольных частиц в результате захвата газовых ионов // Ж. техн. физ.- 1960.- Т. 30, N. 5.- С. 573-588.

6. Hoppel, W.A. Ion-aerosol attachment coefficients and diffusional charging of aerosols // Electrical processes in Atmospheres.- Darmstadt: Steinkopff, 1977.- P. 60-69.

7. Fuchs, N.A. On the stationary charge distribution on aerosol particles in a bipolar ionic atmosphere // Geofis. pura e appl.- 1963.- Vol. 56, N 3.- P. 185-193.

8. Kojima, H. Measurements of equilibrium charge distribution on aerosols in bipolar ionic atmosphere // Atmospheric Environment.- 1978.- Vol. 12.- P. 2363-2368.

Translated from:

Таммет Х.Ф. К интерпретации электрической плотности аэрозоля // Уч. зап. Тарт. ун-та.- 1984.- Вып. 669.- С. 31-38.

Comment:

The improved calculation of $w_g(r)$ is published in paper:

Tammet, H. Aerosol electrical density: interpretation and principles of measurement // Report series in aerosol science.- Helsinki, 1991.- N 18.- P. 128-133.

LIST OF PUBLICATIONS OF TARTU UNIVERSITY ON AIR ELECTRICITY IN 1986-1991

Compiled by L. Langus and H. Tammet

1. Арольд М.У., Таммет Х.Ф., Матизен Р.Л., Хыррак У.Э. Атмосферно-электрические наблюдения на о. Вильсанди // Тез. докл. III Всес. симпоз. по атмосферному электричеству.- Тарту, 1986.- С. 20.

Observation of atmospheric electricity on the Island of Vilsandi.

2. Бирюков Ю.Г., Загайнов В.А., Кикас Ю.Э., Мирме А.А., Пейль И.А., Сутугин А.Г., Тамм Э.И., Успаленко Т.Г. Исследование конденсационного роста заряженных аэрозольных частиц // Тез. докл. III Всес. симпоз. по атмосферному электричеству.- Тарту, 1986.- С. 67.

Investigation of condensation growth of charged aerosol particles.

3. Загайнов В.А., Лушников А.А., Бирюков Ю.Г., Успаленко Т.Г., Кикас Ю.Э., Мирме А.А., Тамм Э.И. Исследование образования высокодисперсных аэрозольных частиц в коронном разряде // Тез. докл. V Всес. конф. "Аэрозоли и их применение в народном хозяйстве".- Москва, 1987.- Т. 1. - С. 37.

Investigation of the formation of high-dispersity aerosol particles in corona discharge.

4. Лутс А.М., Сальм Я.Й. Кинетика образования положительных легких аэроионов в тропосфере // Уч. зап. Тарт. ун-та.- 1988.- Вып. 824.- С. 60-68.

The kinetics of the evolution of positive small air ions in the troposphere.

5. Кикас Ю.Э. О качестве калибровочных аэрозолей, полученных электрическим сепарированием // Уч. зап. Тарт. ун-та.- 1987.- Вып. 755.- С. 106-112.

On the quality of electrically separated calibration aerosols.

6. Кикас Ю.Э., Киммель В.А., Мирме А.А., Тамм Э.И. Спектры атмосферного аэрозоля приземного слоя // Тез. докл. IV Всес. симпоз. по атмосферному электричеству.- Нальчик, 1990.- С. 207-208.

Spectra of atmospheric aerosol of the ground layer.

7. Кикас Ю.Э., Коломиец С.М., Корниенко В.И., Мирме А.А., Сальм Я.Й., Сергеев И.Я., Таммет Х.Ф. Комплексное измерение

характеристик аэрозоля и аэроионов в приземном слое атмосферы // Тр. ин-та эксперим. метеорологии.- 1990.- Вып. 51 (142).- С. 109-117.

The complex measurement of the characteristics of aerosol and air ions in the ground layer of the atmosphere.

8. Кикас Ю.Э., Мирме А.А., Круув Х.А., Тамм Э.И. Генератор монодисперсного аэрозоля.- А. с. 1388103 СССР, В 05 В 17/04.- Заявл. 12.09.86, опубл. 15.04.88, Бюл. No. 14.

A generator of monodisperse aerosol.

9. Кикас Ю.Э., Мирме А.А., Тамм Э.И. Наблюдения городского аэрозоля // Тез. докл. XV Всес. конф. Актуальные вопросы физики аэродисперсных систем.- Одесса, 1989.- Т. 2.- С. 114.

Measurement of urban aerosol.

10. Матизен Р.Л. Методика обеспечения эксплуатационной надежности счетчиков аэроионов // Тез. докл. III Всес. симпоз. по атмосферному электричеству.- Тарту, 1986.- С. 82.

Methodology of guaranteeing operational reliability of air ion counters.

11. Матизен Р.Л. Климатические испытания счетчиков аэроионов // Уч. зап. Тарт. ун-та.- 1987.- Вып. 755.- С. 58-61.

Climate tests of air-ion counters.

12. Матизен Р.Л. К методике расчета эксплуатационной надежности аэроэлектрической аппаратуры // Уч. зап. Тарт. ун-та. - 1988.- Вып. 809. С. 103-110.

The methods for computing reliability of air electricity measurement devices.

13. Матизен Р.Л., Маасепп Я.Х., Ээвель Я.Р., Миллер Ф.Г., Таммет Х.Ф., Сальм Я.Й., Сеппер Т.В. Счетчики аэроионов ТГУ // Тез. докл. III Всес. симпоз. по атмосферному электричеству.- Тарту, 1986.- С. 86.

Air ion counters of Tartu State University.

14. Мирме А.А. О калибровке электрического спектрометра аэрозолей // Уч. зап. Тарт. ун-та.- 1987.- Вып. 755.- С. 71-79.

About the calibration of the electrical aerosol spectrometer.

15. Мирме А.А. Учет погрешностей калибровки аэрозольного спектрометра // Уч. зап. Тарт. ун-та.- 1988.- Вып. 809.- С. 111-117.

Calibration errors accounting for aerosol spectrometer.

16. Мирме А.А., Кикас Ю.Э., Тамм Э.И. Динамика спектра

атмосферного аэрозоля приземного слоя // Уч. зап. Тарт. ун-та.- 1988.- Вып. 824.- С. 109-122.

The dynamics of the near ground atmospheric aerosol spectra.

17. Мирме А.А., Кикас Ю.Э., Тамм Э.И. Генератор монодисперсного аэрозоля. - А.с. 1634330 СССР, В 05 В 17/04.- Заявл. 29.07.88, опубл. 15.03.91, Бюл. No. 10.

A generator of monodisperse aerosol.

18. Мирме А.А., Рейнарт А.Э., Кикас Ю.Э., Тамм Э.И., Дубровин М.А., Бернотас Т.П., Пейль И.А. Измерение спектров калибровочных аэрозолей. Сравнение анализатора TSI со спектрометром ТГУ // Уч. зап. Тарт. ун-та.- 1987.- Вып. 755.- С. 80-88.

Measurement of calibration aerosol spectra. Comparison of the TSI aerosol analyzer with the aerosol spectrometer of Tartu State University.

19. Мирме А.А., Тамм Э.И. Многоканальный метод электрической спектрометрии аэрозолей // Тез. докл. Всес. конф. "Примеси - трассеры атмосферных процессов".- Вильнюс, 1989.- С. 36-37.

A multi-channel method of aerosol electric spectrometry.

20. Мирме А.А., Тамм Э.И., Таммет Х.Ф., Кикас Ю.Э. Использование электрической спектрометрии для регистрации аэрозольной загрязненности атмосферы // Современные методы и средства автоматического контроля атмосферного воздуха и перспективы их развития. Тез. докл. - Киев, 1987. - С. 182-183.

Application of electric spectrometry for the registration of aerosol pollution of the atmosphere.

21. Мирме А.А., Таммет Х.Ф., Ноппель М.Г., Тамм Э.И. Пределы применимости электрического метода спектрометрии аэрозолей // Тез. докл. XV Всес. конф. Актуальные вопросы физики аэродисперсных систем.- Одесса, 1989.- Т. 1.- С. 229.

Limits of the applicability of the electrical method of aerosol spectrometry.

22. Незгада В.Ю., Сабутис А.К., Рейнет Я.Ю. Возможности нейтрализации электростатических зарядов текстильных материалов с помощью униполярного аэрозоля // Уч. зап. Тарт. ун-та.- 1987.- Вып. 755.- С. 198-203.

Possibility of neutralizing electrostatic charges of textile materials by means of unipolar aerosols.

23. Ноппель М.Г. Влияние начального распределения на распределение зарядов частиц при их униполярной зарядке в сильном электрическом поле // Уч. зап. Тарт. ун-та.- 1988.- Вып. 809.- С. 118-126.

The influence of initial charge distribution on the charge distribution of particles in unipolar charging in a strong electric field.

24. Ноппель М.Г. О влиянии несферичности частиц при электрической спектрометрии размеров аэрозолей // Уч. зап. Тарт-ун-та.- 1988.- Вып. 824.- С. 84-91.

On the influence of nonsphericality of particles at the electrical spectrometry of aerosol sizes.

25. Ноппель М.Г. Анализ методики измерения спектра размеров аэрозоля прибором TSI-3030 // Тез. докл. Всес. конф. "Примеси - трассеры атмосферных процессов".- Вильнюс, 1989.- С. 37-38.

An analysis of the methodology of aerosol size spectrometry with TSI-3030.

26. Ноппель М.Г. Теория и методика определения аппаратной матрицы электрического анализатора аэрозолей. Автореф. дис. на соиск. учен. степ. канд. физ.-мат. наук.- Л., 1989.- 16 с.

The theory and methodology of the determination of the apparatus matrix of the electrical aerosol analyzer.

27. Ноппель М.Г., Пейль И.А. Электрические заряды мелкодисперсных аэрозольных частиц // Тез. докл. III Всес. симпоз. по атмосферному электричеству.- Тарту, 1986.- С. 56.

Electric charges on fine aerosol particles.

28. Ноппель М.Г., Таммет Х.Ф. Метод и алгоритм вычисления аппаратной матрицы электрического спектрометра аэрозолей // Уч. зап. Тарт. ун-та.- 1987. Вып. 755.- С. 62-70.

Method and algorithm for the calculation of the apparatus matrix for the electrical aerosol spectrometer.

29. Партс Т.М. О природе положительных легких аэроионов односекундного возраста // Уч. зап. Тарт. ун-та.- 1988.- Вып. 824. С. 69-77.

On the nature of small positive air ions.

30. Партс Т.М. Спектрометрия подвижности легких аэроионов - одна из возможностей определения органических веществ в воздухе // Тез. докл. Всес. конф. "Примеси-трассеры атмосферных процессов".- Вильнюс, 1989.- С. 39-40.

Mobility spectrometry of small air ions: one of the

possibilities for the determination of organic compounds in the air.

31. Партс Т.М. О природе легких аэроионов односекундного возраста в приземном слое атмосферы // Тез. докл. IV Всес. симпоз. по атмосферному электричеству.- Нальчик, 1990.- С. 203.

On the nature of small air ions of one-second age in the ground layer of the atmosphere.

32. Партс Т.М., Сальм Я.Й. Воздействие примесей воздуха на подвижность легких аэроионов // Тез. докл. III Всес. симпоз. по атмосферному электричеству.- Тарту, 1986.- С. 53.

The influence of air admixtures on the mobility of small air ions.

33. Партс Т.М., Сальм Я.Й. Воздействие пиридина и некоторых его гомологов на спектр подвижности положительных легких аэроионов // Уч. зап. Тарт. ун-та.- 1988.- Вып. 809.- С. 71-78.

The effect of pyridine and its homologues on mobility spectra of positive small air ions.

34. Пейль И.А. Электростатический разбавитель аэрозоля // Уч. зап. Тарт. ун-та.- 1987.- Вып. 755.- С. 120-125.

An electrostatical aerosol diluter.

35. Пейль И.А., Тамм Э.И. Возникновение узкого биполярного распределения заряда на частицах аэрозоля // Тез. докл. XIV Всес. конф. "Актуальные вопросы физики аэродисперсных систем".- Одесса, 1986.- Т. 1.- С. 74.

Generation of the narrow bipolar charge distribution on aerosol particles.

36. Пейль И.А., Тамм Э.И., Зубченко П.Н., Холм И.К., Мяги Э.К. Генерирование узкого биполярного распределения заряда на частицах аэрозоля // Уч. зап. Тарт. ун-та.- 1987.- Вып. 755.- С. 89-97.

Generation of the narrow bipolar charge distribution on aerosol particles.

37. Прийман Р.Э., Виснапуу Л.Ю., Партс Т.М. Влияние некоторых антропогенных загрязнителей и их очистителей на спектры подвижностей легких аэроионов // Уч. зап. Тарт. ун-та. - 1988. - Вып. 824.- С. 138-145.

The influence of some human pollutants and its purifiers on mobility spectra of small air ions.

38. Прийман Р.Э., Таммет Х.Ф. Оценка допустимой мощности коронного аэроионизатора по критерию химического загрязнения

воздуха // Уч. зап. Тарт. ун-та.- 1987.- Вып. 755.- С. 166-174.

Assessment of the permissible power of the corona ionizer according to the criterion of the chemical pollution of the air.

38. Рейнарт А.Э., Мирме А.А. Автоматизация наблюдений за аэрозольными и аэроионными спектрами // Современные методы и средства автоматического контроля атмосферного воздуха и перспективы их развития. Тез. докл.- Киев, 1987.- С. 75-76.

Automation of the measurement of aerosol and air ion spectra.

40. Рейнарт А.Э., Мирме А.А., Пейль И.А., Таммет Х.Ф., Тамм Э.И., Сальм Я.Й., Бернотас Т.П., Миллер Ф.Г. Автоматизация наблюдений за аэроионами и аэрозолем в ТГУ // Тез. докл. III Всес. симпоз. по атмосферному электричеству.- Тарту, 1986.- С. 83.

Automation of aerosol and air ion measurement in Tartu State University.

41. Рейнет Я.Ю. Характеристика концентрации легких аэроионов // Тез. докл. III Всес. симпоз. по атмосферному электричеству.- Тарту, 1986.- С. 54.

Characteristics of the concentration of small air ions.

42. Сальм Я.Й. Баланс аэроионов при симметричной стационарной ионизации // Тез. докл. III Всес. симпоз. по атмосферному электричеству.- Тарту, 1986.- С. 52.

The balance of air ions at symmetrical stationary ionization.

43. Сальм Я.Й. Очерк истории Аэроэлектрической лаборатории Тартуского государственного университета // Ионизация, аэрозоли, электрометрия. Библиографический указатель науч. публикаций Тарт. гос. ун-та за 1946-1985 гг.- Тарту, 1986.- С. 8-14.

A survey of the history of the Air Electricity laboratory of Tartu State University.

44. Сальм Я.Й. Соединение аэроионов при симметричной стационарной ионизации // Уч. зап. Тарт. ун-та.- 1987.- Вып. 755.- С. 10-17.

Combination of air ions in the case of symmetrical steady-state ionization.

45. Сальм Я.Й. Распределение полярной плотности заряда тропосферных тяжелых аэроионов по подвижностям // Изв. АН

СССР. Физика атмосферы и океана.- 1988.- Т. 24. Вып. 5.- С. 561-563.

The mobility distribution of polar charge density of tropospheric large air ions.

46. Сальм Я.Й. Эквивалентный коэффициент прилипания аэроионов к частице аэрозоля // Тез. докл. XIV Всес. конф. "Актуальные вопросы физики аэродисперсных систем".- Одесса, 1986.- Т. 1.- С. 68.

The equivalent coefficient of the attachment of air ions to an aerosol particle.

47. Сальм Я.Й. Электрические характеристики тропосферного аэрозоля // Тез. докл. V Всес. конф. "Аэрозоли и их применение в народном хозяйстве".- Москва, 1987.- С. 28.

Electrical characteristics of the tropospheric aerosol.

48. Сальм Я.Й., Ихер Х.Р., Миллер Ф.Г. Способ индикации перегрева оборудования.- А.с. 1415080 СССР, G 01 K 7/40.- Заявл. 11.02.86, опубл. 07.08.88, Бюл. No. 29.

A method of indication of overheating of equipment.

49. Сальм Я.Й., Лутс А.М. Кинетика эволюции легких аэроионов // Тез. докл. III Всес. симпоз. по атмосферному электричеству.- Тарту, 1986.- С. 48.

Kinetics of the evolution of small air ions.

50. Сальм Я.Й., Лутс А.М. Кинетика образования отрицательных легких аэроионов в тропосфере // Уч. зап. Тарт. ун-та.- 1988.- Вып. 809.- С. 64-70.

Kinetics of the formation of small negative air ions in the troposphere.

51. Сальм Я.Й., Лутс А.М. Метод вычисления стационарных концентраций одного класса задач химической кинетики // Уч. зап. Тарт. ун-та.- 1988.- Вып. 824.- С. 52-59.

Method of the calculations of steady-state concentrations for a class of problems in chemical kinetics.

52. Сальм Я.Й., Таммет Х.Ф., Ихер Х.Р., Партс Т.М., Миллер Ф.Г. Возможности использования спектрометрии подвижности легких аэроионов для индикации загрязнений воздуха // Современные методы и средства автоматического контроля атмосферного воздуха и перспективы их развития. Тез. докл.- Киев, 1987.- С. 36-37.

Possibilities of using the mobility spectrometry of small air ions for the indication of air pollution.

53. Сальм Я.Й., Таммет Х.Ф., Ихер Х.Р., Хыррак У.Э. За-

висимость спектра подвижности легких аэроионов в приземном слое атмосферы от температуры и давления воздуха // Уч. зап. Тарт. ун-та.- 1988.- Вып. 809.- С. 87-94.

The dependence of small air ion mobility spectra in the ground layer of a... sphere on temperature and pressure.

54. Сальм Я.Й., Таммет Х.Ф., Ихер Х.Р., Хыррак У.Э. Атмосферно-электрические измерения в Тахкузе, Эстония // Вопросы атмосферного электричества.- Ленинград: Гидрометеоиздат, 1990.- С. 168-175.

Atmospheric electricity measurements at Tahkuse.

55. Тамм Э.И., Лангус Л.Э., Мирме А.А. Проверка работы электрического сепаратора аэрозолей в области больших частиц // Уч. зап. Тарт. ун-та.- 1987.- Вып. 755.- С. 98-105.

Checking of the operation of the electric aerosol separator in the range of large particle size.

56. Тамм Э.И., Мирме А.А., Кикас Ю.Э. Коронный разряд как генератор монодисперсного аэрозоля нанометрового диапазона // Уч. зап. Тарт. ун-та.- 1988.- Вып. 824.- С. 123-131.

Corona discharge as a generator of monodisperse aerosols in the nanometer range.

57. Тамм Э.И., Мирме А.А., Ноппель М.Г., Пейль И.А. Роль электрических методов в аэрозольных измерениях // Тез. докл. III Всес. симпоз. по атмосферному электричеству.- Тарту, 1986.- С. 91.

The role of electrical methods in aerosol measurements.

58. Тамм Э.И., Тамме В.Б., Кикас Ю.Э., Пейль И.А., Мирме А.А., Лангус Л.Э. Система получения эталонных аэрозолей с размерами от 10 нм до 10 мкм // Тез. докл. XIV Всес. конф. "Актуальные вопросы физики аэродисперсных систем".- Одесса, 1986.- Т. 2.- С. 102.

A system for obtaining etalon aerosols in the range 10 nm ... 10 μm.

59. Тамме В.Б. Повышение эффективности улавливания аэрозольных частиц отработавшими волокнистыми фильтрами // Уч. зап. Тарт. ун-та. 1988.- Вып. 824.- С. 132-137.

Enhancement of the filtering efficiency of aerosol particles by dust-filled fabric filters.

60. Тамме В.Б., Коппелмаа И.В. Вибрационный генератор монодисперсных аэрозолей // Уч. зап. Тарт. ун-та.- 1987.- Вып. 755.- С. 113-119.

Vibrating generator of monodisperse aerosols.

61. Таммет Х.Ф. Работы Н.Н. Комарова по теории аэроионных измерений // Тез. докл. III Всес. симпоз. по атмосферному электричеству.- Тарту, 1986.- С. 80.

The works of N.N. Komarov in the theory of air ion measurement.

62. Таммет Х.Ф. Теория метода совместного измерения интенсивности ионообразования и электрической плотности аэрозоля // Тез. докл. III Всес. симпоз. по атмосферному электричеству.- Тарту, 1986.- С. 92.

The theory of the method of simultaneous measurement of the intensity of ion generation and aerosol electric density.

63. Таммет Х.Ф. Теория метода совместного измерения интенсивности ионообразования и электрической плотности аэрозоля // Тр. III Всес. симпоз. по атмосферному электричеству.- Л., 1988.- С. 83-86.

The theory of the method of simultaneous measurement of the intensity of ion generation and aerosol electric density.

64. Таммет Х.Ф. Использование зарядника аэрозольных частиц как приставки к аэроионометру (счетчику аэроионов) // Уч. зап. Тарт. ун-та.- 1988.- Вып. 809.- С. 127-136.

The use of aerosol particle charger as an additional device to air ion counter.

65. Таммет Х.Ф. Сравнение модельных распределений аэрозольных частиц по размерам // Уч. зап. Тарт. ун-та.- 1988.- Вып. 824. - С. 92-108.

Comparison between model distributions of aerosol particle sizes.

66. Таммет Х.Ф. Отклик наземной антенны на вариации потенциала ионосферы // Магнитосферные исследования.- М., 1990.- N 15. С. 5-9.

Reaction of a ground based antenne to the variations of ionosphere potential.

67. Таммет Х.Ф., Ихер Х.Р., Сальм Я.Й. Спектр атмосферных ионов в диапазоне подвижности 0,32-3,2 см2/(В с) // Уч. зап. Тарт. ун-та.- 1987.- Вып. 755.- С. 29-46.

The spectrum of atmospheric ions in the range of 0.32-3.2 $см^2/(V \cdot s)$.

68. Таммет Х.Ф., Миллер Ф.Г., Матизен Р.Л., Ээвель Я.Р. Малогабаритный прибор для измерения электропроводности воздуха, концентрации и средней подвижности легких аэроионов //

Тез. докл. III Всес. симпоз. по атмосферному электричеству.- Тарту, 1986.- С. 87.

A small-size device for the measurement of air electric conductivity, concentration and average mobility of small air ions.

69. Таммет Х.Ф., Миллер Ф.Г., Матизен Р.Л., Ээвель Я.Р. Малогабаритный аэроионометр высокой предельной подвижности // Уч. зап. Тарт. ун-та.- 1988.- Вып. 809.- С. 95-102.

Small-size air ion meter of high limiting mobility.

70. Таммет Х.Ф., Миллер Ф.Г., Тамм Э.И., Бернотас Т.П., Мирме А.А., Сальм Я.Й. Аппаратура и методика спектрометрии подвижностей легких аэроионов // Уч. зап. Тарт. ун-та.- 1987. Вып. 755.- С. 18-28.

Apparatus and methods for the spectrometry of small air ions.

71. Таммет Х.Ф., Мирме А.А., Сальм Я.Й., Тамм Э.И., Миллер Ф.Г., Бернотас Т.П., Пейль И.А., Ноппель М.Г., Рейнарт А.Э., Лангус Л.Э., Кикас Ю.Э., Тамме В.Б. Аппаратура и методика спектрометрии подвижности аэроионов и аэрозольных частиц // Тез. докл. III Всес. симпоз. по атмосферному электричеству.- Тарту, 1986. С. 85.

Apparatus and methods of the mobility spectrometry of air ions and aerosol particles.

72. Таммет Х.Ф., Сальм Я.Й., Ихер Х.Р., Тамм Э.И., Мирме А.А., Кикас Ю.Э. Спектр подвижности аэроионов в приземном воздухе // Тез. докл. III Всес. симпоз. по атмосферному электричеству.- Тарту, 1986.- С. 47.

Air ion mobility spectrum in the ground layer.

73. Таммет Х.Ф., Сальм Я.Й., Ихер Х.Р., Тамм Э.И., Мирме А.А., Кикас Ю.Э. Спектр подвижности аэроионов в приземном воздухе // Тр. III Всес. симпоз. по атмосферному электричеству.- Л., 1988.- С. 46-50.

Air ion mobility spectrum in the ground layer.

74. Таммет Х.Ф., Сальм Я.Й, Партс Т.М., Лутс А.М. Кластерные аэроионы в тропосфере // Физика кластеров.- Новосибирск, 1987.- С. 86-91.

Cluster ions in the troposphere.

75. Таммет Х.Ф., Сальм Я.Й., Тамм Э.И., Кикас Ю.Э., Ноппель М.Г. Атмосферные ионы и аэрозоли (обзор непубликуемых докладов) // Тр. III Всес. симпоз. по атмосферному электричеству.- Л., 1988.- С. 89-97.

Atmospheric ions and aerosols (A survey of un-

published reports).

76. Хыррак У.Э. Статистические сводки результатов измерения атмосферных ионов и аэрозолей на о. Вильсанди летом 1984 года // Уч. зап. Тарт. ун-та.- 1987.- Вып. 755.- С. 47-57.

Statistical results of air ions and aerosol measurements on the island of Vilsandi in the summer of 1984.

77. Хыррак У.Э., Таммет Х.Ф., Ихер Х.Р., Сальм Я.Й. Зависимость спектра аэроионов от ветра (по измерениям в Тахкузе в 1985 году) // Уч. зап. Тарт. ун-та.- 1988.- Вып. 809.- С. 79-86.

The dependence of air ion spectra on wind by measurements in Tahkuse 1985.

78. Хыррак У.Э., Таммет Х.Ф., Сальм Я.Й., Ихер Х.Р. Суточный и годовой ходы атмосферно-ионизационных величин в Тахкузе // Уч. зап. Тарт. ун-та.- 1988.- Вып. 824.- С. 78-83.

Diurnal and annual variations of atmospheric ionisation quantities in Tahkuse.

79. Хыррак У.Э., Таммет Х.Ф., Сальм Я.Й., Лутс А.М., Ихер Х.Р. Результаты наблюдений за спектром подвижности атмосферных ионов // Тез. докл. IV Всес. симпоз. по атмосферному электричеству.- Нальчик, 1990.- С. 204.

Results of the measurement of the mobility spectrum of atmospheric ions.

80. Hõrrak, U., Miller, F., Mirme, A., Salm, J., Tammet, H. Air ion observatory at Tahkuse: Instrumentation // Acta et comm. Univ. Tartuensis.- 1990.- No. 880.- P. 33-43.

81. Kikas, Ü. Processes transforming near-ground aerosol spectra // Abstracts of Papers of European Aerosol Conference - Karlsruhe, 1991.- P. 161.

82. Kikas, Ü., Mirme, A., Tamm, E. Size distribution dynamics of rural and urban aerosols // Acta et comm. Univ. Tartuensis.- 1990.- No. 880.- P. 84-93.

83. Kikas, Ü., Mirme, A., Tamm, E. Maalähedase aerosooli allikatest ja levikust // Kaasaegse ökoloogia probleemid. Eesti V ökoloogiakonverentsi teesid. - Tartu, 1991.- Lk. 74--76.

Sources and transfer of near-ground atmospheric aerosol.

84. Kikas, Ü., Mirme, A., Tamm, E. Variability of near-ground atmospheric aerosol // Abstracts of Papers of European Aerosol Conference. - Karlsruhe, 1991.- P. 160.

85. Luts, A., Salm, J. Electrostatic scattering of two air ion groups of different mobilities // Acta et comm. Univ. Tartuensis.- 1990.- No. 880.- P. 105-110.

86. Mirme, A., Kikas, Ü., Tamm, E. Time-size structure of atmospheric aerosol // Atmospheric Aerosols and Nucleation. Lecture Notes in Physics. - Vienna: Springer-Verlag, 1988. - No. 309.- P. 52-55.

87. Mirme, A., Tamm, E. Measurement of the rate of aerosol particles formation and decay processes // Report Series in Aerosol Science. - No. 18 (1991). - Helsinki, 1991. - P. 119-123.

88. Mirme, A., Tamm, E. Comparison of sequential and parallel measurement principles in aerosol spectrometry // Abstracts of Papers of European Aerosol Conference. - Karlsruhe, 1991.- P. 316.

89. Noppel, M. Analysis of measurement methods of aerosol size spectrum with electrical analyser TSI-3030 // Acta et comm. Univ. Tartuensis.- 1990.- No. 880.- P. 67-83.

90. Noppel, M. On the La Mer-Sinclair method of aerosol size measurement based on higher order Tyndal spectra // Report Series in Aerosol Science. - No. 18 (1991). - Helsinki, 1991 - P. 16-21.

91. Parts, T. On the nature of negative small air ions of an ageing time of one second // Acta et comm. Univ. Tartuensis.- 1990.- No. 880.- P. 52-61.

92. Reinart, A. A universal controller for long-term experiments // Acta et comm. Univ. Tartuensis.- 1990.- No. 880.- P. 100-104.

93. Reinet, J. A generator of electroaerosols for the neutralization of static electricity // Acta et comm. Univ. Tartuensis.- 1988.- No. 809.- P. 143-146.

94. Salm, J. Air Electricity Laboratory of Tartu State University: a historical survey // Ионизация, аэрозоли, электрометрия. Библиографический указатель науч. публикаций Тарт. гос. ун-та за 1946-1985 гг.- Тарту, 1986.- С. 15-21.

95. Salm, J. The average mobility spectrum of large ions of the troposphere // Research Letters on Atmospheric Electricity. - 1988.- Vol. 8.- P. 21-24.

96. Salm, J. TRÜ AEL 20 // Füüsika 1984.- Tallinn: Valgus, 1986.- Lk. 15-22.

20 years of AEL of Tartu University.

97. Tamm, E., Kikas, Ü., Langus, L., Mirme, A., Reinart,A.

Mõnedest antropogeense aerosooli allikatest // Kaasaegse ökoloogia probleemid. Eesti V ökoloogiakonverentsi teesid. - Tartu - 1991 - Lk. 166-168.

Some sources of aerosol pollution.

98. Tamme, V. Charge generation and separation in the evaporation of water aerosol droplets // Acta et comm. Univ. Tartuensis.- 1990.- No. 880.- P. 94-99.

99. Tammet, H. Models of size spectrum of tropospheric aerosol // Atmospheric Aerosols and Nucleation. Lecture Notes in Physics. - Vienna: Springer-Verlag, 1988. - No. 309. - P. 75-78.

100. Tammet, H. Fair-weather electricity on ground level //Proc. 8th Int. Conf. on Atmospheric Electricity. - Uppsala, 1988. - P. 21-30.

101. Tammet, H. Model calculation of global components in tropospheric electric field variation // Proc. 8th Int. Conf. on Atmospheric Electricity.- Uppsala, 1988.- P. 827-832.

102. Tammet, H. Air Ion Observatory at Tahkuse: Software //Acta et comm. Univ. Tartuensis.- 1990.- No. 880.- P. 44-51.

103. Tammet, H. Aerosol electrical density: Interpretation and principles of measurement // Report Series in Aerosol Science. - No. 19 (1991).- Helsinki, 1991 - P. 128-133.

104. Tammet, H., Salm, J., Luts, A., Iher, H. Mobility spectra of air ions // Proc. 8th Int. Conf. on Atmospheric Electricity. - Uppsala, 1988.- P. 147-151.

105. Tammet, H., Salm, J., Iher, H. Observation of condensation on small air ions in the atmosphere // Atmospheric Aerosols and Nucleation. Lecture Notes in Physics.- Vienna: Springer-Verlag, 1988.- No. 309.- P. 239-240.